# HUMAN AND AUTOMATIC CONTROL INTERACTION WITH A REMOTELY PILOTED VEHICLE

BY

CHAD RAYMOND BURNS

DISSERTATION

Submitted in partial fulfillment of the requirements
for the degree of Doctor of Philosophy in Mechanical Engineering
in the Graduate College of the
University of Illinois at Urbana-Champaign, 2011

Urbana, Illinois

Doctoral Committee:

Associate Professor Dušan M. Stipanović, Chair
Associate Professor Ranxiao Frances Wang
Professor Naira Hovakimyan
Professor Geir E. Dullerud

# Abstract

In this dissertation, we present results from a study on the performance of humans and automatic controllers in a general remote navigation task. The remote navigation task is defined as driving a vehicle with nonholonomic kinematic constraints around obstacles toward a goal. We conducted experiments with humans and automatic controllers; in these experiments, the number and type of obstacles as well as the feedback delay was varied. Humans showed significantly more robust performance compared to that of a receding horizon controller. Using the human data, we then train a new human-like receding horizon controller which provides goal convergence when there is no uncertainty. We show that paths produced by the trained human-like controller are similar to human paths and that the trained controller improves robustness compared to the original receding horizon controller. We also show the impact of feedback delay on five metrics of human operator performance and for each metric characterize the impact as linear or superlinear. Finally we propose a human-inspired strategy for the automatic controller to robustly handle feedback delay.

*For my parents who educated me*

# Acknowledgments

First I would like to acknowledge my Lord and Savior Jesus Christ. The past three years of grad school have been surprisingly formative in my life. A number of individuals have crossed my path who pointed me back to the reality that Jesus is the water that our thirsty souls restlessly seek; for their impact on my life I am grateful.

I'd also like to mention a few people at this university, without whose help this dissertation would not have been possible. Dusan Stipanovic, my advisor, has tirelessly pointed me back into the way. Frances Wang, my co-advisor from Psychology, took an interest in my work and provided much patient help to me. She also provided the Psychology expertness and human subjects to allow this interdisciplinary work to come to completion. Joe Zearing, my good friend and working companion for the most enjoyable year out of six that I did research, was an invaluable aid. Joe is an outstanding programmer who knows how to innovate and follow instructions at the same time. Whitney Street, a psychology graduate student that I collaborated with for the Maze Study, was a pleasure to work with. The work could not have been done without the multi-year effort of Juan Mejia, Dan Block, and others who put together our robotics testbed. I am grateful to my MechSE committee members Naira Hovakimyan, and Geir Dullerud for their time and input. I am also grateful to Becky Lonberger of CSL and Kathy Smith of the MechSE department. Finally, I'd like to thank my beautiful and supportive fiancée Angela Sekerak, who graciously helped me with formatting and proofing this document and a number of others.

# Table of Contents

# Chapter 1

# Introduction and Literature Review

In 1983 D. L. Akin, a researcher at MIT working under contract for NASA's Marshal Space Flight Center, defined telepresence as the following:

> "At the worksite, the manipulators have the dexterity to allow the operator to perform normal human functions. At the control station, the operator receives sufficient quantity and quality of sensory feedback to provide a feeling of actual presence at the worksite." [1]

Today, almost 30 years later, we have not yet realized this dream. Although Akin's vision has not yet been fully realized the applications for telepresence continue to expand. The work contained in this dissertation tackles a piece of the telepresence challenge by studying and characterizing aspects of a human piloting a vehicle in a remote environment. Our aim is to better understand how to blend the strengths of automatic controllers and human drivers. The goal is to provide insight that will be helpful to researchers and practitioners that hope to improve fully automated navigation algorithms and improve the performance of remotely operating human navigators. The main work covered in this dissertation considers human and automatic controllers performance of a "drive to goal without collision" task. We also train and evaluate a human-like controller. Later we provide analysis of the human's strategy for dealing with delay and apply this to our trained human-like controller.

## 1.1 Motivation

A significant proliferation of "human-in-the-control-loop" remotely navigated vehicles is occurring in our society today. This proliferation is occurring in both unmanned ground and unmanned air vehicles (UAVs), where

unmanned does not mean unpiloted as many of these vehicles have humans in a remote navigation and control loop. The UAV market is expected to expand greatly due to predictions such as the following one:

> "Teal Group's 2010 UAV market study predicts a worldwide demand of more than $80 billion for UAVs systems through the coming decade." [2]

Human-in-the-loop remote navigation systems are found in many applications [3]: undersea oil and gas exploration robots swimming in the ocean miles below their human navigators [4], UAVs flying missions half a world away from their human supervisors [5], and bomb disposal robots being remotely navigated by police officers in the next room [6], and many other real [7, 8] and research applications [9, 10]. Although not remote, modern automobiles are another example of a system with humans in a navigation control loop who receive increasingly sophisticated support from onboard controllers [11, 12, 13, 14, 15]. The level of human involvement in the navigation tasks varies between these applications, but in many instances there is a human in the navigation control loop because a purely automatic controller is not capable of performing the task solo [16], or because humans offer superior performance. This fact led us to ask two questions: first, what can we learn from studying human remote navigation that can be applied to fully automatic navigation, and second, what can we learn about human performance of the remote navigation task that will help researchers design smarter controllers for systems where a human will be in the navigation control loop. These important questions were studied in the context of humans and automatic controllers participating in a remote navigation task.

## 1.2 Overview of the Work

The controller study was evenly split between engineering and psychology: it trained receding horizon controllers with human-like characteristics and evaluated the performance of both humans and automatic controllers as feedback time delay was increased, and number and type of obstacles was varied.

The study started with the design of a software-based simulator that tested both human and automatic controller's ability to navigate a vehicle from a starting region to a goal location. The simulator was flexible allowing for arbitrary controller, map, and feedback delay to be selected. Data for the controller's performance on a particular scenario was automatically generated and saved to a file for detailed post-processing which could occur later.

In this study we used factorial experiment design which is explained in more detail in [17, 18]. This is relatively common in studies that analyze human performance (see Section 1.3). The experiment was broken into test cases know in the literature as scenarios. The factors and their levels that determined a scenario were *obstacle type* (concave or convex), *number of obstacles* (one obstacle, two obstacles), *delay* (0, 0.2 and 0.4 seconds) and *controller type* (human, receding horizon, human-like receding horizon). The performance metrics we choose to use were completion time and success rate.

The human-like controller was developed by studying the human path data and identifying key characteristics. By trial and error, terms were developed for the receding horizon controller's objective function which resulted in the identified human behavior being expressed by the receding horizon controller. Finally the entire objective function was trained on selected human paths to render human-like controllers.

We needed a framework sufficiently rich to capture the basic constraints of the 'real world' navigation task, while also being simple enough to allow meaningful identification and modeling of human behaviors. We considered driving a vehicle with nonlinear nonholonomic kinematic constraints with bounded control inputs through a course with convex and concave obstacles toward a goal. The nonlinear vehicle model and concave obstacles made the analysis broadly relevant as many remote navigation tasks are a concatenation of these elements. Similar scenarios that test various representative map configurations were adopted by [19, 20, 21].

Based on this framework, we conducted experiments with human subjects acting as drivers and providing the control inputs for the vehicle. We also did a series of experiments with automatic navigation controllers. These experiments revealed two main facts. First, the automatic controllers worked well in the absence of feedback time delay uncertainty, although when uncertainty was introduced, performance degraded much more rapidly for the automatic control than it did for human operators. Second, humans seemed to complete the navigation task differently from automatic controllers as evidenced by the fact that human paths do not look like automatic controller paths.

From these observations we developed two broad goals: first, to formulate a provably feasible and provably convergent controller that handles the same general navigation task given to humans, and second, to train the controller to perform the navigation task in a human-like way.

After the above work was completed the human data for each scenario was analyzed for the second time focusing exclusively on the impact of feedback delay. We introduced four new metrics (used in addition to completion time and success rate) that shed light on the impact of feedback time delay. This analysis fits linear or quadric trends to the effect of feedback time delay on the given metric. This characterization will allow engineers to make design trade-offs when creating human-in-the-loop remote navigation systems with specific performance objectives in mind.

## 1.3 Methodology

This work has been cross disciplinary between controls engineering and psychology, and we have made an effort to blend ideas from both. A common technique of investigation used by psychologists is factorial experiment design. This approach divides the independent variables of interest into orthogonal factors and levels and provides suggested standard analysis techniques to determine the statistical significance and interaction between the factors. This technique is widely used in the study of human performance [17, 18, 19, 21, 22, 23]. The work presented in this

dissertation is much less common because we apply the technique across both humans and automatic controllers. Frequently engineers are concerned with "yes" or "no" questions: does the controller yield bounded error, does the controller converge, etc. Engineers will also speak of a controller's level of robustness such as gain margin. For a navigation task being performed by a receding horizon controller it is very difficult to directly assign a level of robustness, but using factorial experiments we can draw many useful and rigorous (in the sense of being statistically significant) conclusions about the controller's performance and the impact of the independent variables.

Another area where the blended methodology impacted our work was in how we approached training our human-like controller. The typical approach of engineers is to train the "best" possible controller, for example see [24, 25]. Our training objective was different; we did not aim to train the "best" possible controller, we aimed to train a human-like controller. Our goal was to identify how many human-like controller realizations were necessary to recreate path data similar to that which we collected from real drivers. It turned out that only one realization was necessary suggesting that the human-like controller we designed did a good job capturing the human behaviors expressed in our data. Thus the human-like controller structure we develop may be well suited to capture an expert performance, but we did not study this explicitly.

## 1.4 Contributions of Merit

These are the conclusions and contributions that resulted from the work described in this dissertation:

a. Human drivers take paths that are less-optimal compared to simple time minimizing controllers.

b. We can capture human-likeness with our trained human-like receding horizon controller. We also provide non-restrictive sufficient conditions for the receding horizon controller's boundedness and convergence.

c. Humans are far more effective at dealing with feedback time delay than the receding horizon controller.

d. Our trained human-like receding horizon controller recovers much of the gap between performance of humans and the original receding horizon controller for the cases with feedback time delay.

e. We quantify the impact of feedback delay on human performance from the viewpoint of 5 dependent metrics which we formulate.

g. We provide a formulation of the receding horizon controller, inspired by the observed human stop-and-wait strategy, which gives goal convergence for bounded feedback delays.

## 1.5 Literature Review

This work is interdisciplinary in nature and the themes from literature that have inspired and informed our work are traced and cited in this section. We identified 3 major themes of importance. They are 1) human navigation studies, 2) receding horizon controller theory and implementation, 3) training methods relevant to our work. These themes are discussed in Subsections 1.5.1 – 1.5.3. In each subsection an effort is made to contextualize our work by explaining similarities and differences compared to other studies.

### 1.5.1 Humans and Delay

Feedback time delay in a system controlled by a human may be considered as a temporal lag between issuing a command and seeing its effect. One of the earliest systems developed by man that exhibited this type of lag between command and event was the throwing spear. To hit a running animal, the operator must account for flight time during which the target will move. Throwing a spear to hit a moving target is harder than throwing at a stationary target. This increased difficulty and drop in accuracy that occurs as humans compensate for time lag is studied in this dissertation as it relates to the modern task of driving a vehicle in a remote environment.

In the 1960's NASA's interest in the question of how delay impacts the performance of a remote manipulation task [26, 27] led to extensive study of the topic. It was found that delays as small as 300ms (the smallest studied in [26]) impacted completion time and task accuracy. The researchers also observed that two strategies of compensating for delay exist: drive slowly or stop and wait. We look at these alternatives more closely in the context of our human subjects in Chapter 7 and as it relates to the receding horizon controller in Chapter 8.

A general method of dealing with delay between human operators and remote vehicles is to create a forward prediction based on a model of the system and the most recently given commands. Such forward prediction schemes for a general task [28], driving [29], and specifically driving while avoiding collision [19, 20, 21, 30] are explored in these papers. These studies share many similarities with our work, including scenario iteration and basic factorial design and testing of human performance when completing a feedback delayed remote navigation task. The referenced studies compare unaided human control to augmented human control; unlike these studies, our work compares humans, receding horizon controllers, and trained human-like controllers.

Our work also quantifies trends in the impact of delay on human performance as linear or superlinear (quadratic). The value of similar trend analysis in making engineering judgments about implementing real systems is suggested by [28] (in that case relating task complexity, direct vs. supervisory control and completion time). We offer statistically justified trend analysis of the impact of feedback delay on five human remote-navigator performance metrics.

### 1.5.2 The Controller

Previous work has modeled human navigation and obstacle avoidance as the response of an automatic controller [32, 33, 35] or the solution of an optimization problem [34]. This work considered how humans navigate, either through free space or in the presence of obstacles. Researchers have collected human data and matched or compared it with theoretical results or with controllers designed to be human-like. The work was interdisciplinary and bridged psychology, human factors, and controls engineering, and it offered ideas and inspiration for comparing a human's performance of a navigation task quantitatively with the performance of an automatic controller.

Our work showed that humans handle non-convex obstacles very well. Thus to train a human-like controller to capture human-like performance, it was essential to have an automatic controller formulation that could deal with non-convex obstacles. In general, the simple dynamic control models previously used to capture human-like obstacle avoidance behavior in [35, 32, 33] were unable to deal with non-convex obstacles so a more powerful automatic controller needed to be considered. This shortcoming of the controller used in [35] was verified by replicating in simulation the trained human-like dynamic controller from [35] and observing that it was incapable of completing the simple concave obstacle scenarios we used in our study. We thus selected a receding horizon controller built on the collision avoidance work of [36] and extended it to handle non-convex obstacles. Stability analysis for receding horizon controllers in general has been presented in [37] and how to guide vehicles around convex obstacles in particular has been presented in [36, 38]. These stability guarantees all relied on the basic idea of adding a contractive constraint to the receding horizon controller formulation that contracts an error function. In this paper we adopted a similar approach. Our guarantees are also similar to those found in [39, 40] in the sense that we provide feasibility and convergence results for a receding horizon controller guiding an input constrained vehicle around non-convex obstacles toward a goal. Our guarantees are different, however, because we have a different model, different input constraints, and different proof approach than that offered in [39, 40]. The difference is also due to our interest in "bounded convergence" and not stability in the classical sense of Lyapunov, as considered in [40].

We also provide non-restrictive conditions necessary to ensure collision free goal convergence for zero, bounded constant, and bounded time varying delay, based on a stop-and-wait strategy inspired by the human operator's method of coping with delay.

### 1.5.3 Training Human-Like Controllers

As mentioned in Subsection 1.5.2, we choose to capture the human operator's execution of the navigation task using a receding horizon controller trained on human data. This controller is based on minimizing an objective function – the training was carried out by modifying the objective function of the controller to create human-like behaviors. There are many ways of training automatic controllers based on human data; these include such methods as neural networks (which we examined and simulated before discarding) and apprenticeship learning (which we will reference). Our training method is very similar to the training done in [35] in that we attempt to capture human-like behavior and to better understand the human behavior by examining the results of training the controller. In this sense we are not training with particular performance in mind but with the idea of characterizing the behaviors that exist in the human path data. This training is very unlike [35] in that we are training parameters of a receding horizon controller objective function while [35] trained parameters of a simple dynamic controller.

One method of using human data to train objective function parameters for a receding horizon controller is called apprenticeship learning; a relevant example would be the work in [25, 41]. The similarity to our work is the training of an objective function for a form of receding horizon control. A key difference is what data is used for training. In

[25] expert human data is used; in other work by the same author several expert performances are combined using dynamic time warping to create a single high quality expert path [24]. This emphasis on expert data is dissimilar to our work where we run the training on many real human paths that have not been smoothed or averaged. We trained controllers on selected human paths, then examined their similarity to other human paths. One purpose was to capture real human behavior in our training instead of idealized behavior. Another purpose behind our approach was to determine how many human-like realizations of the controller were necessary to create paths similar to all other human paths. We expected to need several realizations, but one turned out to be sufficient, suggesting in the end that the differences between the individual human performances were less significant than we originally thought.

## 1.6 Outline

This thesis is divided into ten chapters. Chapter 1 presents an introduction and a literature review. Chapter 2 looks at humans acting as the navigation controller and explains our methods for testing and factorial experiment design. Chapter 3 develops the receding horizon controller stability guarantees and tests this controller on the same conditions given to humans and offers analysis of the results. In Chapter 4, we present a modification to the receding horizon controller's objective function which allows us to train the controller to make human-like decisions, and we discuss the training in Chapter 5. Chapter 6 tackles the analysis between the trained human-like controller and the humans themselves. In Chapter 7, we move away from the factorial analysis approach to look at the human operators' response to the single independent variable: feedback delay. In Chapter 8, we discuss the impact of the feedback delay on the receding horizon control formulation, give an upper delay bound for which the controller will still have bounded goal error, and show how adopting a human-like stop-to-wait strategy can give robust performance for bounded error. Conclusions and future research directions are discussed in Chapter 9.

# Chapter 2*

# The Human as Navigator

As pointed out in the introduction, there are many real world instances where humans are used to provide navigation control input to remote vehicles. To study this, we needed to collect data for humans performing a controlled remote navigation task. The purpose was three fold: 1) to allow characterization of human performance as independent factors of importance were varied, 2) to establish baseline human performance for comparison to automatic controllers, and 3) to collect human operator data that could later be used to train human-like automatic controllers.

To test human remote navigation, we designed an experiment that presented humans with the important navigation challenges we identified in Chapter 1; namely, variable obstacle configurations and variable feedback time delay. The experiment was then coded in MATLAB as a modular simulator which supported scenario iteration and batch testing. The simulator was also designed to batch test automatic controllers on the same scenarios given to humans. Care was taken in the design of this simulator to ensure that the comparison between the automatic controller and the humans was equivalent. Similar knowledge of the vehicle model, simulator saturations limits and equivalent levels of map information were presented to both humans and automatic controllers. Further, the same dependent performance metrics and independent facts were studied. Finally, the humans and automatic controllers were given instructions with similarly ranked priorities. All this was done to ensure relevant comparisons could be made later between human navigators and automatic controllers.

* Chapters 2-6 are based on work also contained in a journal submission which is reference [31]; the SYSTAT analysis in these chapters was run by Frances Wang, a co-author on the submission.

## 2.1 The Simulator

The simulator was designed to allow analysis of the human's behavior as important parameters and environmental options were varied, according to our factorial experiment design. A map module held map definitions with non-convex and convex obstacles constructed from line segments and vertices. The vehicle plant module was composed of two blocks: one was an uncertainty block, the other accepted a mathematical model of the vehicle along with input saturation limits. The uncertainty was a time delay unknown to the human navigator. Taken together, the vehicle model and uncertainty block became the vehicle plant module. The controller module contained the human operator who was fed information about the vehicle's state from the vehicle's plant module and relevant obstacle data from the map module. This information was provided to the human navigator as an overhead view of the map with extents that included the obstacles, vehicle, and goal. The controller module output a control command for the vehicle. All the modules were flexible and could be changed for various scenarios. The simulator is depicted in Figure 2.1. Figure 2.3 shows a human navigator and a screen shot of a sample human navigation experiment in progress. For additional information on the simulator see [42].

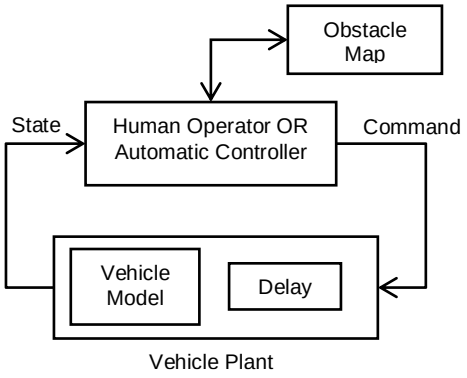


**Figure 2.1** The simulator. The blocks show individual components of the simulator.

### 2.1.1 The Vehicle Model

For this study, we asked humans to provide commands for a vehicle which could only move in the direction it was pointing, meaning it has a nonholonomic kinematic constraint. In robotics literature, such a model was sometimes called a "simple unicycle model" [43]. We used a discrete-time unicycle model [44] which we will refer to as the "vehicle model" and which is given by the following:

$$x_{k+1}^{cor} = \begin{cases} x_k^{cor} + \frac{v_k}{\omega_k}\left[\sin\left(\theta_k + \omega_k \Delta t\right) - \sin\left(\theta_k\right)\right] & \text{if } \omega_k \neq 0 \\ x_k^{cor} + v_k \cos\left(\theta_k\right)\Delta t & \text{if } \omega_k = 0 \end{cases}$$

$$y_{k+1}^{cor} = \begin{cases} y_k^{cor} - \frac{v_k}{w_k}\left[\cos(\theta_k + w_k \Delta t) - \cos(\theta_k)\right] & \text{if } w_k \neq 0 \\ y_k^{cor} + v_k \sin(\theta_k)\Delta t & \text{if } w_k = 0 \end{cases}$$

$$\theta_{k+1} = \theta_k + \omega_k \Delta t.$$

In the above model $x_k^{cor}$, $y_k^{cor}$ and $\theta_k$ are vehicle position and heading coordinates which belong to a continuous domain but were computed at discrete-time instances $k$. The above equations will be written in the compact form:

$$x_{k+1} = f(x_k, u_k), \tag{1}$$

where $x_k = [x_k^{cor}, y_k^{cor}, \theta_k]$ and $u_k = [v_k, \omega_k]$. The vehicle's position state is referred to as: $x_k^{pos} = [x_k^{cor}, y_k^{cor}]$. Just as a real vehicle has upper bounds on its maximum velocity and turn rate, the command inputs given by the human were also saturation limited. The command limits used are expressed as follows:

$$\begin{matrix} 0 \leq v_k \leq \bar{v} \\ |\omega_k| < \bar{\omega} \end{matrix}.$$

The vehicle moved in a 2-dimensional space defined by the map.

### 2.1.2 Maps

Four maps were used in the study, and they were selected to represent tasks with increasing difficulty for the human navigator. Both convex and concave obstacles were tested; the four maps are shown in Figure 2.2. The blue dotted circles are the starting regions where the starting location initial conditions (ICs) for the human navigators and controllers were located. For the human experiments, the ICs chosen all lay on a diameter of the circle which was roughly perpendicular to a line stretched to the goal. The green dot in the lower right corner of each map denotes the goal.

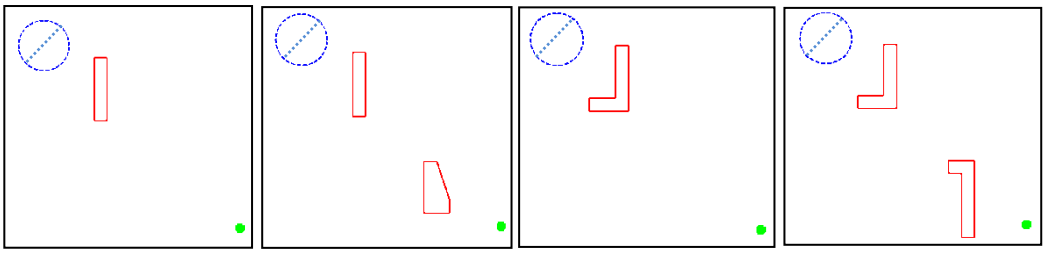


**Figure 2.2** The maps used in this research. The blue circle shows the starting region within which the initial conditions will lie; the line across the starting region shows where the human ICs were selected to fall. The green dot marks the goal.

### 2.1.3 Delay

In addition to varying difficulty maps, we introduced quantifiable uncertainty by adding delay to the vehicle plant. The vehicle model, which is the conception of the vehicle held by the human operator's mind, was fixed. The vehicle plant, which is the actual vehicle in the simulation, had an input delay attached to it. When set to a nonzero value, this time delay meant the actual vehicle plant would not respond the way our operator expected.

To quantify and understand the navigation data, two performance metrics were defined. Completion time was the average time that a human takes to successfully guide the vehicle to the goal. Success rate (robustness) was the average percent probability of success for a human operator facing a particular navigation task. These measures could be used to compare the relative difficulty of two tasks or the relative performance of human operators, as experimental conditions, such as map or uncertainty are varied**.**

## 2.2 Testing Procedure

In this study, 1056 IC to goal paths were created by eleven subjects. Each subject was given a practice session to learn the nonholonomic constraints of the vehicle and how to use the joystick to drive the vehicle to the goal while avoiding the obstacles. These practice sessions had no feedback delay and served as a learning period for humans allowing them to conceptualize the vehicle model without time delay. The subject continued practice until s/he completed five consecutive runs without obstacle collision; then the actual testing session started. Allowing this conceptualization to form before testing began kept humans on equal terms with the controllers we tested in later sections of this paper, which were given the mathematical vehicle model, equation (1). The process of first learning the no-delay vehicle model and then encountering the effect of delay later during a trail is exactly analogous to how we dealt with the automatic controller. The automatic controller was given a copy of the vehicle model without delay and then later during trail runs feedback delay was added as a "surprise" to the controller.

On each of the four maps the subject was given four ICs. For each IC, each subject attempted 6 runs to the goal; two at zero delay, two at 0.2 seconds of delay and two at 0.4 seconds of delay.

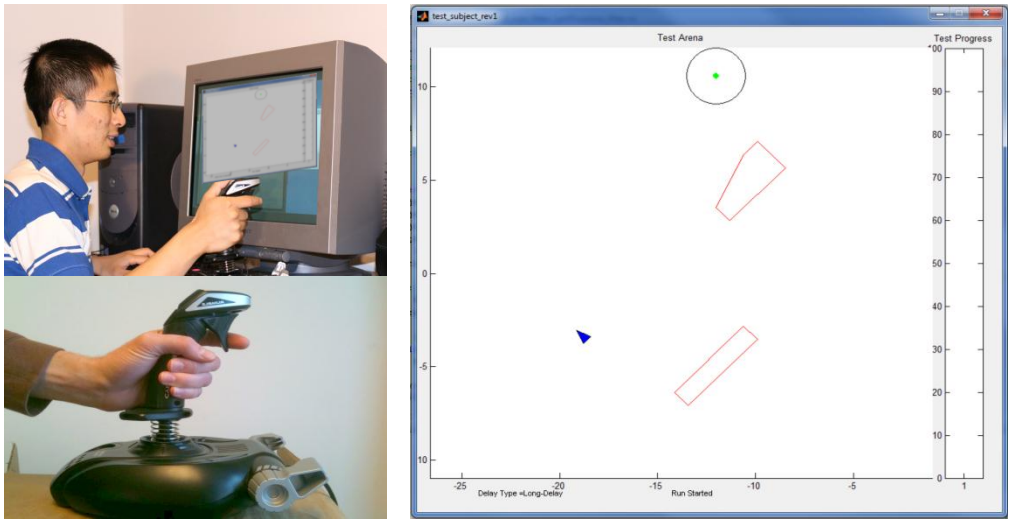


**Figure 2.3** Top: Cartoon of human operator (not a subject). Bottom: Joystick. Right: Overhead view of obstacles (red), vehicle (blue triangle) and goal (green) as presented to humans.

The human subjects were instructed to drive the vehicle to the goal with two ranked priorities in mind: first, to avoid collisions with obstacles, and second, to reach the goal as quickly as possible. The subjects were informed that sometimes there would be unknown but fixed time delays which could make completion of the task more challenging.

## 2.3 Results for the Human Navigator

The human subject data for maps three and four is shown in Figure 2.4a & b. These were the paths created by all the subjects with no uncertainty, i.e. zero delay. The human path data was recorded as an x-y trajectory and a velocity. In Figure 2.4 c & d we show two representative human paths from map three. The top view shows the x-y path. Tipped on its side, the velocity of the vehicle at each instant is recorded as the vertical path height. These two paths started off slow and sped up to about ½ of the vehicle maximum velocity. The completion time data and averaged success rate for the human navigators are shown in Figure 2.5.

A 3 delays X 2 obstacle number X 2 obstacle type ANOVA [45] was conducted on the rate of success and on the mean completion time of the successful runs. For the success rate, there was a significant main effect of delay ($F(2, 516)=16.03$, $p<.001$) and no other effects (all $Fs<1$, $ps>.48$). For the completion time, there was a significant main effect of delay ($F(2, 513)=160.88$, $p<.001$), a significant main effect of the number of obstacles ($F(1, 513)=27.07$, $p<.001$), and a marginal effect of obstacle type ($F(1, 513)=3.56$, $p=.06$). There were no significant interactions (all $Fs<1.4$, $ps>.24$).

The data first shows that humans were slower and less successful as the delay increased. Second, humans were slower as the number of obstacles increased, although their success rate remained unaffected. Third, people tended

to be slower for concave than convex obstacles, but the success rates were comparable. This data is interesting by itself and confirms the expected result that feedback delay degrades human remote navigator performance. We look at this effect in more detail in Chapter 7. The data also serves as reference for comparison to the automatic controllers in the following chapters.

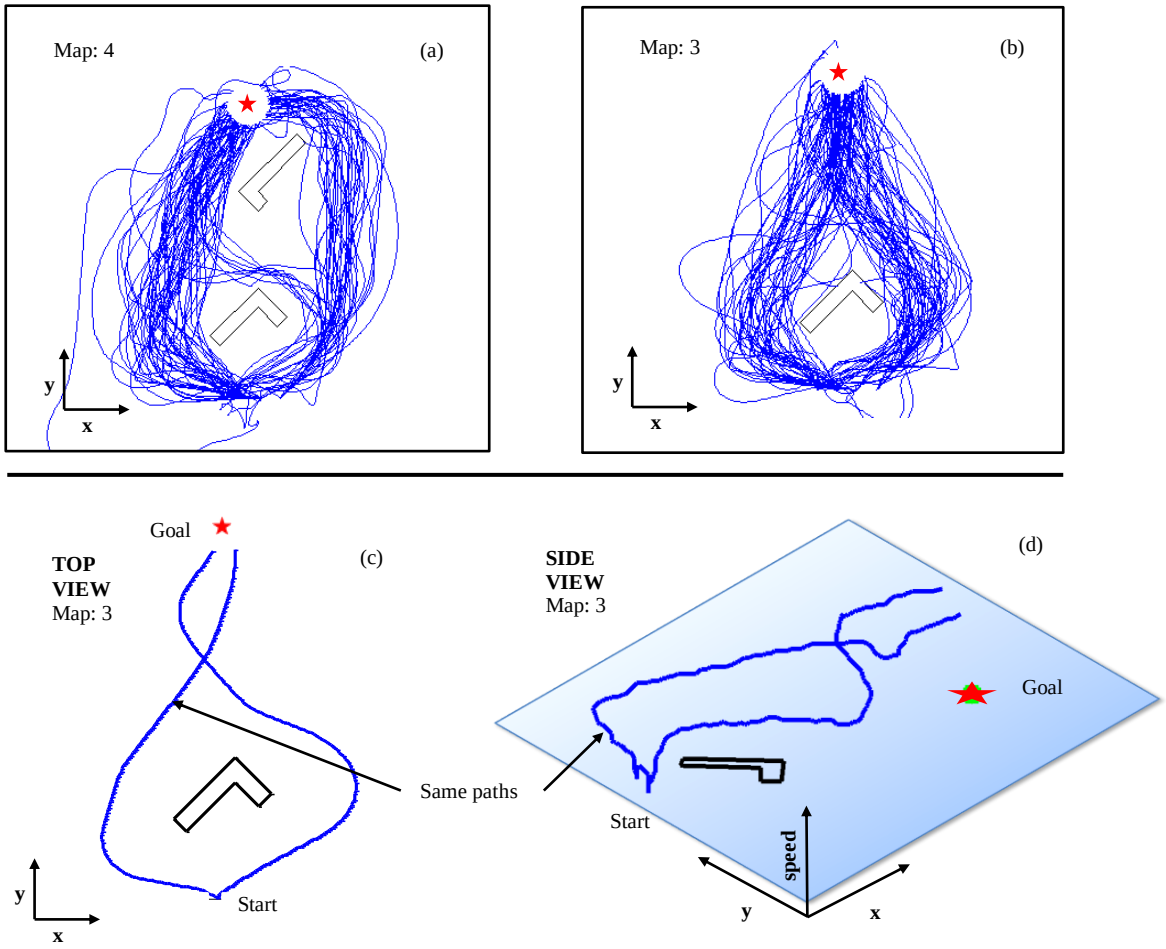


**Figure 2.4** Representative human path data. Zero delay human path data from maps three and four, (a) & (b). Shown in (c) are two representative human paths; (d) shows the same paths as (c) but from the side we can now see vehicle's speed represented by the vertical height of the path at each point in the x-y plane.

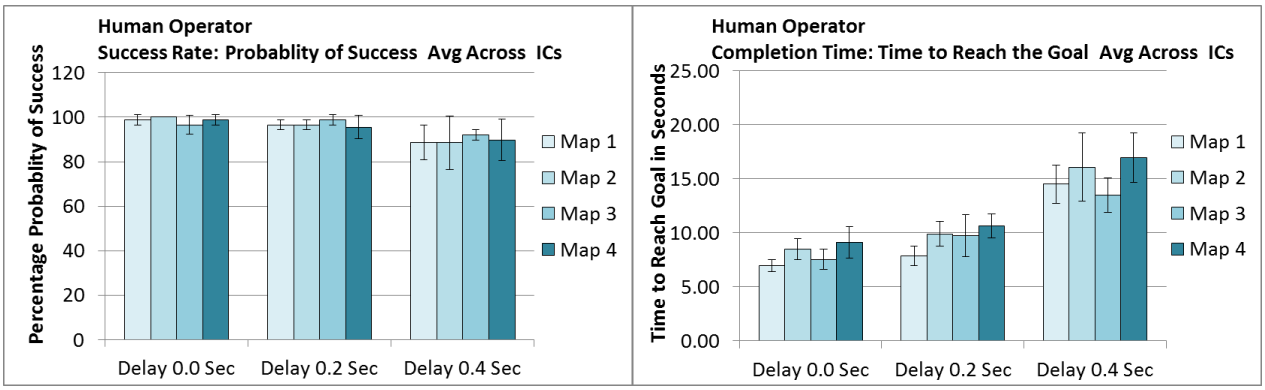


**Figure 2.5** Human success rate and completion time data. Data for the human navigators, averaged across ICs for each map. The error bars show plus/minus one standard deviation of the data for each of the four ICs on a given map.

# Chapter 3

# Automatic Receding Horizon Controller as Navigator

In the previous chapter, the simulator was used to test human operators acting as controllers. In this chapter we perform similar experiments with automatic receding horizon navigation controllers. The controller we used needed to be capable of handling the same navigation task given to the humans; based on this criterion we identified five essential controller properties:

1. Capability of prediction in order to plan the best route based on map information, vehicle model, and present state.
2. Capability of handling convex, non-convex obstacles and a nonlinear vehicle model.
3. Guaranteed feasibility.
4. Guaranteed convergence to the goal.
5. Flexibility to be trained to adopt human-like behavior while maintaining 1-4.

These criteria lead very naturally to the consideration of a receding horizon controller as opposed to simple non-linear feedback control, such as that used in the work of [35]. Because no receding horizon controller was available in the literature which met all the specifications, a new formulation was required.

## 3.1. The Receding Horizon Controller Formulation

Receding horizon controllers are both powerful and flexible, anticipating the future to plan the best path and capable of handling nonlinear vehicle models. To formulate a receding horizon control, a plant is given and an objective function is designed to capture a desired performance metric. An optimization package then produces a set of control commands that satisfy constraints, if they are given, while minimizing the objective function over a finite horizon. Once a minimizing control has been found, that control is applied to the plant in an open-loop fashion for a period of time, called the execution horizon, $n$, which is shorter than the computation horizon, $N$. Three events occur at the end of the execution horizon: the plant state is sampled, a new minimizing control input is computed, and the whole process repeats. In this way, receding horizon control is a feedback control strategy [46]. To guarantee that the vehicle will converge to the goal, we can impose a contractive constraint requiring the controller to produce a command which leads to the contraction of a goal distance error function [37]. Such a contractive constraint was added to the receding horizon formulation. The constraint has two key properties: flexibility and feasibility. First, the constraint is flexible: it gives the controller maximum flexibility in how it satisfies the constraint because it deals with the next execution horizon, not just the next step. Practically this means the vehicle does not always have to move toward the goal for the contractive constraint to be satisfied. The vehicle's behavior is often governed by the objective function and the terms designed to render human-like behavior and not by the contractive constraint. The second important property of the contractive constraint is continuous feasibility over a space with non-convex obstacles. The formulation places a Dijkstra algorithm in the constraint facilitating the proof of convergence. It is important to note that Dijkstra functions have a long history of use in solving navigation problems; one example being [47, 48, 49, 50].

### 3.1.1 Receding Horizon Controller Structure

Equation (1) explains the nonlinear vehicle model being controlled. All control inputs $u_k$ must satisfy $u_k \in U$, where $U$ is a convex compact set which defines the set of all admissible control inputs (for a computation horizon of length $N$). For example, the inputs in our model are absolute value bounded (with the same bounds used in Section 2):

$$0 \le v_k \le \bar{v} \text{ and } \left|\omega_k\right| < \bar{\omega}.$$

Future predicted states starting from an initial condition $x_k$ are defined by $x_{k+i|k}, i \in \{1,...,N\}$ and these were generated by the proposed control inputs $u_{k+i|k}, i \in \{1,...,N\}$ and the vehicle model. A sequence of control inputs on the finite horizon starting from initial condition $x_k$ was defined as $U_N(x_k) = \{u_{k+1|k}, u_{k+2|k}, ..., u_{k+N|k}\}$ and the sequence of states produced by these inputs was denoted as $X_N(x_k) = \{x_{k+1|k}, x_{k+2|k}, ..., x_{k+N|k}\}$. The function being minimized in (2), $J_N(\cdot)$, may be any scalar function dependent on $U_N(x_k)$, and $X_N(x_k)$. For example, the objective function,

in this section, is a cost-to-go term that measures or approximates the cost for the vehicle to move from the end of the computation horizon to the goal.

A general form of the receding finite time horizon optimal control problem, denoted as $P(k)$, starting from the initial condition $x_k$ at time $k$, can be stated as follows:

$$\begin{aligned} &P(k): \quad J_N^{\circ}(x_k) = \min_{u_{k+i|k}} \{ J_N(x_{k+i|k}, u_{k+i|k}) : \; u_{k+i|k} \in U, i \in \{1,...,N\} \} \\ &s.t. \begin{cases} h(k,i) = 0, \forall i \in \{1,...,N\} \\ g(k,i) \le 0, \forall i \in \{1,...,N\} \end{cases} . \end{aligned} \tag{2}$$

The formulation in (2) was subject to a set of obstacle and equality constraints. Obstacle constraints, $g(k,i) \le 0$, required the computed path to not intersect an obstacle. The problem was solved over the computation horizon $N$, but only $n$ commands were implemented before the solution was recomputed from the new location. The execution horizon $n$ satisfied $n < N$. Equality constraints, $h(\cdot) = 0$, representing the system model in equation (1) required that the solutions be kinematically feasible over a finite computation horizon $N$.

Two new indices are here introduced that clarify the notation to follow. A new sequence, $\{\hat{k}\}$, will be defined as a subsequence of $\{k\}$. The $\{\hat{k}\}$ subsequence contains the values of $k$ at which time the optimizer re-computes the solution. Every time an execution horizon finishes, the solution is recomputed, thus $\hat{k}$ takes values at 0, *n*, 2*n*, 3*n*, and so on. The computation horizon for a single solution will be $\hat{k}+1$ to $\hat{k}+N$. The optimizer is planning into the future $N$ steps, by choosing a command set $U_N$ and matching state set $X_N$. The $x_k$'s in $X_N$ are future states, predicted on the current real location $x_{\hat{k}}$. Thus we write them as: $x_{\hat{k}+i|\hat{k}}$ for $i = \{1,...,N\}$ We introduce a final sequence, $\{\ell\}$, which will indicate the number of times the optimizer has run.

### 3.1.2 Dealing with Obstacles

To ensure that computation of the Dijkstra algorithm is feasible, we require the obstacles, convex or non-convex, to be represented (or over bounded) by a closed shape with boundaries consisting of vertices and straight line segments. This requirement is not restrictive, because shapes with a finite number of edges and vertices can be found to approximate a closed two-dimensional path to any desired level of accuracy. This is true, so long as the path is continuous, continuously differentiable except at a finite number of points, and has a finite number of inflections. Many algorithms have been proposed for path polygonization, the one in [51] is given as a reference; additional information on this topic can be found in [52, 53]. For any given map let $m_{vert}$ be the number of vertices required to over bound all obstacles to a satisfactory degree of accuracy. If the obstacles are made up only of straight lines and vertices then $m_{vert}$ will simply equal the total number of obstacle vertices appearing in the domain.

As in [39, 40] the basis of our convergence proof will be the contraction of a special function, which we call distance to goal and is computed according to the Dijkstra algorithm. The Dijkstra algorithm is a simple but powerful method of computing the shortest collision-free distance to the goal from any point in a map with a finite number of obstacles and obstacle vertices. It was introduced in [54] and a formal mathematical statement can be found in [55]. The algorithm can be simplified as follows:

1. Place points (call them nodes) at the vertices of all obstacle segments, the present vehicle location, and the goal.
2. Compute the Euclidian distances between each node and every other node. If an edge passes through an obstacle, its cost is set to infinity.
3. Compute the shortest path through the nodes from the current vehicle location node to the goal node. This path cost is the sum of the edge lengths

Our simulation code adheres to the three conditions, 1-3 above, and returns the length of the shortest straight line path to the goal as a function of the position state. Throughout this work we denote the Dijkstra distance to goal as $V(x_k^{pos})$.

Moving in a direction that $V$ decreases always results in progress toward the goal, even when the present state is behind a non-convex obstacle. The ability of the Dijkstra algorithm to deal with non-convex obstacles is why we choose to use it. The function is also continuous, though not smooth. Dijkstra is realized at some cost; computation is more expensive than a simple distance norm and global knowledge of the environment is assumed. Figure 3.1 shows $V(x_k^{pos})$ plotted on a map with two non-convex obstacles.

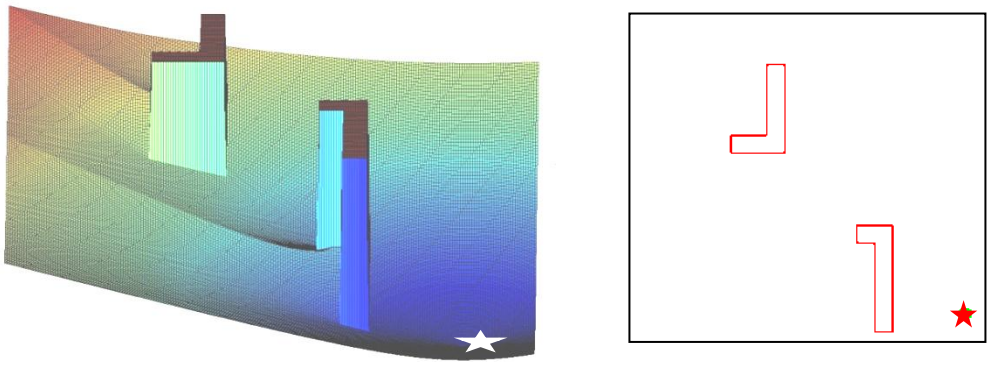

**Figure 3.1** The Dijkstra distance to a goal function plotted on map 4. The goal is in the lower right hand corner.

### 3.1.3 A Contractive Constraint

The role of a contractive constraint is to contract a function of the goal distance. The distance to the goal is not a function of the vehicle's heading, and furthermore, the vehicle heading is always bounded by $2\pi$. Thus the vehicle location state is our only concern. Due to the contractive constraint, the maximum error on the present execution horizon must be less than or equal to the maximum error on the previous execution horizon.

The constraint is expressed by the following inequality:

$$\max_{i\in\{1,\ldots,n\}}\{V(\hat{x}^{pos}_{k+i\,|\hat{k}})\} - c\max_{j\in\{1,\ldots,n\}}\{V(\hat{x}^{pos}_{k-n+j})\}\le 0\,, \tag{3}$$

where $c$ is between zero and one. For the first computation, when history is not available and $\max_{j\in\{0,\ldots,n\}}\{V(\hat{x}^{pos}_{k-n+j})\}$ does not exist, $V(x_0^{pos})+n\Delta t\,\bar{v}$ will be substituted. This can be thought of as an upper bound to the position error on a previous horizon *if* a previous horizon had existed. Requiring the vehicle to always make the greatest possible progress toward the goal is the optimal way of solving the navigation problem. But, in a world of non-convex obstacles, this may not be feasible or such a path may be undesirably aggressive. The constraint in (3) is less restrictive; it requires contraction from one horizon to the next, not for each new vehicle location.

Having introduced the contractive constraint, the convergent constrained version of the receding horizon control problem, $P_{SC}(k)$, starting from initial conditions $x_k$ at time $k$ can be formulated as follows:

$$\begin{aligned} &P_{SC}(k):\quad J_N^{\circ}(x_k) = \min_{u_{k+i|k}}\{J_N(x_{k+i|k},u_{k+i|k}):\\ &u_{k+i|k}\in U_N, i\in\{1,\ldots,N\}\},\\ &s.t.\begin{cases} h(k,i)=0, \forall i\in\{1,\ldots,N\}\\ g(k,i)\le 0, \forall i\in\{1,\ldots,N\}\\ \bar{g}(k,n,c)\le 0, \end{cases} \end{aligned} \tag{4}$$

Where $\bar{g}(k,n,c)\le 0$ represents the convergent contractive constraint given in (3). For the objective function we choose to minimize the Dijkstra distance from the end of the solution horizon.

### 3.1.4 The Final Formulation

The final formulation of the receding horizon controller can be summarized thus:

**Objective:** Minimize Dijkstra distance from the end of the solution horizon to the goal.

**Constraints:**

- Vehicle Model
- Command Saturation Limits
- No Obstacle Collisions
- Distance to Goal Contracts on Each Execution Horizon

## 3.2 Feasibility and Convergence of the Receding Horizon Controller

To guarantee that the vehicle reached the goal (feasibility/convergence) and that along the way maximum goal error was finite (boundedness), we needed to show that for every point in the domain a solution existed which satisfied the constraints. Further, we needed to show that satisfying the constraints meant the vehicle must ultimately converge to the goal. The following assumptions were needed to accomplish the task:

**A1** *For all* $x_k^{pos} \in D$ *an obstacle free path always exists in a direction of decreasing* $V(x_k^{pos})$**.**

**A2** $(n-1)\bar{\omega} > \pi$**.** *This assumption means that the vehicle can always turn 180 degrees and still move forward on one execution horizon.*

**A3** *The size of the closed domain D within which the vehicle will move, and the contraction coefficient, c, are related; c is chosen to satisfy* $c \le 1$*. Together, c and D must satisfy:* $\forall x \in D, \max_x cV(x^{pos}) < \Delta t \bar{v}$ .

**A4** *The receding horizon controller can either satisfy (3) for c<1 directly, OR if that is not possible it may move the vehicle to a new node with lower distance-to-goal than the position it started from.*

**A5** *The coordinates of the goal lie at the origin.*

**A6** *An over bound for the total number of obstacle vertices exists and is denoted by* $m_{vert}$ .

By definition of the Dijkstra algorithm, Assumption (A1) is true. Assumption (A2) can be added as a constraint condition to the receding horizon controller formulation, Assumption (A3) will be satisfied by selecting the appropriate domain and contraction coefficient, and Assumption (A4) can be enforced as a constraint in the receding horizon formulation. The impact of Assumption (A4) is explained in the convergence guarantee which follows. Assumption (A5) can always be realized through a coordinate transformation, and as explained in Subsection 3.1.2, Assumption (A6) is not restrictive.

With these assumptions in place the guarantees are formulated as follows.

*Guarantee of Feasibility:* The Dijkstra distance measure will always decrease in a direction that avoids obstacles (A1). It is always feasible on one execution horizon to point in the direction of maximally decreasing $V(x_k^{pos})$ (A2). After turning to a point in this direction it is always feasible for the vehicle to move a distance of at least $cV(x_k^{pos})$ (A3). The only time a movement of at least $cV(x_k^{pos})$ is not feasible is when motion results in the vehicle reaching an obstacle vertex before travelling the full $\Delta t\,\bar{v}$ distance. In that case the second half of (A4) is satisfied; see Figure 3.2. Thus feasibility is assured under (A1-A4).

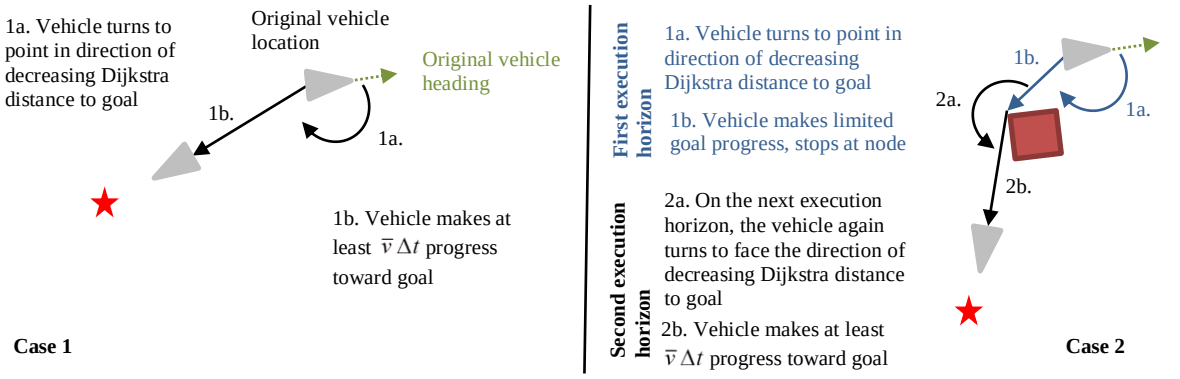


**Figure 3.2** Explanation for assumption (A4). In Case 1, the vehicle turns nearly 180 degrees and then makes goal progress at least equal to one execution step, $\bar{v}\,\Delta t$. In Case 2 the vehicle turns nearly 180 degrees but it cannot make full $\bar{v}\,\Delta t$ progress toward the goal because it encounters an obstacle vertex (where a node has been placed). So the vehicle stops and waits for the next horizon to continue making progress. It is in Case 2 that assumption (A4) is needed.

*Guarantee of Boundedness: The proposed receding horizon control (4) with* $c=1$ *from contraction constraint (3) will result in the vehicle position state* $x_k^{pos}$ *being explicitly bounded by a function of the initial vehicle position state,* $x_0^{pos}$. *That is,* $\left\|x_k^{pos}\right\| \le r(x_0^{pos})$.

*Proof:* It is sufficient to supply the bound $r(x_0^{pos})$, to prove explicit boundedness. From the definition of Dijkstra and since we know that the goal is at the origin we concluded $\left\| x_k^{pos} \right\| \le V(x_k^{pos})$. By equation (3) we have that for the first execution horizon:

$$\max_{i\in\{1,\ldots,n\}} \{V(x_{\hat{k}+i|\hat{k}}^{pos})\} \le V(x_0^{pos}) + n\,\Delta t\,\bar{v}\,,$$

which for $c=1$ will also be true on every subsequent execution horizon as well. Thus,

$$V(x_k^{pos}) \le V(x_0^{pos}) + n\Delta t\bar{v},\ \forall k\,.$$

Combining all the above we find,

$$\left\| x_k^{pos} \right\| \le V(x_0^{pos}) + n\Delta t\,\bar{v},\ \forall k\ ,$$

And thus,

$$V(x_0^{pos}) + n\Delta t\,\bar{v} = r(x_0^{pos}), \forall k$$

which gives the desired global bound on $\left\| x_k^{pos} \right\|$ for $c$=1 as a function of the time step $\Delta t$, maximum velocity $\bar{v}$ initial configuration $x_0$ and the receding horizon controller design parameters, and number of steps in each execution horizon, $n$.

*Guarantee of Convergence: The proposed receding horizon control (4) with contractive constant $c<1$ will result in the vehicle state converging to the goal after sufficient time $T$ has passed, i.e. for any $\varepsilon>0$ there exists $T$ such that if $\ell > T$ then $\left\| x_k^{pos} \right\| < \varepsilon$.*

*Proof:* From above: $\left\| x_k^{pos} \right\| < V(x_k^{pos}),\ \forall\ x_k$. From (3) and $c<1$ we have:

$$V(x_k^{pos}) \le \max_{i\in\{1,\ldots,n\}} \{V(x_{\hat{k}+i\,|\,\hat{k}}^{pos})\} \le c^{\ell}[V(x_0^{pos}) + n\Delta t\,\bar{v}\,]$$

By observation for $c<1$ we can always find $T$ such that for any $\varepsilon>0$, $\ell > T \ \Rightarrow\ c^{\ell}[V(x^{pos}_0) + n\Delta t\,\bar{v}\,] < \varepsilon$. Now combining from above:

$$\left\| x_k^{pos} \right\| < \varepsilon, \forall\ \ell > T\ .$$

There may be a finite number of times, less than the number of vertices in the map, $m_{vert}$, where full '$c$' decrease does not occur. In these instances, the motion for the execution horizon terminates at an obstacle vertex (A4), preventing the full '$c$' decrease from occurring. However, because $m_{vert}$ is finite (A6) we can simply add $m_{vert}$ to $T$ to arrive at the same result; namely, that for sufficiently large $\ell > T + m_{vert}$, we can force $\left\| x_k^{pos} \right\|$ arbitrarily small goal convergence.

## 3.3 Testing the Receding Horizon Controller

To compare the receding horizon controller to the human operators, we used the simulator developed for human testing. To do this, it was important that the input given to (by) the receding horizon controller be comparable to that given to (by) the human operator.

The humans were presented with an overhead view that displayed all obstacles and the goal. The Dijkstra cost-to-go employed by the receding horizon controller effectively used data from the entire map to compute the shortest straight line path to the goal. The humans were instructed to avoid obstacles as their primary concern and to reach the goal as quickly as possible, as a secondary objective. Following similar priorities, the receding horizon controller was constrained away from obstacles, and then it optimized the time to reach the goal. The saturation limits for turn rate and driving speed used for the humans were also used for the receding horizon controller.

In a similar way that human performance was measured, we measured performance of the automatic controller. Traditionally, robustness in mathematical terms is a relation between task performance (stability of the system) and environmental perturbations or model uncertainty. Some closed-form controllers admit direct computation of robustness measures (such as phase margin – a measure related to permissible feedback delay before instability). An open-form controller, such as the receding horizon controller, does not permit such direct computation of robustness. Similar to the way success rate was measured for human navigators, success rate (robustness) of the receding horizon controller was measured as the percentage of solutions which reached the goal, averaged over many simulator runs. Completion time was measured as the average time required for a successful solution to reach the goal.

## 3.4 Simulator Results for the Receding Horizon Controller

The receding horizon controller was run 200 times for zero delay on all four maps. Figure 3.3a & b displays about 100 of the zero delay paths on maps three and four. Two individual paths which represent some of the smoother trajectories from map three were shown in c & d. When there is no uncertainty (zero delay), the receding horizon controller performed impressively; many vehicle paths showed nearly constant travel at maximum speed. For zero delay the controller had a 100% success rate: no collisions occurred, even on map four.

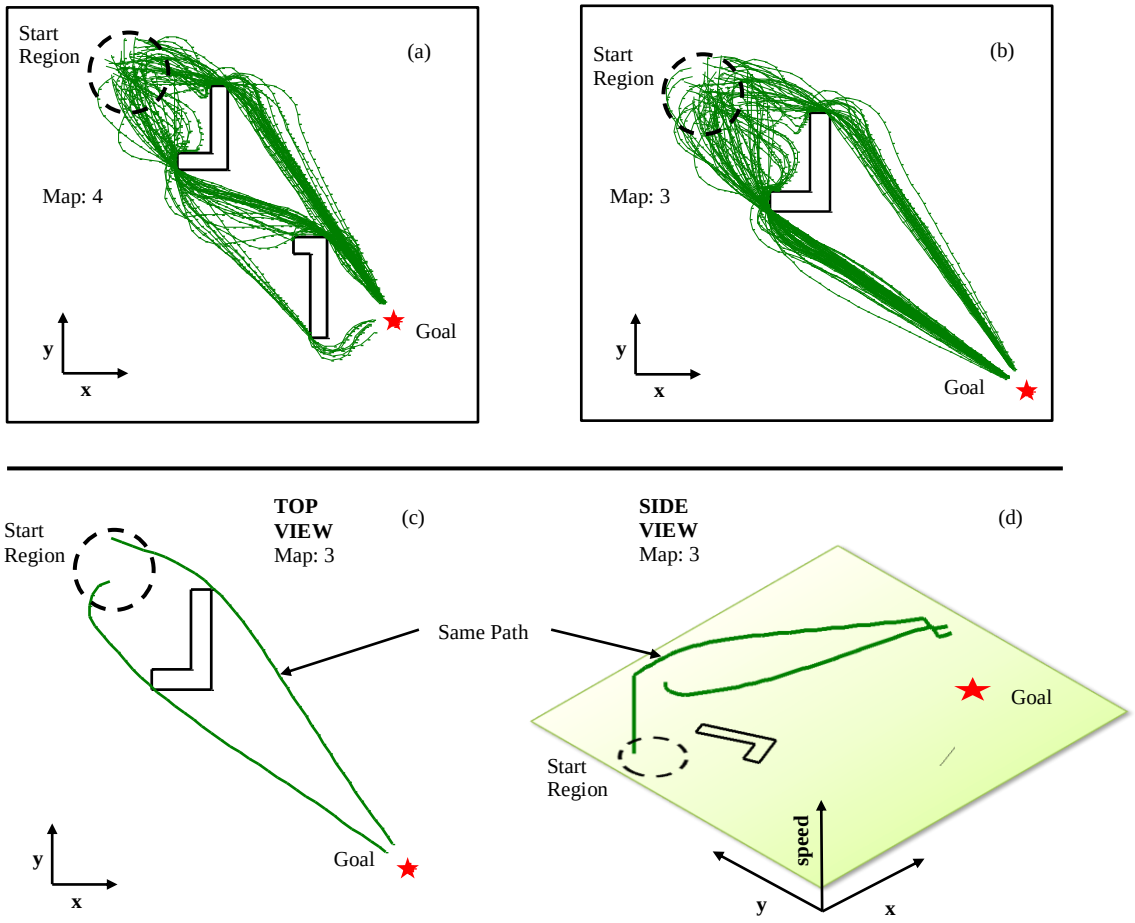


**Figure 3.3** Sample of receding horizon controller paths. Top: Path data from maps three (a) and four (b), for zero delay. Bottom: Two receding horizon controller paths. In (c) a top view is shown and in (d) the side view shows vehicle speed; the controller dictates travel at constant speed most of the way to the goal.

To compare the performance of the receding horizon controller to humans, the same 4 ICs given to humans were tested on the receding horizon controller as well. The results are shown in Figure 3.4. A 2 controller (receding horizon controller vs human) X 3 delay ANOVA was run on the success rate and on the completion time. For the mean completion time of the successful runs, there was a significant main effect of controller ($F(1, 76)=166.93$, $p<.001$), of the delay ($F(2, 76)=21.89$, $p<.001$), and an interaction between the two factors ($F(2, 76)=26.31$, $p<.001$). For the success rate, there was a main effect of controller ($F(1, 90)=15.88$, $p<.001$), of the delay ($F(2, 90)=7.32$, $p<.001$), and a significant interaction between the two factors ($F(2, 90)=4.56$, $p<.01$). This data showed that overall humans are slower than the receding horizon controller but have a higher success rate in reaching the goal without collision. Moreover, humans were less affected by the delay than the receding horizon controller.

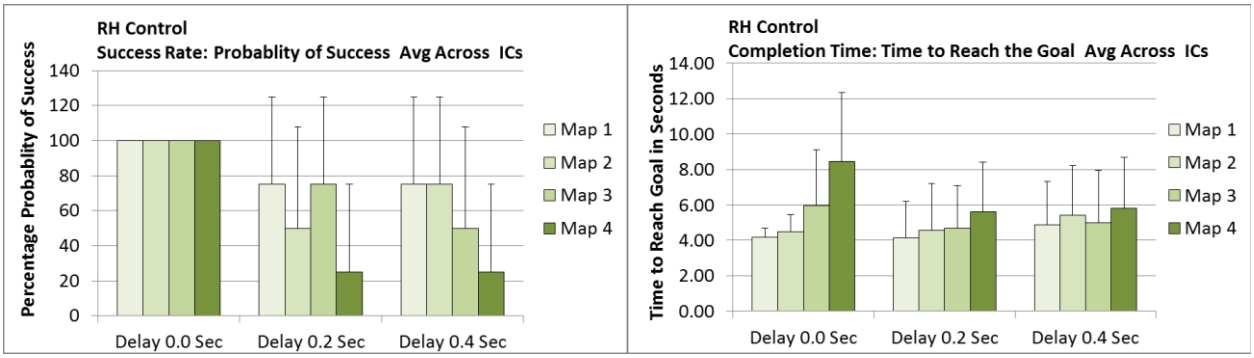


**Figure 3.4** Receding horizon controller success rate and completion time data. Data averaged across ICs for each map. The error bars show one standard deviation of the data for each of the four human ICs.

A careful examination of the data showed that the types of paths chosen by the humans were different from those chosen by the receding horizon controller. Figures 2.4 and 3.3 c and d reveal that humans did not tend to drive at maximum speed all the time, while they did tended to choose paths that swept wide around obstacles. The optimizing receding horizon controller tended to choose aggressive paths that called for rapid movements, high speed, and close approaches to obstacles. These paths were exactly the kind of aggressive paths we expected to see from a controller trying to minimize time to reach the goal, as was the receding horizon controller. The time to reach the goal, averaged across all maps, was almost 2 seconds faster for the receding horizon controller than for the human.

# Chapter 4

# Designing a Human Inspired Receding Horizon Controller

Because of the success rate disparity, and because the original receding horizon controller paths were different from their human counterparts we set out to train a new human-like receding horizon controller that would capture some of the features observed in the human paths. This was a much more complex task than designing a path following controller. The new human-like controller was trained not to follow human paths but to behave like the human, selecting similar paths and strategies when given similar circumstances.

The training of a human-like receding horizon controller started with the basic receding horizon controller from Chapter 3 which nominally drove the vehicle toward the goal without collision. Then a collection of weighting terms (that are functions of parameters $\Theta$), which were adjusted by the training algorithm, were added to the objective function. The weighting terms were designed with the generation of human-like behavior in mind. The range over which the parameters produced acceptable results was determined before training began. For each setting of the parameters, the human-like controller drove the vehicle toward the goal, the generated path was compared to the human path being trained against, and an error for that parameter set was calculated. The goal of training was to minimize this error. The performance of the trained human-like receding horizon controller is compared to the original receding horizon controller and to the humans' own paths in Chapter 6.

## 4.1. Structure of the Human-Like controller

The difference between the original receding horizon controller and the human-like controller was in the objective function. All other constraints and parameters remained similar. The original objective function, $J_N = V(x_{k+N|k})$, was expanded to include the new objective function weighting terms which themselves were dependent on one or more parameters. Developing the correct weighting terms was crucial to the success of the training process. First, the human data was examined and three main characteristics of the human behavior that differed from the receding horizon controller were identified. These behaviors were speed limiting, stop-to-turn, and sweeping wide around obstacles. Second, weighting terms for the objective function which resulted in human-like behavior from the receding horizon controller were designed. The following discussion in Sections 4.1.1 – 4.1.3 explains the underlying motivation behind the weighting terms' construction.

### 4.1.1 The Speed Limit Weighing Term

The original receding horizon controller frequently drove the vehicle at the maximum speed because its objective was to minimize the distance-to-goal on each computation horizon. It is observed that humans often chose not to drive as quickly as the controller, frequently selecting speeds bellow the maximum. In order to give the receding horizon controller a chance to adopt human-like speeds, a speed limit weighing term was added to the objective function. Unlike a constraint, such as "no obstacle collisions," which must always be satisfied, a weighing term is one of several competing values in the receding horizon controller objective. The relative importance of this weighing term and the shape of its interaction with the chosen velocity command were both controlled by a parameter. This flexibility meant the training algorithm could iteratively 'zero in' on parameter values that best approximated the behavior of the human path being used for training. The speed limiting weight was designed around a sigmoid function which steeply increases the penalty for speeds above the speed limit, $\Theta_2$. The multiplier, $\Theta_1$, adjusted how much penalty was assessed. Thus, the Speed Limit weighting term took the following form:

$$\sum_{k=1}^{N} \frac{\Theta_1}{1+e^{-c_1(v_k-\Theta_2-c_2)}}$$

In Figure 4.1 a human path that exhibits variable speed is shown along with the sigmoid function and the desired effect on the human-like receding horizon controller's path.

### 4.1.2 The Obstacle Avoidance Weighting Term

Many human paths exhibited a tendency to sweep wide around the obstacles. On the other hand, the receding horizon controller tended to drive aggressively close to the obstacle vertices, see Figure 3.4. To give the human-like

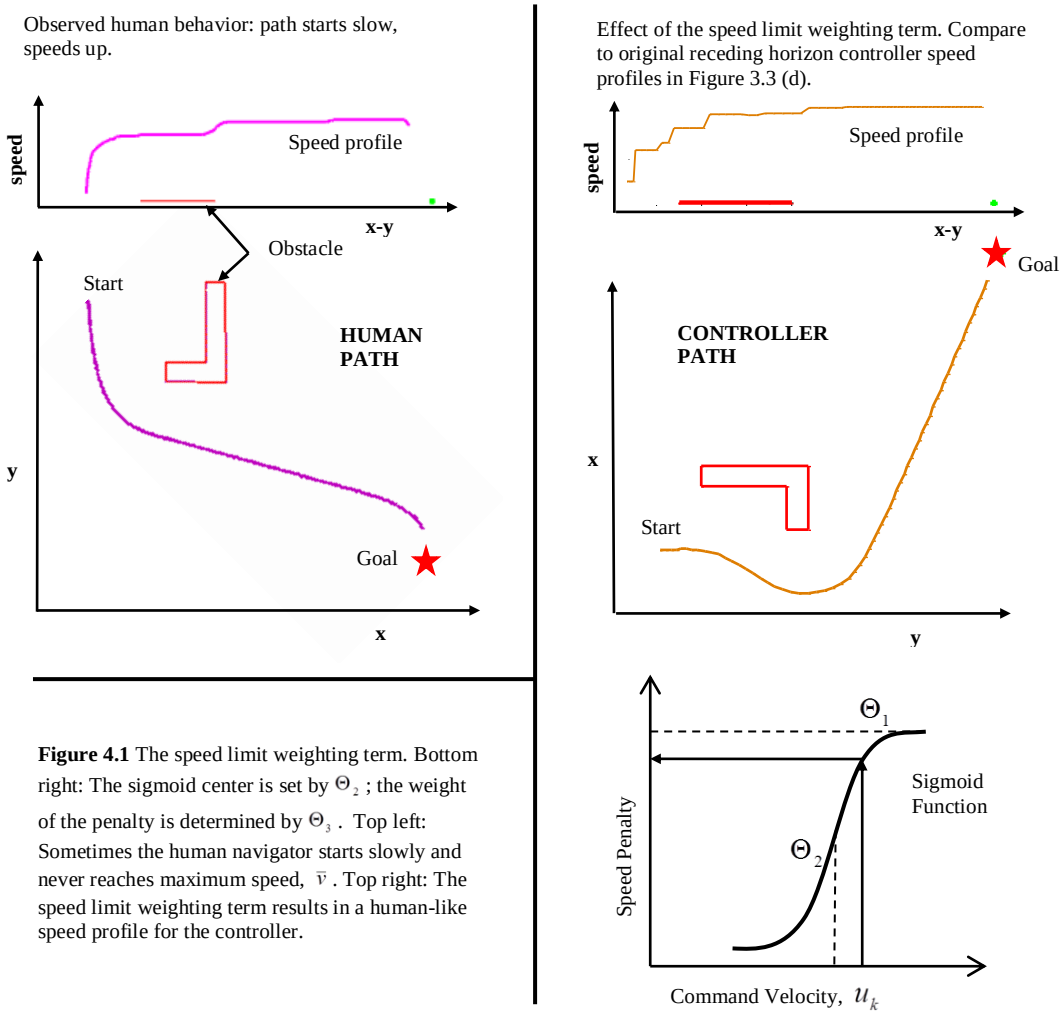


**Figure 4.1** The speed limit weighting term. Bottom right: The sigmoid center is set by $\Theta_2$; the weight of the penalty is determined by $\Theta_3$. Top left: Sometimes the human navigator starts slowly and never reaches maximum speed, $\bar{v}$. Top right: The speed limit weighting term results in a human-like speed profile for the controller.

controller the ability to learn from and imitate the human's more cautious behavior, an Obstacle Avoidance weighing term was designed which penalizes nearness of approach to obstacles in order to produce human-like avoidance behavior:

$$\text{Obstacle Penalty}(x_k, \Theta_4) = \left( \max\left(0, \frac{\Theta_4 - \text{distance to obstacle}}{\text{distance to obstacle}}\right)\right)$$

$$\text{The Obstacle Avoidance weight: } \Theta_3 \sum_{path} \text{Obstacle Penalty}(x_k, \Theta_4)$$

Like the Speed Limit weighing term, the Obstacle Avoidance weighing term is composed of two parameters. The first parameter, $\Theta_4$, governed how close to the obstacle the controller could drive without incurring any penalty.

The penalty started at zero when the vehicle is distance $\Theta_4$ from the obstacle, and asymptotically increases toward infinity at the wall. The second parameter, $\Theta_3$, governed how rapidly the penalty increases as the vehicle approached the obstacle. For example, a high $\Theta_4$ and low $\Theta_3$ meant the vehicle would begin taking the obstacle into account while it was far away but did not experience an urgent need to steer clear until it got closer. The relative nature of this language was consistent with how the weights in the objective function traded against each other based on the relative size of their respective parameters.

The Obstacle Avoidance weight, as a function of vehicle position on map 4, is plotted in Figure 4.2. The obstacles appear as mountains with a radius of $\Theta_4$. Also shown is a human path that sweeps around the obstacle and two receding horizon controller paths, illustrating the effect of the weighting term.

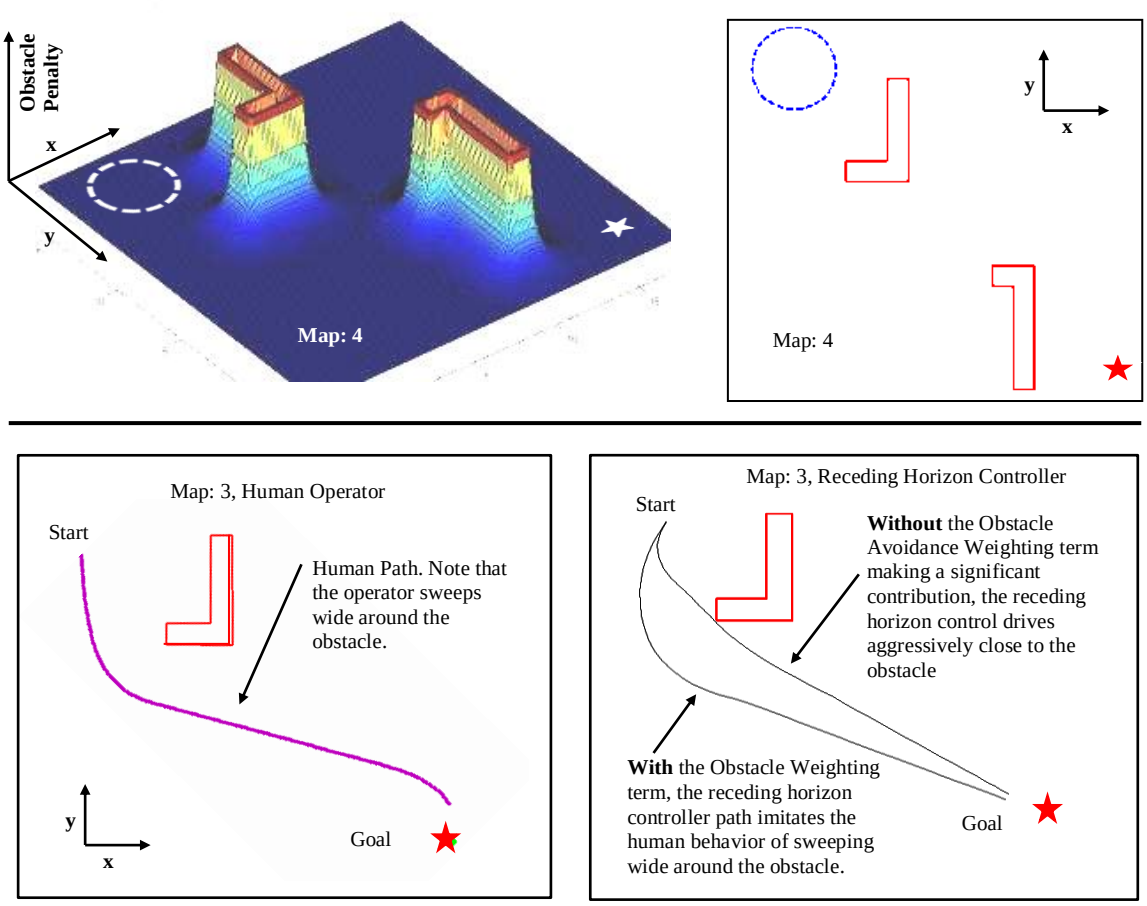


**Figure 4.2** The Obstacle Avoidance weighting term. Top: The Obstacle Avoidance weight appears as a mountain in the objective function. Bottom left: Observed human behavior. Bottom right: The simulation shows the effect of larger parameters $\Theta_3 \& \Theta_4$, which result in a more human-like sweeping path around the obstacle.

### 4.1.3 The Stop-to-Turn Weighting Term

Many human paths exhibited a tendency to stop before executing a turn. A study of this phenomenon and possible explanation are offered in Chapter 7. The original receding horizon controller almost never chose to stop before executing a turn: instead, it drove nearly full speed while turning. To give the trained human-like controller an opportunity to imitate this human tendency, a weighting term was developed which can produce this behavior. The Stop-to-Turn weighing term multiplied the forward velocity command with the turning command; if $\Theta_5$ is large, the human-like controller was strongly encouraged to stop forward motion before it executed a turn. Thus, the Stop-to-Turn weighting term is given by the following:

$$\Theta_5 \sum_{j=1}^{N} \frac{1}{N} |v_k(j) w_k(j)| .$$

Figure 4.3 illustrated the effect of the Stop-to-Turn weighing term. Human stop-to-turn behavior was shown on the left. The human came to a full stop before executing their turn. On the right, the human-like receding horizon controller with the Stop-to-Turn weighing term was shown producing similar stop-to-turn behavior.

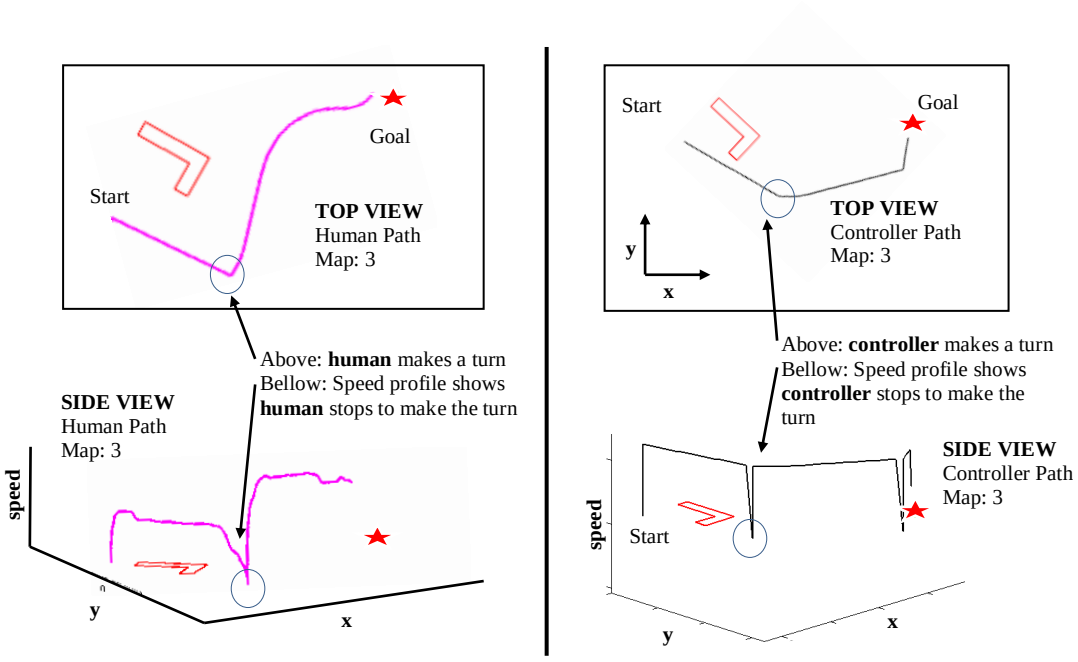


**Figure 4.3** The Stop-to-turn weighting term. Comparison between human behavior, and the impact of the Stop-to-Turn weighting term on the receding horizon controller's path. Left: Observed human behavior. Right: Effect of the Stop-to-Turn weighting term.

## 4.2 The New Human-Like Objective Function

The new human-like receding horizon controller formulation had the same constraints as the original receding horizon controller but the new objective function contained the three weighting terms we developed. The new objective function was formulated as follows:

$$J_N^{\circ}(x_k) = \min_{u_{k+i|k}} \{ J_N(x_{k+i|k}, u_{k+i|k}) : u_{k+i|k} \in U_N, i \in \{1,\ldots,N\} \}$$

$$J_N = V(x_{k+N|k}) + \sum_{k=1}^{N} \frac{\Theta_1}{1+e^{-c_1(v_k-\Theta_2-c_2)}} + \Theta_3 \sum_{path} Obstacle\ Penalty(x_k, \Theta_4) + \Theta_5 \sum_{j=1}^{N} \frac{1}{N} |v_k(j) w_k(j)|$$

The feasibility and convergence guarantees of Chapter 3 were independent of the objective function and still hold for the new human-like receding horizon controller. In Chapter 5 we develop and apply a training algorithm that selects values of the parameters $\Theta_1 - \Theta_5$ based on comparison and training with human path data.

# Chapter 5

# Training the Human-Like Receding Horizon Controller

With the structure of the human-like receding horizon controller established in the previous chapter, we turn our attention to the training of the parameters. The overall training goal was two-fold. The first of goal was to find a collection of parameter sets that characterized all human strategies expressed in the zero delay human path data. This was done by training one human-like controller for each homotopic path group (defined in Section 5.2). The second goal was to find one human-like receding horizon controller realization that best reproduced all human behaviors on all maps. “Best” in the sense of being able to produce automatic behavior with lowest error measured relative to the median human behavior. The criterion for successfully creating a general human-like controller was for that controller to produce paths with lower error relative to median human paths than the average error of all human paths to their own medians. Analysis in Chapter 6 shows that this was achieved.

Since the human data encoded a variety of different human choices and strategies for each scenario, designing a training method was non-trivial. In the following subsections the two-step approach which we adopted is explained. First, a method to capture the human strategy expressed in a single path with a human-like receding horizon controller was developed; second, many human-like receding horizon controllers were trained and evaluated on aggregated human path data; ultimately, the best performer was selected as the final winner.

## 5.1. Training from a Single Human Path

To train the human-like receding horizon controller from a single human path a metric was needed by which to compare the human path and the new path generated by the human-like controller. Comparing two temporally parameterized paths extended in *m*-dimensional space, which have varying velocities, is generally considered a difficult problem and one without a unique solution [56, 57]. Two common path comparison metrics, the Fréchet [58, 59, 60] distance and the Hausdorff [61, 62] distance are maximum distance measures, returning a value based only on the greatest distance between one point on each path. A summing method, such as Dynamic Time Warping (DTW) [63], seemed more appropriate for the purpose of capturing the level of similarity between two paths. DTW works well for matching features between curves that occur at different times by remapping the time domain. Because our scenarios included obstacles, choosing to use a comparison metric that remapped features could return a comparison for paths that were no longer feasible. Thus traditional DTW was not a good choice; this led us to develop a similar integrative method.

The components, or dimensions, of our path data are x-position, y-position, heading, and velocity. One method of comparison was to define the error metric in the x-y plane as the integration of the area between the human path and the human-like receding horizon controller path. Because of the vehicle model constraint, the heading must be tangent to the path; thus this metric would capture a little more than two of the four dimensions. This simple x-y error metric was unsatisfying because velocity data is ignored. Thus to capture the impact of velocity in the error metric, the vehicle path was considered in three spatial dimensions where the third dimension is velocity.

The three-dimensional representation of the path was normalized by placing N points along the path at evenly spaced intervals. A path, such as $path_1$, once it has been uniformly resampled, will be denoted as $path_1^N$. The three-dimensional path distance between any two points was path length/N. This normalization was executed for both paths to be compared and the error metric was defined as the sequential sum of the 3D Euclidian distances between the points of each normalized path.

The path error was defined as follows:

$$PathError(path_1^N, path_2^N) = \sum_{i=1}^{N} \left\| path_1^N(i) - path_2^N(i) \right\|_2 ,$$

where the two-norm for vectors is defined as usual to be $\| x \|_2 = \sqrt{x^T x}$. This error metric has no units and was useful as a comparison not an absolute measure.

A training procedure that adjusts the parameters was formulated around the goal of minimizing the path error between a human training path and the path generated by the controller being trained.

The Training Procedure (see Figure 5.1):

1. Select a human IC and path to use as training data.
2. Select new set of parameters for the human-like controller.
3. Give the human-like controller the obstacles as they were presented to the human and IC where the human training path originates.
4. Run the human-like controller to generate a path to the goal.
5. Compare the human-like controller's path with the actual human path to produce an error value.
6. If number of iterations has reached a maximum exit loop or if error has fallen to threshold value exit loop.
7. Return to step 2.

In this way the training algorithm adjusted the parameters of the weighting terms in the objective function looking for a controller realization that produced a path that well matched the human path. The training was done using the MatLab *patternsearch* function, with the following argument settings: 'CompletePoll', 'on', 'TolFun', 1e-3,' TolCon', '1e-3', 'MaxFunEvals', '200.' The *patternsearch* algorithm is a non-gradient based decent algorithm [64**].** For this experiment the threshold value was set below 1, meaning that the training always ran until the maximum number of iterations had been reached.

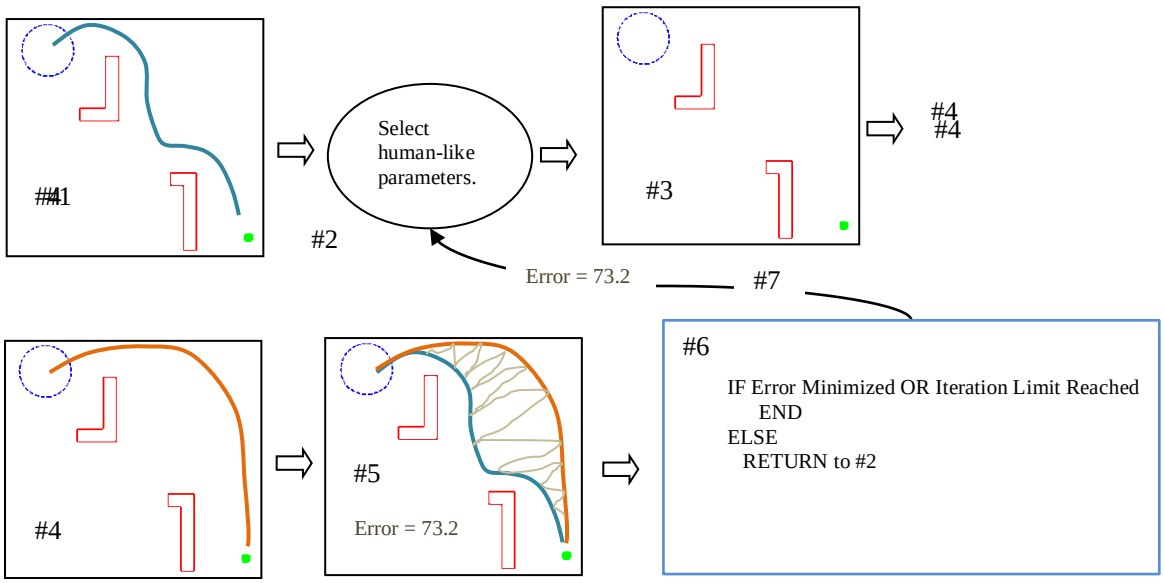


**Figure 5.1** Flowchart showing training process.

## 5.2. Identifying the Homotopic Groups in the Human Data

The human path data was rich in variety; thus determining a reasonable procedure to select the human paths, that would be used as training data required careful consideration. The human paths fell into natural groupings depending on which direction the operator drove around each obstacle. It did not make sense to average together paths where the human operators choose to drive on opposite sides of the same obstacle, as the resulting average path might pass directly through the obstacle even if none of the individual paths did. Paths were thus divided into 'homotopic groups' where all paths per group take the same general route so that any convex weighted combination (average) of the paths in a group was collision-free.

A homotopic group was defined as a collection of paths that followed a similar route to the goal. They were homotopic to each other, meaning they shared the property of being related to each other through continuous collision-free deformations, such as bending and stretching [54]. Thus, as shown in Figure 5.2, with one obstacle there were 2 homotopic groups and with two obstacles there were four homotopic groups.

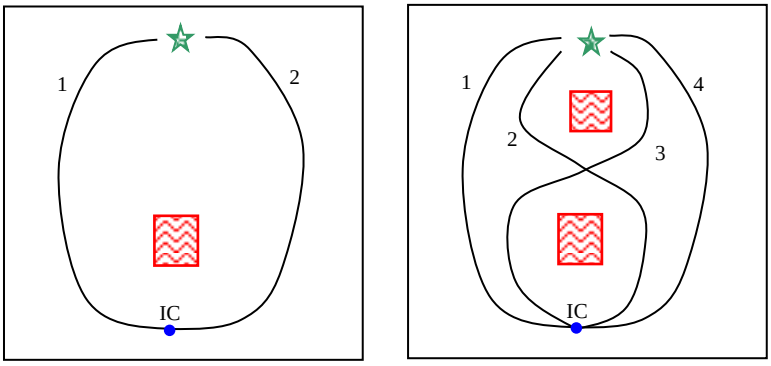


**Figure 5.2** Examples of the homotopic path groups possible for one- and two-obstacle maps.

An example of a homotopic group of human paths is shown in Figure 5.3. To carry out the analysis, all paths were discretized in three spatial dimensions (two position dimensions and velocity) into 200 equally-spaced points. All the paths from a given homotopic group, $N_{T_g}$, were averaged together, point by point, to give the average path, $\tilde{x}^{T_g}(i)$ as,

$$\tilde{x}^{T_g}(i) = \frac{1}{N_{Tg}} \sum_{j=1}^{N_{Tg}} x_j^{T_g}(i)$$

The median human path, $\bar{x}^{T_g}(i)$ was selected as the human path with the lowest summed Euclidian distance between its 200 points and the 200 points of the average path, that is, it had the lowest path error:

$$\bar{x}^{T_g}(i) \equiv x_j^{T_g}(i) \ ,$$

Where $j$ is the argument minimizing:

$$\min_{j \in \{1 \ldots N_t\}} \sum_{i=1}^{200} \left\| x_j^{T_g}(i) - \tilde{x}^{T_g}(i) \right\|_2 .$$

As mentioned earlier, each of our four maps had four initial conditions that were given to the human operators; there were two maps with one obstacle and two maps with two obstacles. Thus there were a total of 48 possible homotopic groups, across the four maps. The human data showed that only 36 of the 48 groups were used (i.e., each of these homotopic groups contained at least one human path that reached the goal). For each of the 36 used groups, a human-like receding horizon controller was trained. The training path was the median human path from each group.

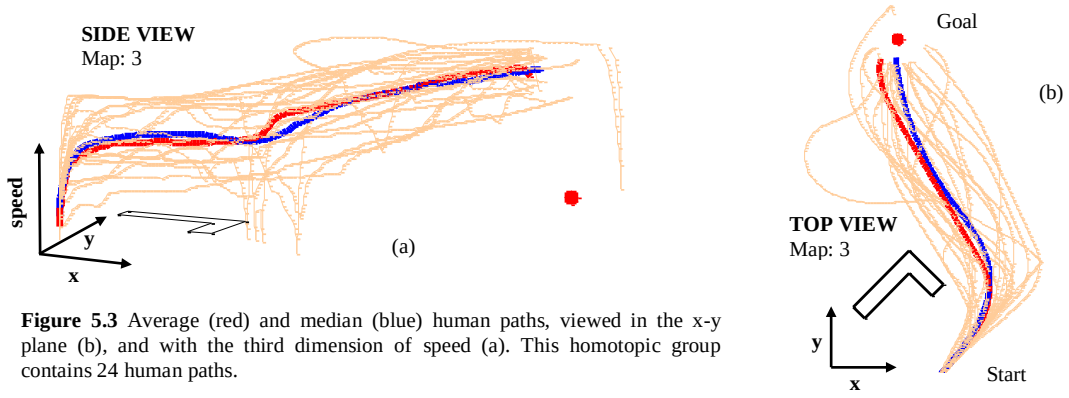


**Figure 5.3** Average (red) and median (blue) human paths, viewed in the x-y plane (b), and with the third dimension of speed (a). This homotopic group contains 24 human paths.

## 5.3. Training a Human-Like Receding Horizon Controller for Each Homotopic Group

Following the procedure outlined in Section 5.1, a human-like receding horizon controller was trained on each of the homotopic groups of the human path data for zero feedback delay. The resulting controller parameter realizations are listed in Table 5.1. The group number on the far left is the homotopic group. The Quality of Fit was the final error between the human-like receding horizon controller path and the human median path being used for training:

$$HL\,RHC_{\text{var}}^{T_g} = \sum_{i=1}^{200} \left\| x_{HL}^{T_g}(i) - \bar{x}^{T_g}(i) \right\|_2 .$$

For the purpose of training, upper and lower bounds $(ub, lb)$ for each parameter were selected based on testing. These values were as follows:

$$lb = [0.75 \ .25 \ \ 0 \ \ 2 \ \ \ 0],$$

$$ub = [3.5 \ \ .8 \ \ 10 \ \ 5.7 \ 8].$$

For each training simulation, the starting value of the parameters was taken to be $P0 = [2.75 \ \ .25 \ 5 \ \ 2.8 \ 0]$.

Figure 5.4 contains three histograms that show distributions for the values of Fit Quality and distributions of the parameter values Obstacle Radius and Stop-to-Turn. In Figure 5.5, the median human paths (blue) and the trained human-like receding horizon controller paths (orange) are shown for six of the homotopic groups.

| group # | Subject | Map | IC | Quality of Fit | obs radius | obs wgt | thr wgt | thr cnt | stop_to_turn |
|---|---|---|---|---|---|---|---|---|---|
| 1 | 13 | 1 | 1 | 380.90 | 0.75 | 0.77 | 8.86 | 2.29 | 0.00 |
| 2 | 6 | 1 | 1 | 301.46 | 2.75 | 0.25 | 9.16 | 3.30 | 0.50 |
| 3 | 12 | 1 | 2 | 392.34 | 0.75 | 0.25 | 0.88 | 3.05 | 0.00 |
| 4 | 9 | 1 | 2 | 175.26 | 3.25 | 0.50 | 8.00 | 2.55 | 0.75 |
| 5 | 6 | 1 | 3 | 340.51 | 2.00 | 0.50 | 8.98 | 3.80 | 3.50 |
| 6 | 5 | 1 | 3 | 84.05 | 1.81 | 0.25 | 6.50 | 2.80 | 0.92 |
| 7 | 14 | 1 | 4 | 231.85 | 1.88 | 0.75 | 7.00 | 2.80 | 0.00 |
| 8 | 11 | 2 | 1 | 484.57 | 1.75 | 0.25 | 4.51 | 4.86 | 0.00 |
| 9 | 12 | 2 | 1 | 773.71 | 1.50 | 0.38 | 7.00 | 2.49 | 2.00 |
| 10 | 8 | 2 | 1 | 189.05 | 2.79 | 0.25 | 6.88 | 2.80 | 0.00 |
| 11 | 12 | 2 | 2 | 329.59 | 1.75 | 0.25 | 2.13 | 2.80 | 1.02 |
| 12 | 14 | 2 | 2 | 216.25 | 2.75 | 0.50 | 6.38 | 3.05 | 0.00 |
| 13 | 6 | 2 | 3 | 398.56 | 1.63 | 0.75 | 3.00 | 4.80 | 4.00 |
| 14 | 12 | 2 | 3 | 559.65 | 0.75 | 0.25 | 10.00 | 2.55 | 0.00 |
| 15 | 14 | 2 | 3 | 204.68 | 2.75 | 0.75 | 5.60 | 2.71 | 0.00 |
| 16 | 12 | 2 | 4 | 548.56 | 1.00 | 0.38 | 7.70 | 3.05 | 0.00 |
| 17 | 5 | 2 | 4 | 251.88 | 3.48 | 0.27 | 3.97 | 2.30 | 0.00 |
| 18 | 6 | 3 | 1 | 956.46 | 1.75 | 0.25 | 8.97 | 4.80 | 0.00 |
| 19 | 8 | 3 | 1 | 117.13 | 2.81 | 0.50 | 4.93 | 2.18 | 0.00 |
| 20 | 4 | 3 | 2 | 370.82 | 1.75 | 0.25 | 1.50 | 2.80 | 2.42 |
| 21 | 5 | 3 | 2 | 273.77 | 1.75 | 0.25 | 9.75 | 2.05 | 0.00 |
| 22 | 8 | 3 | 3 | 449.25 | 1.88 | 0.25 | 7.50 | 4.30 | 3.75 |
| 23 | 14 | 3 | 3 | 172.36 | 3.50 | 0.75 | 3.19 | 2.86 | 0.08 |
| 24 | 14 | 3 | 4 | 228.02 | 1.75 | 0.38 | 5.88 | 2.74 | 0.00 |
| 25 | 10 | 4 | 1 | 298.48 | 3.25 | 0.25 | 9.97 | 2.30 | 0.52 |
| 26 | 15 | 4 | 1 | 482.13 | 1.75 | 0.25 | 5.00 | 4.68 | 0.94 |
| 27 | 5 | 4 | 1 | 454.70 | 2.72 | 0.25 | 6.00 | 3.80 | 0.00 |
| 28 | 6 | 4 | 2 | 216.96 | 3.00 | 0.25 | 6.19 | 2.55 | 0.05 |
| 19 | 14 | 4 | 2 | 510.29 | 1.75 | 0.25 | 7.75 | 2.55 | 0.00 |
| 30 | 14 | 4 | 2 | 485.86 | 2.75 | 0.25 | 4.98 | 3.27 | 0.03 |
| 31 | 6 | 4 | 3 | 379.49 | 1.75 | 0.38 | 8.13 | 3.80 | 3.25 |
| 32 | 15 | 4 | 3 | 974.82 | 1.75 | 0.25 | 4.50 | 3.80 | 2.00 |
| 33 | 14 | 4 | 3 | 398.37 | 2.22 | 0.50 | 6.00 | 3.74 | 0.02 |
| 34 | 9 | 4 | 4 | 1193.03 | 0.75 | 0.25 | 8.98 | 2.80 | 0.00 |
| 35 | 10 | 4 | 4 | 458.97 | 2.25 | 0.25 | 5.74 | 2.80 | 0.00 |
| 36 | 14 | 4 | 4 | 401.62 | 2.75 | 0.28 | 7.00 | 3.82 | 0.00 |

**Table 5.1** This table shows the parameter values for the 36 controllers trained on the median human paths from the 36 homotopic groups of human paths data.

As shown in the histogram in Figure 5.4, most of the trained controllers resulted in a Quality of Fit roughly equal to 400. Homotopic groups 3 and 13 (from Figure 5.5) both had fit qualities close to 400. It should be noted that the groups in 5.5 did not show the third dimension of velocity, which did impact Quality of Fit. Group 34 is presented as an example of the worst Quality of Fit among all the trained controllers.

The Stop-to-Turn parameter was frequently not expressed (trains to zero), but when it is, there are two modes, high and low. This modality suggested that humans either drove smoothly or drove with a stop-and-go strategy. Group 13, shown in Figure 5.5, had the highest Stop-to-Turn parameter value of any trained human-like receding horizon controller; the effect was seen in the sharp angular path.

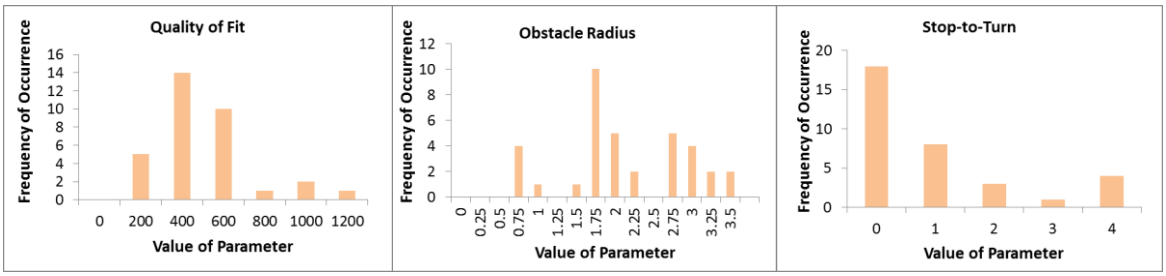


**Figure 5.4** Distribution of parameter values from the full training. Data from Table 5.1.

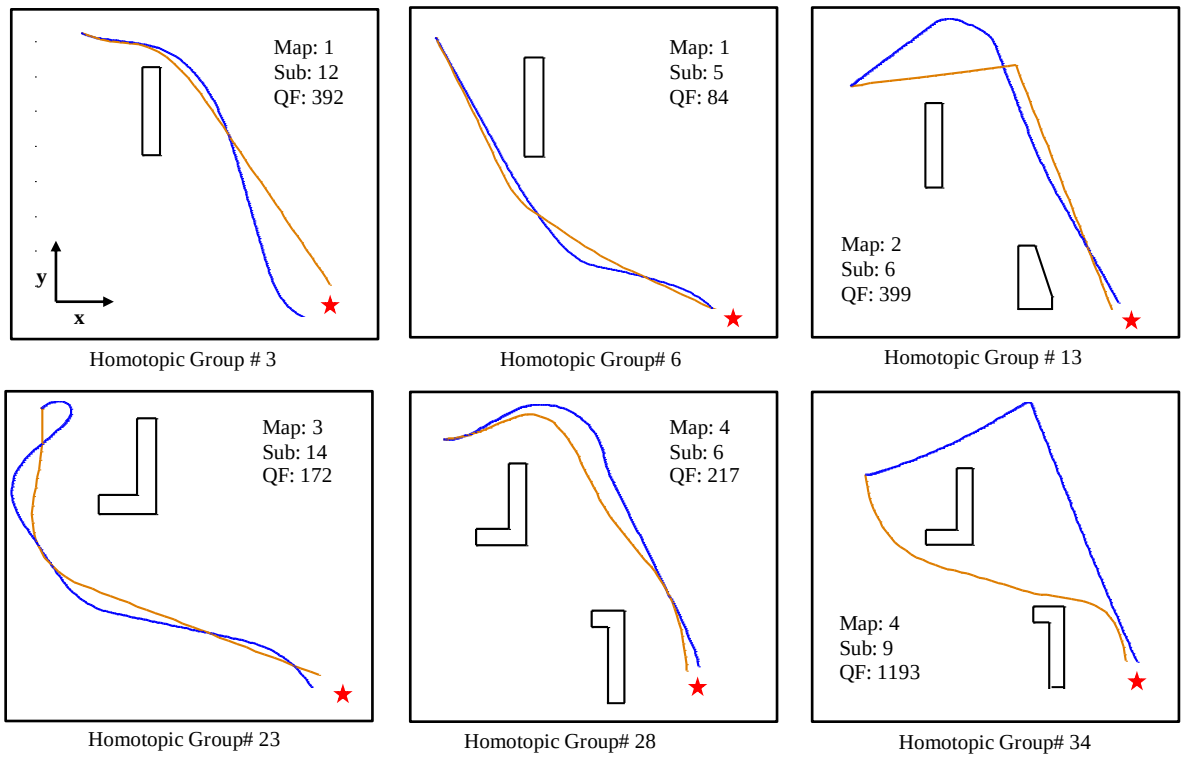


**Figure 5.5** Representative selections of trained human-like controllers. Shown are paths generated by 6 of the 36 trained human-like controllers from Table 5.1. Human-like receding horizon controller paths (orange) were each trained to the median human path (blue) from a homotopic group. QF stands for Quality of Fit.

## 5.4. Selecting the "Best" Human-Like Receding Horizon Controller

To identify a single "best" human-like controller, the 36 trained controllers were graded against one another and then given a performance test with the simulator and graded again. First 16 controllers were selected by keeping only the human-like realization that had the best Quality of Fit for each initial condition (there were 4) and each map (there were 4). The finalist controllers are highlighted in blue in Table 5.1. Re-tabulating the histograms for just the 16 finalist controllers resulted in Figure 5.6.

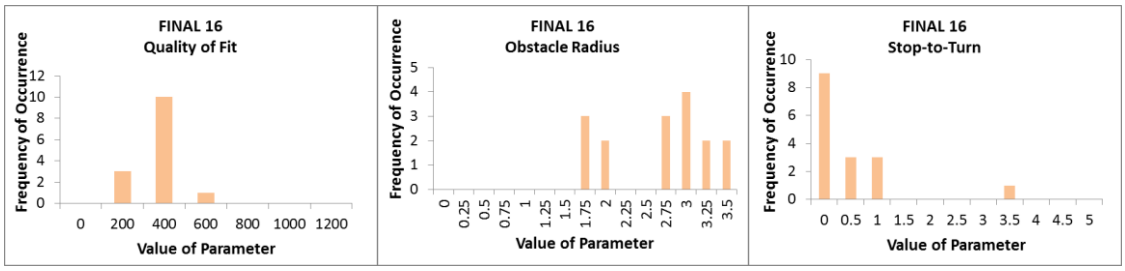


**Figure 5.6** Distribution of parameter values for the 16 finalist human-like receding horizon controllers. Data from the blue-highlighted rows of Table 5.1.

The 16 finalist controllers were then each run from the 4 ICs on all 4 maps. The controller's path error was computed relative to the human median path that resulted in the lowest error. That is, each finalist controller path was compared to the nearest human median path. The overall performance of each finalist controller was measured as its average error across all 16 of its runs. The winning controller was the controller with the lowest overall error. This was the controller which most consistently produced behavior that matched at least one human median solution for each map and IC combination.

All the computations were carried out on a main frame computer using multithreaded Matlab. The winning controller was the one trained on homotopic group# 28; the path was shown in figure 5.5. This winning controller will be called the human-like receding horizon controller.

## 5.5. Simulation Results for the Human-Like Receding Horizon Controller

To compare the human-like receding horizon controller to the humans and the original receding horizon controller, paths were generated on each map for each delay. Some paths from maps three and four were shown in figure 5.7. To compare to the humans, the same 4 ICs given to humans were tested on the human-like controller. The completion time and success rate for this test is displayed in Figure 5.8.

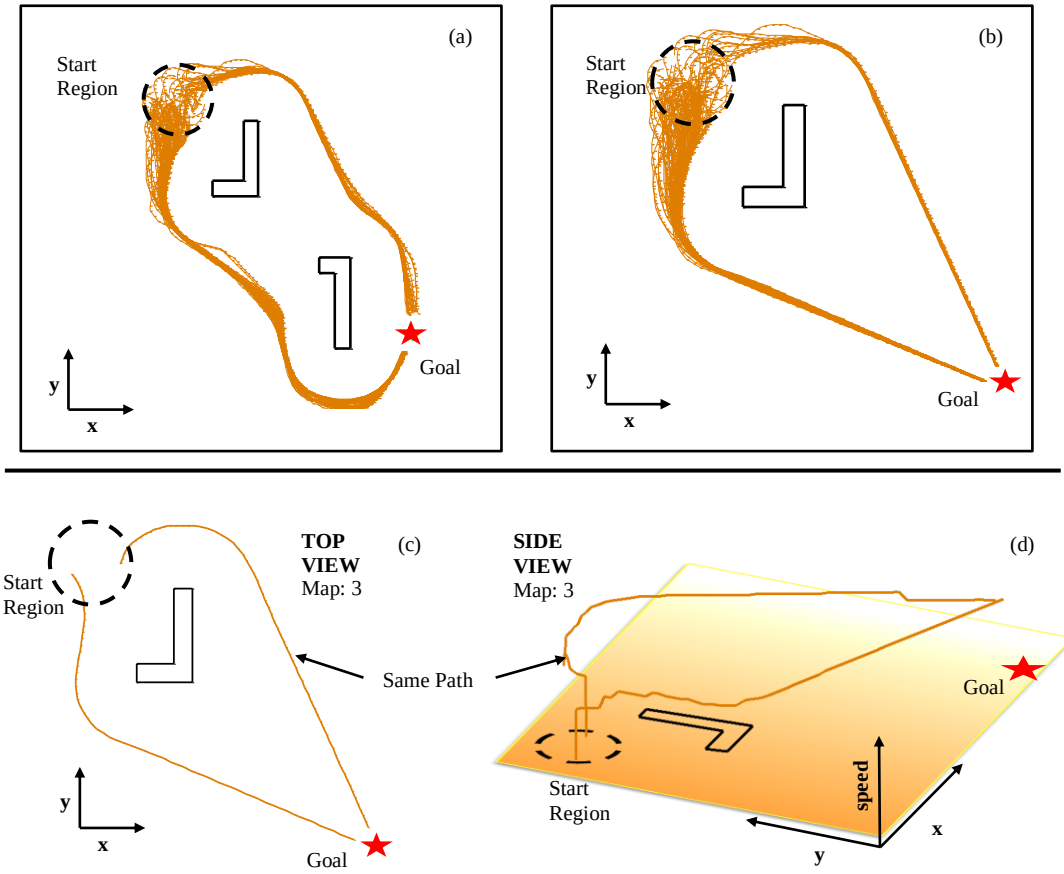


**Figure 5.7** Paths from the human-like receding horizon controller (the controller trained on human data from homotopic group #28). Above: (a) & (b) show zero delay paths when starting from same region given to humans. Bellow: (c) & (d) show two paths from map 3.

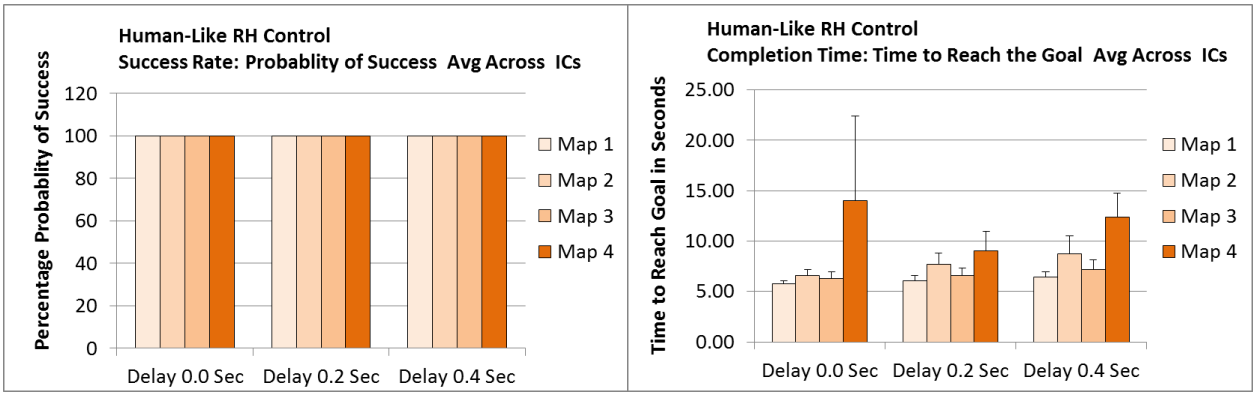


**Figure 5.8** Human-like receding horizon controller success rate and completion time data. Data for the human-like receding horizon control started from each of the four human ICs. Data is averaged across ICs for each map. The error bars showed one standard deviation of the data for each of the four human ICs. Note that success rate is 100% even for high delay.

# Chapter 6

# Analysis of the Human and Automatic Controllers

In this chapter we provide analysis of the paths chosen by the automatic controller and the human operators. We also provide additional between controller performance analysis based on the success rate and completion time metrics. Two goals were presented in Chapter 1. The first goal, to formulate a provably feasible and provably convergent controller that handles the same general navigation task given to humans, was accomplished in Chapters 2 & 3. The success in achieving the second goal, training the baseline controller to perform the navigation task in a human-like way, is analyzed in Sections 6.1 & 6.2. A quantitative comparison is made among the paths taken by humans, the original receding horizon controller and the human-like controller and it is shown that the human-like receding horizon controller is more robust than the original receding horizon controller.

## 6.1. Analysis of the Controller Paths

One way of comparing the controllers to one another was to assess the similarities and differences between the paths they generate for the same initial conditions on the same scenarios. Because this is fundamentally different than comparing the controllers based on their relative performance, as done in Subsection 6.2, this path analysis gives an additional degree of insight.

For each initial starting point that had been given to the humans, the original controller and the human-like controller were allowed to generate their own path to the goal. The controller's path would follow one of the available homotopic path groups from that IC to the goal. The path variance (or error) was defined as the difference

between a path taken by the controller (receding horizon or human-like receding horizon) and the median human path from the same homotopic group. The human's own path variance (or error), $H_{\text{var}}^{T_g}$, for a given homotopic group was computed as follows:

$$H_{\text{var}}^{T_g} = \frac{1}{N_{T_g}} \sum_{j=1}^{N_{T_g}} \sum_{i=1}^{200} \left\| x_j^{T_g}(i) - \bar{x}^{T_g}(i) \right\|_2 .$$

This was a measure of the variability between the human median paths and all the other human paths from the same homotopic group. For humans, this was averaged across the homotopic groups originating from a given IC. Figure 6.1 shows the three comparisons side by side.

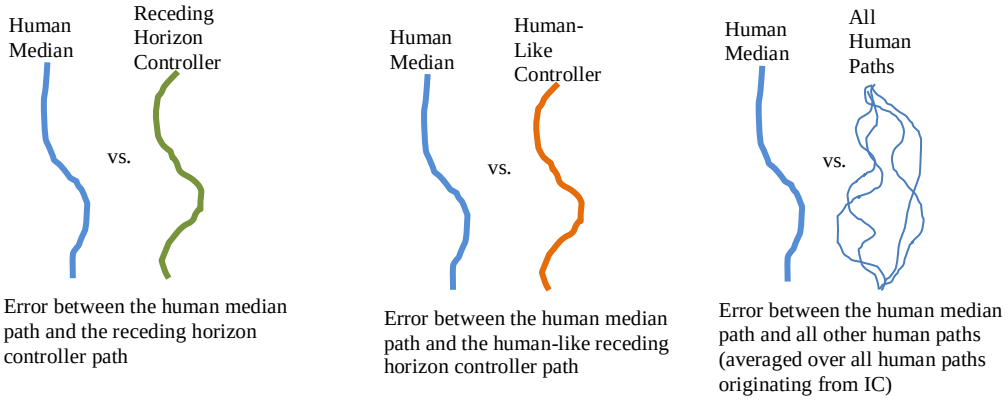


**Figure 6.1** This cartoon illustrates the three types of path comparisons discussed in the text. Each comparison was made within a homotopic group and the values rendered by these comparisons are shown in Table 6.1.

This comparison was carried out for each IC on each map, meaning that each of the three comparisons generates a total of 16 values. These are shown in Table 6.1 and plotted in Figure 6.2. A 3 controller (human, receding horizon, and human-like receding horizon) X 3 delay ANOVA on the path errors showed a significant main effect of controller ($F(2, 121)=30.48$, $p<.001$), a main effect of delay ($F(2, 121)=17.86$, $p<.001$), and significant interactions between the two factors ($F(4, 121)=5.29$, $p<.001$). A pair-wise comparison of the path errors between human vs. human-like receding horizon controller showed a significant main effect of delay ($F(2, 90)=29.45$, $p<.001$) and controller ($F(1, 90)=58.40$, $p<.001$), and an interaction between controller and delay ($F(2, 90)=4.19$, $p<.05$). For human vs. receding horizon controller, there was a marginal effect of controller ($F(1, 76)=3.23$, $p<.08$), a significant effect of delay ($F(2, 76)=21.28$, $p<.001$) and interactions between controller and delay ($F(2, 76)=17.85$, $p<.001$). Specifically, the path error for the receding horizon controller was significantly larger than those of humans when there was zero delay ($t(30)=3.21$, $p<.01$). However, when there was a delay the trend was reversed ($t(48)=3.80$, $p<.001$). Finally, a comparison between receding horizon control and human-like receding horizon control showed a significant effect of controller ($F(1, 76)=19.15$, $p<.001$), but no effect of delay ($F(2, 76)=2.15$, $p=.12$) or interactions ($F(2, 76)=1.26$, $p=.29$).

| Error Relative to the Median Human Paths | | | | |
|---|---|---|---|---|
| map | IC | Humans | RHC | HL RH Controller |
| 1 | 1 | 403 | 443 | 361 |
| 1 | 2 | 478 | 524 | 230 |
| 1 | 3 | 467 | 355 | 155 |
| 1 | 4 | 357 | 497 | 317 |
| 2 | 1 | 467 | 689 | 496 |
| 2 | 2 | 327 | 550 | 276 |
| 2 | 3 | 420 | 663 | 213 |
| 2 | 4 | 405 | 557 | 307 |
| 3 | 1 | 400 | 593 | 155 |
| 3 | 2 | 300 | 260 | 386 |
| 3 | 3 | 417 | 633 | 333 |
| 3 | 4 | 369 | 420 | 266 |
| 4 | 1 | 347 | 706 | 342 |
| 4 | 2 | 285 | 531 | 217 |
| 4 | 3 | 440 | 1000 | 461 |
| 4 | 4 | 352 | 674 | 488 |
| | Average: | 390 | 568 | 313 |

**Table 6.1** Path errors relative to human median.

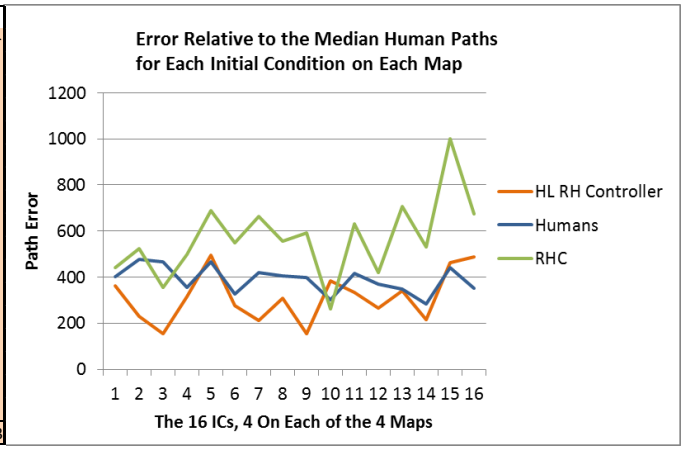


**Figure 6.2** Plot of the data in Table 6.1.

Taken together, the analysis showed that when there was zero delay, the paths generated by the human-like receding horizon controller were closer to the human median path than other human paths, while the original receding horizon controller generated paths farther away from the human median path. These results suggest that the weighting functions designed in Section 4 to capture human like path characteristics were, by this measure, successful in creating human-like paths. However, humans were more affected by the delay than both the original and the human-like controllers, generating paths more dissimilar to their own zero delay median paths than the two controllers did. These results suggest that the characteristics of human steering captured by the controllers trained with the zero delay condition may not generalize to the delay trials.

## 6.2 Analysis of the Controllers' Performance

In training the human-like controller the goal was to produce paths that were similar to the human paths. The design of the weights and the training algorithm considered this as the only objective. Success rate and completion time were never explicitly mentioned and no objective function terms were designed to capture these characteristics. Now the question remains, does the human-like controller which is capturing human-like path behavior (shown in Subsection 6.1), show signs of being human-like in its performance as well?

The performance data for all three controllers is presented in Figure 6.3. For each delay, the data for each controller has been averaged across all maps. A 2 controller (human vs. human-like receding horizon) X 3 delays ANOVA was run on the success rate and on the mean completion time. For the success rate, there was a significant effect of controller ($F(1, 90)=43.80$, $p<.001$), of the delay ($F(2, 90)=13.13$, $p<.001$), and an interaction between the two factors ($F(2, 90)=13.13$, $p<.001$).For the mean completion time, there was a significant main effect of controller ($F(1, 90)=23.40$, $p<.001$), of the delay ($F(2, 90)=17.71$, $p<.001$), and an interaction between the two factors ($F(2, 90)=11.10$, $p<.001$).

To compare receding horizon controller to human-like receding horizon controller, a 2 controller (original receding horizon controller vs. human-like receding horizon controller) X 3 delays ANOVA was run on the success rate and on the mean completion time. For the mean completion time, there was a main effect of controller ($F(1, 76)= 17.95$, $p<.001$), but no effect of the delay ($F(2, 76)=.90$, $p=.41$), and no interaction between the two factors ($F(2, 76)=.22$, $p=.80$). For the success rate, there was a significant effect of controller ($F(1, 90)=23.33$, $p<.001$), of the delay ($F(2, 90)=5.83$, $p<.01$), and an interaction between the two factors ($F(2, 90)=5.83$, $p<.01$).

This analysis shows that the human-like receding horizon controller out-performed the human operators, both in terms of time to reach the goal and in terms of percentage of successful runs. The trained human-like controller was also more tolerant of the delay than the human operators. When compared with the original controller, the human-like receding horizon controller was significantly better in terms of success rate and was less affected by the delay, although it was significantly slower in time to reach the goal. Thus by training the objective function, but without explicitly considering delay, we realized an increase in success rate compared to the original controller.

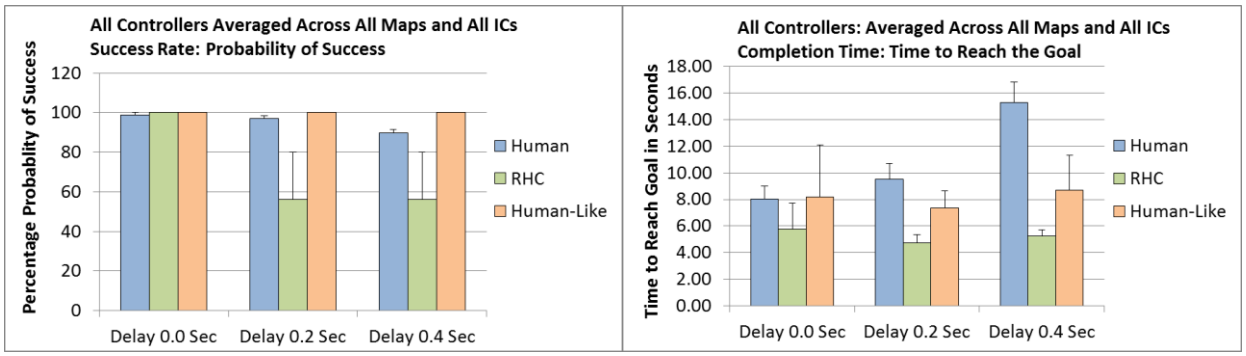


**Figure 6.3** Performance data showing success rate and completion time for the human, receding horizon controller, and human-like controller. The data has been averaged across maps. Error bars show one standard deviation of the across map average.

## Chapter 7

# Analysis of the Human Data as a Function of Delay

In previous chapters we have studied human performance in the context of other controllers and used Feedback Delay as one of 3 independent variables. These variables are as follows: number of obstacles (2 values), type of obstacle (2 values), and amount of feedback delay (3 values). Our approach was to use the zero delay human data to train a human-like automatic controller and then compare the success rate, completion time, and path similarity between the human's and our human-like controller's paths. The delay was treated as an important independent variable that allowed us to inject regulated amounts of uncertainty into the system to see how the zero-delay trained controller would react or to see how the humans themselves would react. The perspective of our investigation was to look at delay as a disturbance to our zero delay models and humans. Now we shift our perspective and consider the impact of delay explicitly on the human operators. Looking at all of the human data (collapsed across number and type of obstacle) and considering the independent variable to be delay, we quantify its impact on human performance and human strategy. We also offer suggestions to the researcher and practitioners that can help them make design tradeoffs and understand the impact of delay on their remotely navigated human in-the-loop systems.

### 7.1 Cataloging and Interpreting the Effect of Feedback Delay

In Sections 7.2 and 7.3 we look at the effect of delay on the human operator's performance from five different perspectives. The analysis catalogues the impact of feedback delay on the human navigator's performance and fits models to this interaction. The delays we consider are the same used in previous chapters: 0, 0.2 and 0.4 seconds. These delays are similar to the kind of latency founded on the public internet. See Table 7.1.

| Country | Server | RTT |
|---|---|---|
| Afghanistan | flag.ep.net | 71ms |
| China | 7x24.cn | 272ms |
| Africa | joburg.org.za | 118ms |
| S. Korea | visitkorea.or.kr | 220ms |

**Table 7.1** Round trip times for packet "pings" recorded on 3/18/2011 from the Coordinated Science Laboratory, University of Illinois at Urbana-Champaign.

The public internet latencies are noted because it is easy to envision a human operator remotely navigating a vehicle on a connection with similar latency. It is noted in [19] that round trip communication to a satellite in orbit is about 0.4 seconds; this is relevant because some remotely piloted vehicles include satellite links in their communication networks. For each of the five delay impact studies in Section 7.3, we provide a practical connection between the esoteric metrics we define and real world applications of interest to practitioners.

In section 7.4 we explain why human operators choose to stop the vehicle more often as delay increases. We show that this is related to a loss of control by comparing the vehicle heading errors that occurred directly before and after stops. This conclusion matches other work which found human's stopping to wait for delayed commands to purge from the system [26]. This provides inspiration for a method of dealing with delay in the receding horizon control implantation which is discussed in Section 7.5 and further in Chapter 8.

## 7.2 Methods and Analysis Technique

The statistical analysis provided in Section 7.3 answers the question: What order model is statistically significant for the data? The data is presented in part in Table 7.3 and in full in Appendix B. The analysis results for significance of model fit was run on the data in Appendix B after averaging the data by subject. This means there were 11 data points for each metric for each delay case. The analysis was run using SYSTAT. The figures showing the raw data and model fits were created in MATLAB and are based on the full data set. For those who may not be familiar with determining the significance of regression parameters, a detailed explanation is presented in Appendix A.

## 7.3 Data and Analysis for the Five Effects

The human path data collected across three delays was processed from 5 different points of view and the results are presented in the following sub-sections. In each case a metric was defined to capture the dependent variable of interest, then code was written to process the data according to the metric. The data was then analyzed using the statistical methods described in Section 7.2. The analysis revealed linear or quadratic trends in the effect of the feedback delay on the metrics. The variables are organized by type (discrete/continuous) in Table 7.2.

| |
|---|
| **Dependent Variables:**<br>Average Success Rate (**)<br>Average Completion Time (*)<br>Average Path Error (*)<br>Number of Stops (**)<br>Average Heading Error(*)<br>**Independent Variable:**<br>Feedback Time Delay(**)<br><br>*Domain: (*) continues, (**) discrete.* |

**Table 7.2** List of dependent and independent variables and their domain type.

A sample of the data produced by applying the metric to each scenario is given in Table 7.3. Each line of data shown in the table corresponds to a particular human subject attempting a particular scenario. A scenario is defined by map-type, Feedback Delay, and initial condition. For each scenario each subject was given the chance to drive the vehicle twice, thus generating two paths. The data for each line in the table is a sum or average over the two paths generated by the human operator for that particular scenario.

| | A | B | C | D | E | F | G | H | I |
|---|---|---|---|---|---|---|---|---|---|
| Notes: | Each line of data represents two human path attempts. Total Successful indicates how many of these attempts were successful. | | | | | | If this column is "0" dependant data will be listed as Not A Number, "NaN" | This is the completion time for successful paths averaged | The median is from zero delay human data, even when compariing to a path with delay. |
| | Subject | Map | Delay | IC | num obst | concave | Total Successful summed across both paths | Avg Cmpltn Time **(Seconds)** | Average error relative to nearest median human path **(Unitless)** |
| | 4 | 1 | 1 | 1 | 1 | 0 | 2 | 6.23 | 585 |
| | 4 | 1 | 1 | 2 | 1 | 0 | 2 | 5.65 | 641 |
| | 4 | 1 | 1 | 3 | 1 | 0 | 1 | 5.65 | 422 |
| | 4 | 1 | 1 | 4 | 1 | 0 | 2 | 4.75 | 449 |
| | 4 | 1 | 2 | 1 | 1 | 0 | 2 | 7.03 | 397 |
| | 4 | 1 | 2 | 2 | 1 | 0 | 2 | 7.15 | 736 |
| | 4 | 1 | 2 | 3 | 1 | 0 | 2 | 9.63 | 667 |
| | 4 | 1 | 2 | 4 | 1 | 0 | 2 | 6.18 | 499 |
| | 4 | 1 | 3 | 1 | 1 | 0 | 2 | 10.55 | 782 |
| | 4 | 1 | 3 | 2 | 1 | 0 | 2 | 15.65 | 1242 |
| | 4 | 1 | 3 | 3 | 1 | 0 | 2 | 9.43 | 785 |
| | 4 | 1 | 3 | 4 | 1 | 0 | 2 | 14.90 | 1038 |
| | 4 | 2 | 1 | 1 | 2 | 0 | 2 | 10.10 | 1131 |
| | 4 | 2 | 1 | 2 | 2 | 0 | 2 | 7.58 | 531 |
| | 4 | 2 | 1 | 3 | 2 | 0 | 2 | 5.53 | 278 |
| | 4 | 2 | 1 | 4 | 2 | 0 | 2 | 6.15 | 474 |
| | 4 | 2 | 2 | 1 | 2 | 0 | 2 | 12.95 | 669 |
| | 4 | 2 | 2 | 2 | 2 | 0 | 1 | 6.90 | 967 |
| | 4 | 2 | 2 | 3 | 2 | 0 | 2 | 8.40 | 497 |
| | 4 | 2 | 2 | 4 | 2 | 0 | 2 | 8.75 | 880 |
| | 4 | 2 | 3 | 1 | 2 | 0 | 2 | 15.53 | 1008 |
| | 4 | 2 | 3 | 2 | 2 | 0 | 2 | 19.50 | 723 |
| | 4 | 2 | 3 | 3 | 2 | 0 | 2 | 25.40 | 1100 |
| | 4 | 2 | 3 | 4 | 2 | 0 | 2 | 20.08 | 1233 |
| | 4 | 3 | 1 | 1 | 1 | 1 | 1 | 8.50 | 457 |
| | 4 | 3 | 1 | 2 | 1 | 1 | 2 | 5.50 | 107 |
| | 4 | 3 | 1 | 3 | 1 | 1 | 1 | 5.95 | 326 |

| J | K | L | M |
|---|---|---|---|
| A stop is only recorded if there is are at least 10 steps follow the resumption of forward movment. | This is measured by computing the heading error at each point on the path and averaging. | This is error based on a window of 10 steps before the stop. For delay cases the window is shifted back by the delay amount. | This error is based on a window of 10 step (.5 sec) following the resumption of forward movment. |
| Number of Stops summed across both paths | Average heading error for two paths, calculated for every point **(Radians)** | Average before stop heading error **(Radians)** | Average after stop heading error **(Radians)** |
| 0 | 0.70 | 0.00 | 0.00 |
| 0 | 0.56 | 0.00 | 0.00 |
| 0 | 0.66 | 0.00 | 0.00 |
| 0 | 0.42 | 0.00 | 0.00 |
| 0 | 0.65 | 0.00 | 0.00 |
| 0 | 0.87 | 0.00 | 0.00 |
| 0 | 0.87 | 0.00 | 0.00 |
| 0 | 0.72 | 0.00 | 0.00 |
| 1 | 0.79 | 0.54 | 0.03 |
| 6 | 0.95 | 0.57 | 0.38 |
| 0 | 0.87 | 0.00 | 0.00 |
| 6 | 0.83 | 1.38 | 0.38 |
| 1 | 1.04 | 1.26 | 0.61 |
| 0 | 0.87 | 0.00 | 0.00 |
| 0 | 0.46 | 0.00 | 0.00 |
| 0 | 0.62 | 0.00 | 0.00 |
| 3 | 0.94 | 0.38 | 0.40 |
| 0 | 0.65 | 0.00 | 0.00 |
| 0 | 0.83 | 0.00 | 0.00 |
| 1 | 0.92 | 1.11 | 0.25 |
| 3 | 1.01 | 0.82 | 0.16 |
| 8 | 0.88 | 0.67 | 0.40 |
| 9 | 1.06 | 1.51 | 0.82 |
| 6 | 1.05 | 1.75 | 0.81 |
| 0 | 0.92 | 0.00 | 0.00 |
| 0 | 0.54 | 0.00 | 0.00 |
| 0 | 0.69 | 0.00 | 0.00 |

**Table 7.3.1** Partial table of the metrics computed for each scenario. Full table is given in Appendix B.

### 7.3.1 Success Rate

The Average Success Rate is a measure of how successful the human operators were at completing the task without looking at any other type of performance indicator, thus a path that reaches the goal is successful even if it takes a very long time for the human to get there. This measure, shown in Column G of Table 7.3, is an integer on the 0 to 2 scale, as there are two human attempts per scenario. Most human paths reach the goal, meaning that zeros are very rare in this column.

A path was deemed successful if it reached a threshold distance from the goal. This is clearly seen by examining the human path data; consider Figure 7.1 which shows a zoomed-in view the goal region. Notice that the paths are terminating not on the goal but when they reach a set distance from the goal.

**Figure 7.1** Once an operator drives closer to the goal than the threshold, the trial is terminated and considered a success.

The Average Success metric is plotted versus Feedback Delay in Figure 7.2. The figure shows only a seemingly 'few' data points. This is because the dependent variable can only take 3 values so the data is "stacked" on itself. Also shown in Figure 7.2 are the linear and quadratic models that minimized the least square error of the residuals, or RSS. It is worth noting that the quadratic fit is passing directly through the mean completion values for each delay. These means are listed as the first three columns in Table 7.4, and appear as black dots in Figure 7.2.

Table 7.4 shows results from the SYSTAT analysis for the regression fit. The p-value listed in column four shows the significance for each order of the regression fit, the degrees of freedom for each parameter are (1,30). The p-value is the probability that the coefficient for this order is zero. An order model is statistically significant when $p < 0.05$. We select the highest order model that is statistically significant as our fit. In this case, the p-value for quadratic fit is 0.16, more than our significance level of 0.05, which means we do not find a significant quadratic trend in the data. Thus we have a linear relationship between Feedback Delay and Success Rate.

*Interpretation*

As a practitioner who might be designing a system the practical implication of this result is that if the task is primarily a "reach the goal" task and if time to reach the goal or path to reach the goal are less important, then feedback delay should be assumed to have a linear impact on the degradation of the operator's performance. If a tradeoff between cost to reduce Feedback Delay and performance is being made (for instance when selecting hardware or setting specifications) then the relationship to use is linear.

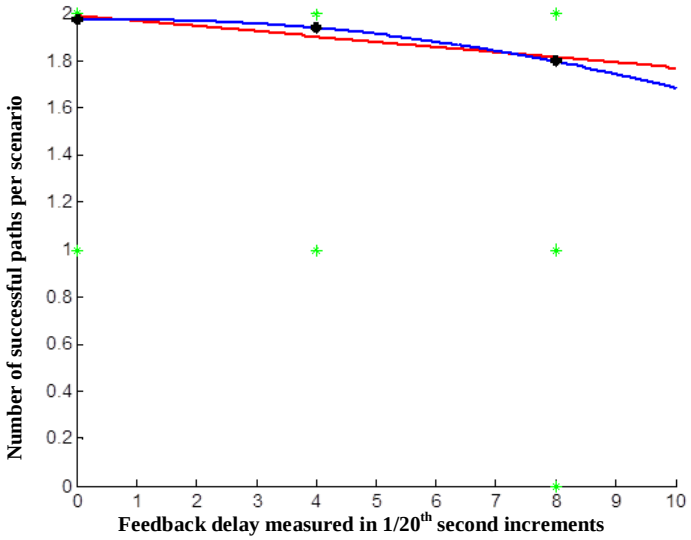


**Figure 7.2** Success Rate data is plotted as a function of Feedback Delay in green. The linear model is shown in red; the quadratic model in blue. The black dots show the mean value for Success Rate for each of the three values of Feedback Delay that were tested.

| Polynomial Coefficients | | | |
|---|---|---|---|
| **Effect** | **Coefficient** | **Standard Error** | **p-Value** |
| CONSTANT | 1.938 | 0.031 | 0.000 |
| (DELAY-U)^1 | -0.088 | 0.022 | 0.000 |
| (DELAY-U)^2 | -0.054 | 0.037 | 0.160 |

**Table 7.4** Results of statistical analysis on Success Rate data.

| Confidence Intervals for Polynomial Coefficients | | | |
|---|---|---|---|
| **Effect** | **Coefficient** | **95.00% Confidence Interval** | |
| | | **Lower** | **Upper** |
| CONSTANT | 1.938 | 1.875 | 2.000 |
| (DELAY-U)^1 | -0.088 | -0.132 | -0.044 |
| (DELAY-U)^2 | -0.054 | -0.130 | 0.022 |

**Table 7.4** Continued from above.

### 7.3.2 Average Completion Time

The Average Completion Time is a measure of how long it takes on average for a human operator to complete the task. This was measured as the average time for the human operators to drive to the goal for paths that reached the goal for each scenario. This metric measures time from the first command until the path reaches the goal and includes any time that the operator may have spent with the vehicle at rest during completion of the task. This dependent variable is continuous and measured in seconds. A sampling of this data is shown in column *H* of Table 7.3.

Figure 7.3 shows the Average Completion Time data for all three values of feedback delay. Notice that the continuous nature of the data means that it is spread out into a "stripe" at each value taken by the discrete Feedback Delay. The black dots show the mean value of Average Completion Time for each Feedback Delay. The regression fitted models are also shown; red for the linear model and blue for the quadratic model, which again passes through the black 'mean value' dots.

Statistical analysis is shown in Table 7.5. There we see that the quadratic model for the interaction between the dependent and independent variables is statistically significant, indicated by the p-value less than our significance level, in the last column.

*Interpretation*

From a practical point of view, this relationship means that if completion time is important, say for a delivery task, then the impact of increasing feedback delay will have a super linear impact on the human operator's performance. The quadratic nature of the relationship can be used to make design tradeoffs between the cost of decreasing the feedback delay and the impact of longer completion times.

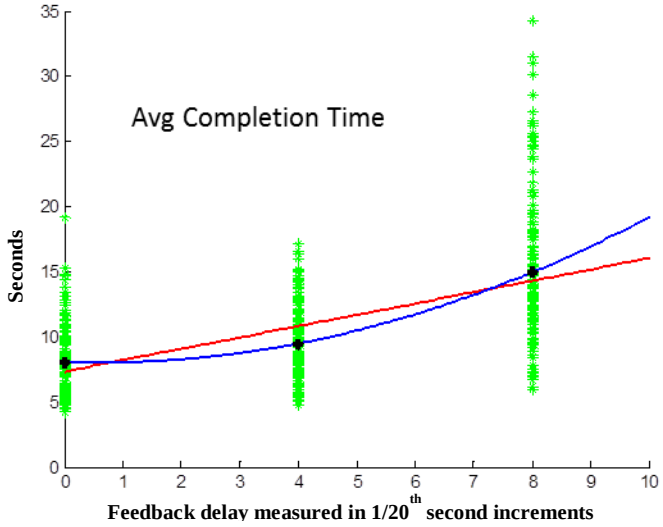


**Figure 7.3** Average Completion Time data is plotted as a function of Feedback Delay in green. The linear model is shown in red, the quadric model in blue. The black dots show the mean value for Average Completion Time for each of the three values of Feedback Delay that were tested.

| Polynomial Coefficients | | | |
|---|---|---|---|
| **Effect** | **Coefficient** | **Standard Error** | **p-Value** |
| CONSTANT | 9.486 | 0.646 | 0.000 |
| (DELAY-U)^1 | 3.462 | 0.457 | 0.000 |
| (DELAY-U)^2 | 1.986 | 0.791 | 0.018 |

| Confidence Intervals for Polynomial Coefficients | | | |
|---|---|---|---|
| **Effect** | **Coefficient** | **95.00% Confidence Interval** | |
| | | **Lower** | **Upper** |
| CONSTANT | 9.486 | 8.167 | 10.804 |
| (DELAY-U)^1 | 3.462 | 2.530 | 4.394 |
| (DELAY-U)^2 | 1.986 | 0.371 | 3.601 |

**Table 7.5** Statistical analysis of the Average Completion Time.

### 7.3.3 Average Path Error

The Average Path Error metric is a measure of variability between the paths chosen by individual operators and median paths selected from the set of all paths produced for zero delay by all operators. The metric is in some sense a measure of how 'spread out' the paths are in relation to a median or central path. Figure 7.4 shows human paths on Map 4 for zero delay, 0.2 seconds of delay and 0.4 seconds of delay.

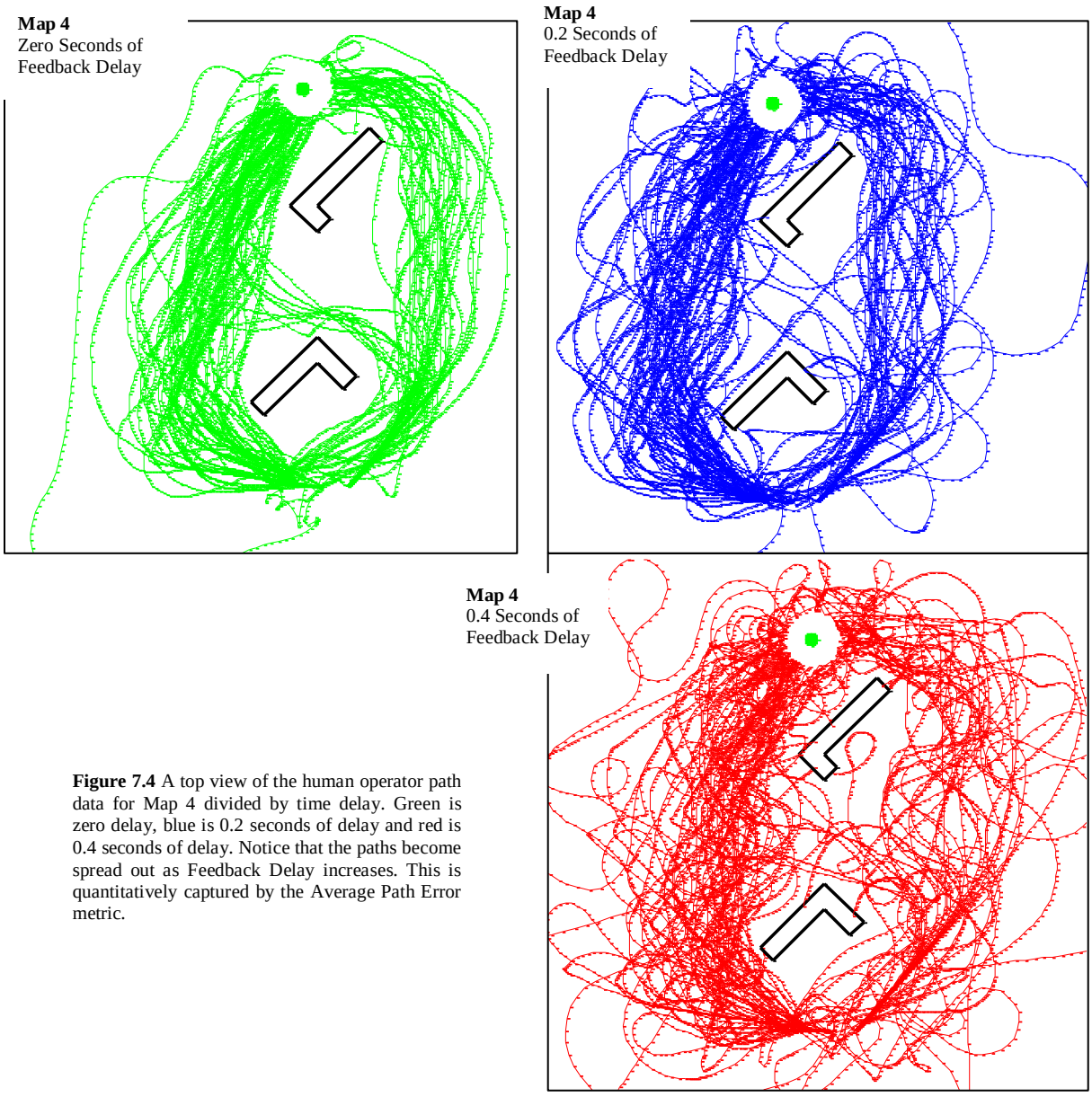


**Figure 7.4** A top view of the human operator path data for Map 4 divided by time delay. Green is zero delay, blue is 0.2 seconds of delay and red is 0.4 seconds of delay. Notice that the paths become spread out as Feedback Delay increases. This is quantitatively captured by the Average Path Error metric.

Figure 7.5 shows the average path error for the paths on each map. The measurement of path error is taken using the technique outlined in Chapter 5 Section 1. The mean values are again shown by black dots; the red line shows the linear fit and the blue line, the quadratic fit. Table 7.6 points to the statistical significance a linear trend.

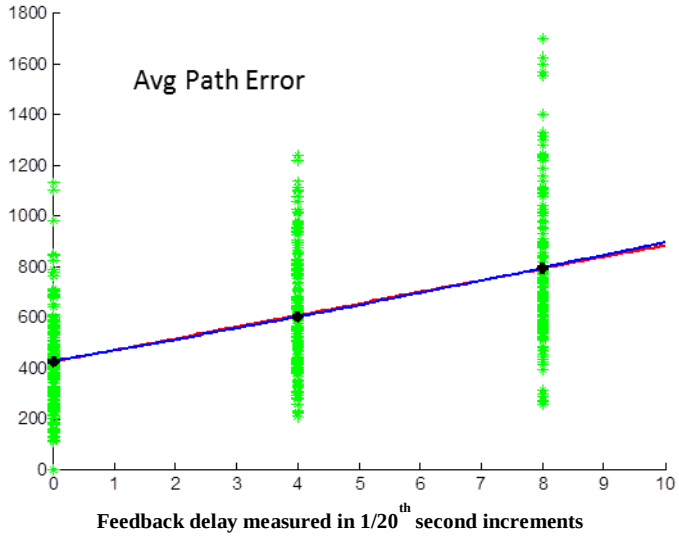


**Figure 7.5** Average Path Error data is plotted as a function of Feedback Delay in green. The linear model is shown in red, the quadratic model in blue. The black dots show the mean value for Average Path Error for each of the three values of Feedback Delay that were tested.

| Polynomial Coefficients | | | |
|---|---|---|---|
| **Effect** | **Coefficient** | **Standard Error** | **p-Value** |
| CONSTANT | 603.609 | 28.603 | 0.000 |
| (DELAY-U)^1 | 184.335 | 20.225 | 0.000 |
| (DELAY-U)^2 | 5.382 | 35.031 | 0.879 |

| Confidence Intervals for Polynomial Coefficients | | | |
|---|---|---|---|
| **Effect** | **Coefficient** | **95.00% Confidence Interval** | |
| | | **Lower** | **Upper** |
| CONSTANT | 603.609 | 545.194 | 662.024 |
| (DELAY-U)^1 | 184.335 | 143.029 | 225.640 |
| (DELAY-U)^2 | 5.382 | -66.162 | 76.926 |

**Table 7.6** Statistical analysis for the Path Error data.

*Interpretation*

The Average Path Error metric is relevant for tasks where repeatability of a path is important. If it is desirable for the operators to create multiple paths that lie close to one other, then minimizing the path error relative to the median of the bundle from which it is drawn is important. A scenario where this might make a difference would be if many robots (or many passes by a single robot) had to be made through an environment where the robot's presence would

be disturbing – say to tundra or root systems, or possibly a crime scene. This metric would be related to the overall footprint of many paths combined. If minimizing the overall footprint is important, the practitioner designing a human in the loop system should consider the delay impact on footprint size as a linear relationship.

### 7.3.4 Number of Stops

The Number of Stops metric, listed in Column J of Table 7.3 as a sum across both paths for a given subject on a given scenario, is the number of times the vehicle comes to a complete halt. This occurs when the operator moves the forward/backward axis of the joystick to neutral and gives a zero velocity command to the vehicle. A stop is measured only on the velocity axis, and in many cases the operator will choose to execute a turn while the vehicle is stopped. A stop is considered to have ended when the vehicle resumes forward motion. Why human operators choose to stop will be explored in Section 7.4, but in this section we report the effect on human operator performance.

We only count stops that occur during the course of the trail which happen at least 1 second after the first command is given at least 0.5 seconds before the path terminates. This is done to allow for the before and after stop processing of data presented in Section 7.4. Figure 7.6 shows pictures of the same human operator path data that was presented in Figure 7.4 but from the profile view. It is qualitatively clear from this data that as the delay increases the number of stops also increases.

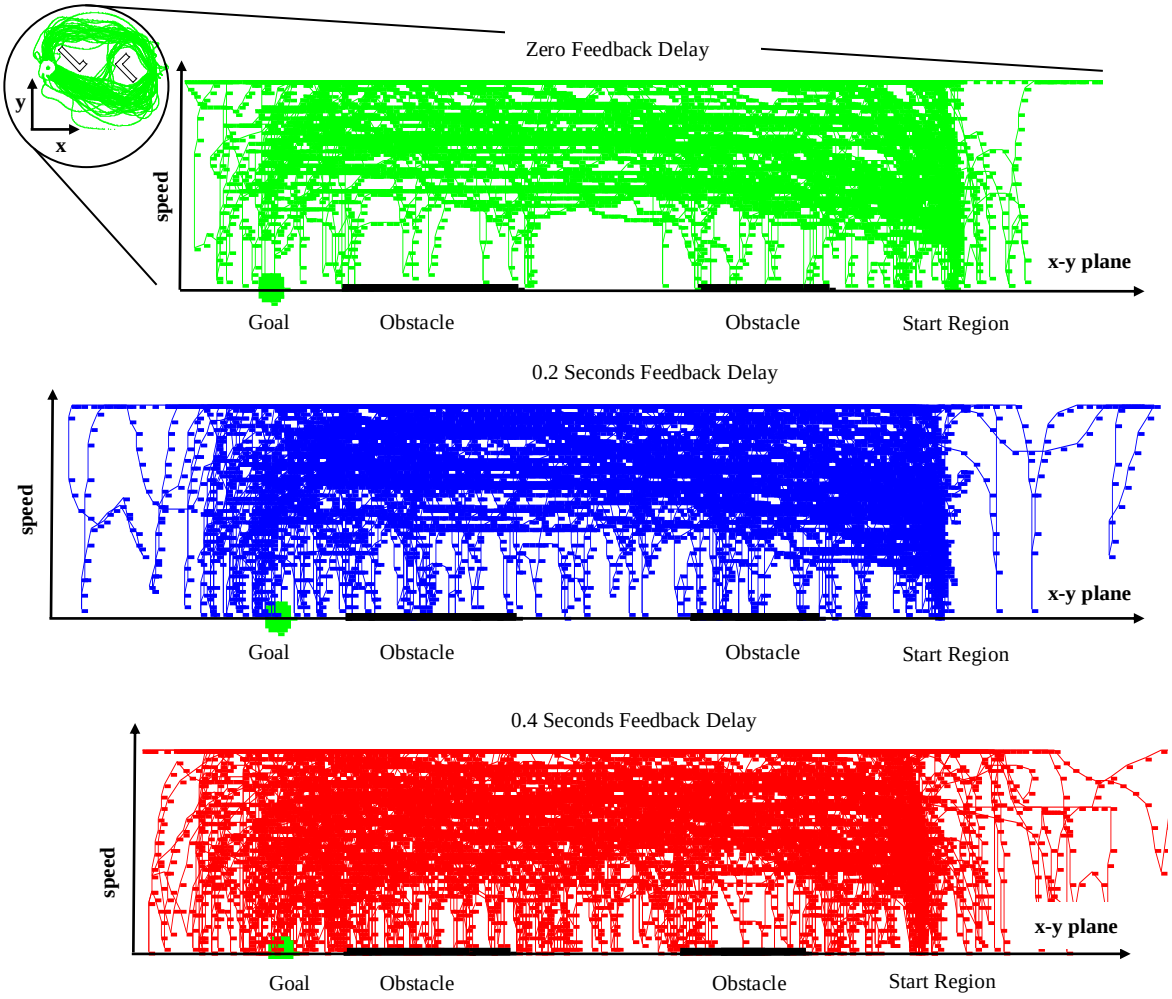


**Figure 7.6** The same path data presented in Figure 7.4 is presented here from the side view. This is a picture of all the human path data from Map 4, the vertical axis in each figure is speed, and the horizontal axis is position. The large green "dots" are the goal; the heavy black lines are the obstacles. All the starting path points (ICs) are on the right. From top to bottom, feedback delay increases from 0 to 0.2 to 0.4 seconds. Any time a vehicle path touches the horizontal axis, this indicates that the drive has issued a zero velocity command and this corresponds to a vehicle stop. It can be seen that stops are more frequent for increasing values of feedback delay.

The stopping data collapsed across maps and subjects is shown in Figure 7.7. The Number of Stops is a discrete variable taking only integer values. As such, each green data tick on the chart frequently corresponds to several paths for that value of delay which had the given number of stops. The black dots show the averages for each delay, and this data is repeated in the table as well. Notice that again the quadratic model passes through the Average Number of Stops for each Feedback Delay value.

*Interpretation*

At a point 0.05 significance level, the relationship between the number of stops and delay is linear. But with a p-value of 0.103 for the quadratic term, we note that the effect of Feedback Delay is trending toward super linear, Table 7.7.

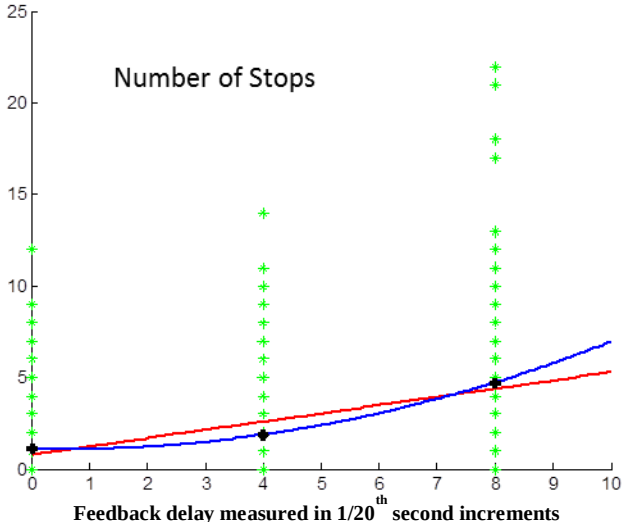


**Figure 7.7** Number of Stops data is plotted as a function of Feedback Delay in green. The linear model is shown in red, the quadratic model in blue. The black dots show the mean value for Number of Stops for each of the three values of Feedback Delay that were tested.

| Polynomial Coefficients | | | |
|---|---|---|---|
| **Effect** | **Coefficient** | **Standard Error** | **p-Value** |
| CONSTANT | 1.892 | 0.513 | 0.001 |
| (DELAY-U)^1 | 1.801 | 0.363 | 0.000 |
| (DELAY-U)^2 | 1.057 | 0.628 | 0.103 |

| Confidence Intervals for Polynomial Coefficients | | | |
|---|---|---|---|
| **Effect** | **Coefficient** | **95.00% Confidence Interval** | |
| | | **Lower** | **Upper** |
| CONSTANT | 1.892 | 0.845 | 2.939 |
| (DELAY-U)^1 | 1.801 | 1.061 | 2.542 |
| (DELAY-U)^2 | 1.057 | -0.226 | 2.340 |

**Table 7.7** Statistical analysis for Number of Stops.

The significant linear model indicates that an operator's propensity to stop the vehicle is not accelerating as a function of increasing feedback delay. If the practitioner is designing the system for a task where coming to a complete stop should be avoided, the tradeoff between feedback delay and stopping likelihood should be considered as linear. Such a task may be battlefield navigation, where coming to a complete stop might allow an enemy to lock onto the vehicle or designate it for a weapon suitable for use only against static targets. If the human operator is driving the lead vehicle in an otherwise automated convey, such a stop would put the entire convoy at risk. Likewise for the convoy task, frequent stopping and starting will also put a strain on the control system responsible for

maintaining safe vehicle separation. Even in convoys that are string stable stopping and starting the lead vehicle may create an undesired ripple effect in the separation distance for following vehicles.

### 7.3.5 Average Heading Error

The Average Heading Error for a vehicle path is computed by summing the heading error for every point along the path, after the first second until the end of the trial, and dividing by the number of points, see Figure 7.8. The Heading error is a positive continuous value between zero and pi.

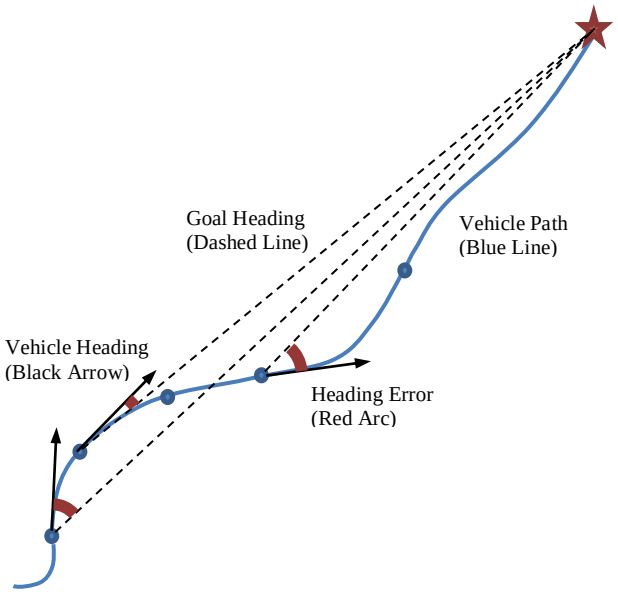


**Figure 7.8** This figure shows how the vehicle heading error was computed as the difference between the current vehicle heading and the goal heading.

The Heading Error for each point was averaged across both paths for a given scenario to produce the K column of data in Table 7.3. The Heading Error is plotted in Figure 7.9. The independent variable is again Feedback Delay. The Heading Error for individual scenarios is plotted as green dots. Notice that the data is spread out as the dependent variable is continuous. The linear and quadratic models after fitting are shown in the figure as red and blue lines respectively. The black dots show the mean values for Heading Error for the three Feedback Delays. The statistical analysis shows no justification for fitting a model of order higher than linear.

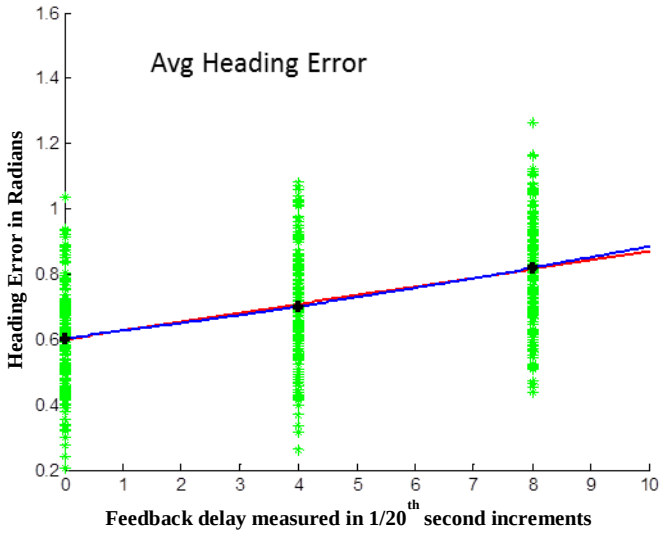


**Figure 7.9** Average Heading Error data is plotted as a function of Feedback Delay in green. The linear model is shown in red, the quadratic model in blue. The black dots show the mean value for Average Heading Error for each of the three values of Feedback Delay that were tested.

| Polynomial Coefficients | | | |
|---|---|---|---|
| **Effect** | **Coefficient** | **Standard Error** | **p-Value** |
| CONSTANT | 0.704 | 0.023 | 0.000 |
| (DELAY-U)^1 | 0.107 | 0.016 | 0.000 |
| (DELAY-U)^2 | 0.008 | 0.028 | 0.772 |

| Confidence Intervals for Polynomial Coefficients | | | |
|---|---|---|---|
| **Effect** | **Coefficient** | **95.00% Confidence Interval** | |
| | | **Lower** | **Upper** |
| CONSTANT | 0.704 | 0.657 | 0.751 |
| (DELAY-U)^1 | 0.107 | 0.074 | 0.141 |
| (DELAY-U)^2 | 0.008 | -0.049 | 0.066 |

**Table 7.8** Statistical analysis for Average Heading Error.

*Interpretation*

Large Heading Error could result from several types of behavior. For instance, a path that zigzags toward the goal, or a path that spirals toward the goal would both have very high average Heading Error. Heading error is also a function of obstacle type and map configuration, but this effect is canceled in our analysis because the same set of maps and obstacles are considered for each delay. For zero delay, we are getting a baseline for the set of maps and obstacles. For the other delays, we are seeing an increase in heading error. If the task for which a human in the loop control system is being designed is highly dependent on heading, such as collecting video footage with a camera mounted to the vehicle, then higher delay will have a linear impact on the degradation of task performance.

## 7.4. Stopping Phenomenon

In the previous section, we catalogued the interaction between feedback delay and five dependent metrics as either linear or quadratic. Now we ask a behavioral question about the choice of human operators to stop more frequently for the higher delay scenarios. We examine the question, why do they choose to stop? Based on non-quantifiable observations of human operators, it "appears" that people may be stopping because they have lost control of the vehicle. To get a quantitative handle on this issue, we measured the heading error for 0.5 seconds before the operators choose to quit moving forward and compared this to the heading error in 0.5 seconds after they began moving forward again. The heading error is significantly less after stops compared to before stops, and this suggests that the stopping action is helping operators to regain control. In Section 7.4.2 we propose a simple mechanism by which this may be occurring.

### 7.4.1 The Before and After Stop Heading Error Data

The data was collected by looking at each stop and computing the average heading error before the stop and after the stop. A stop was included for analysis if there was at least 1.0 seconds of data before the stop and 0.5 seconds of data after the stop. This is a natural requirement since the window size is fixed. The need for more data before a stop is related to Feedback Delay. For a delay case of 0.4 seconds, the vehicle will actually come to rest 0.4 seconds after the operator stops giving commands. To make the analysis relevant to the conditions that were occurring just before the stop command was issued, we look back in the data 0.4 seconds to 0.9 seconds. See Figure 7.10.

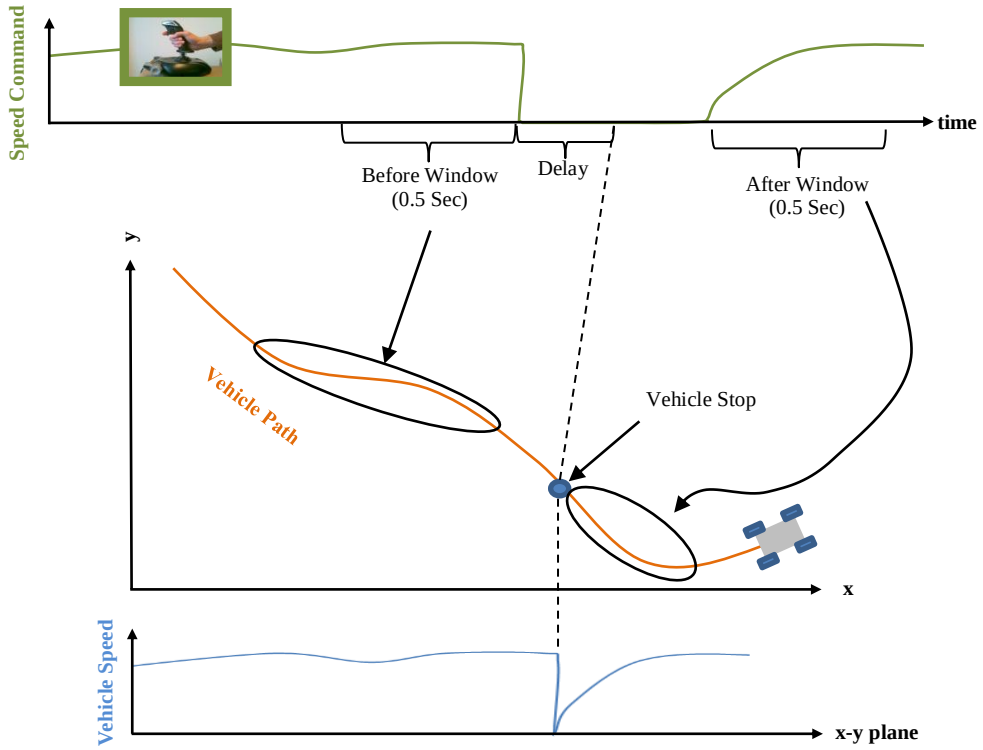


**Figure 7.10** Shows how the windowing works with non-zero delay. Shows a plot of command signal and vehicle path and shows when the command signal comes to rest being before the actual vehicle stops.

The data presented in Columns L & M of Table 7.3 for the Before and After Windows is the average Before Window heading error for that subject and scenario for the two trials and the average After Window heading error for the same two trials. The data for each stop (not averaged across paths) is plotted in histograms in Figures 7.11, 12, 13. The total number of stops across all subjects and scenarios for each delay are as follows: 202 stops for zero Feedback Delay, 333 stops for 0.2 seconds and 836 stops for 0.4 seconds. The data is divided into a 50 bucket histogram, with buckets ranging from 0 to $\pi$ radians.

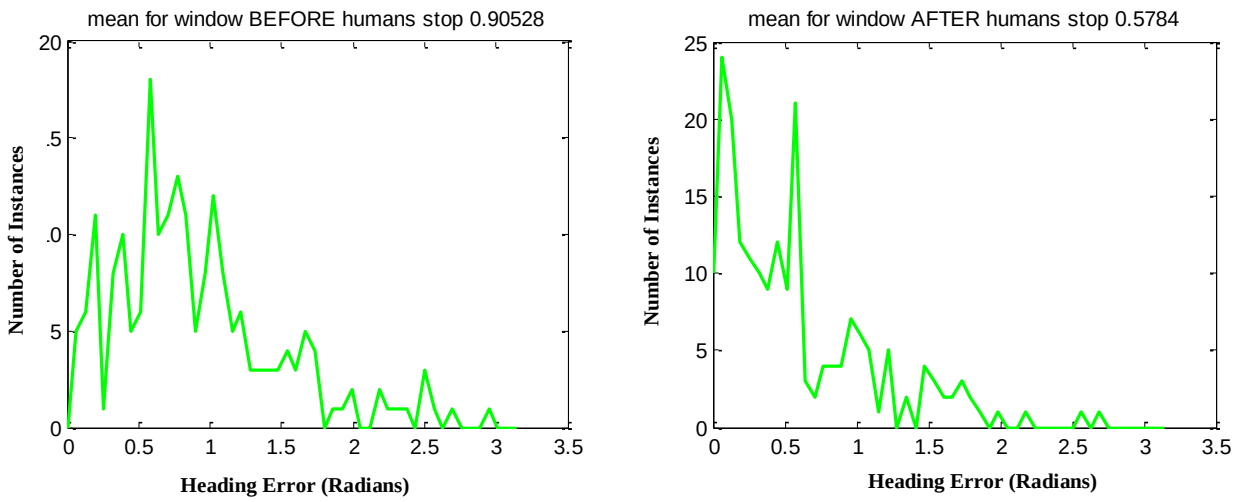


**Figure 7.11** The heading error measured before and after the 202 stops that the human operators chose to make during zero Feedback Delay operation. The histograms each have 50 buckets ranging from 0 to pi radians.

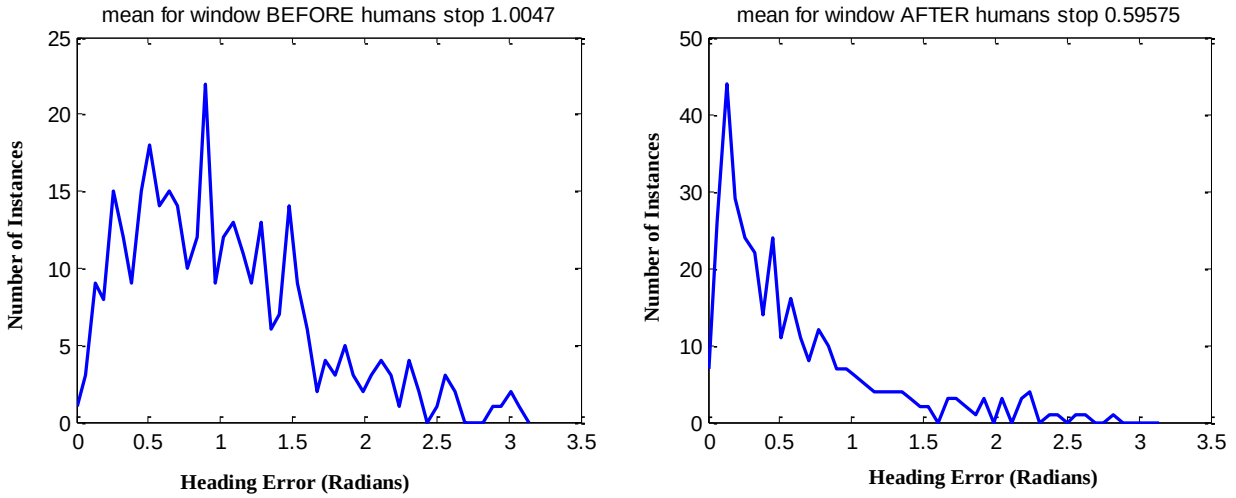


**Figure 7.12** The heading error measured before and after the 333 stops that the human operators chose to make during 0.2 second Feedback Delay operation. The histograms each have 50 buckets ranging from 0 to pi radians.

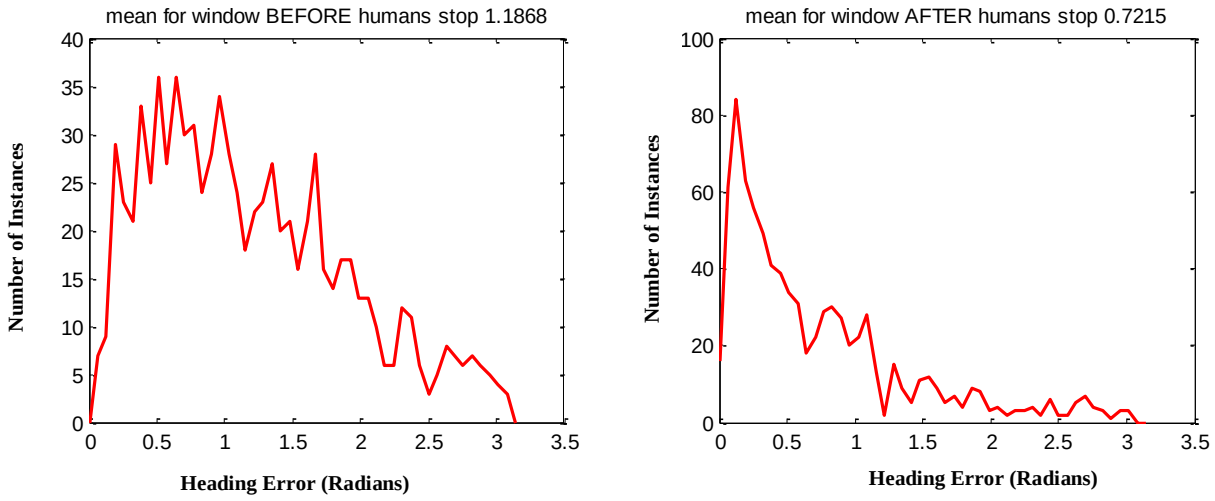


**Figure 7.13** The heading error measured before and after the 836 stops that the human operators chose to make during 0.4 seconds Feedback Delay operation. The histograms each have 50 buckets ranging from 0 to pi radians.

## 7.4.2 Analysis of the Before and After Stop Heading Error Data

A 3 (delays) X 2 (window) ANOVA was run that showed a significant difference between before and after the stop, a significant effect of delay, and an interaction (meaning the error reduction after the stop is larger as the delay increases). Table 7.9 shows the results, Figure 7.14 shows the interaction.

| Analysis of Variance | | | | | |
|---|---|---|---|---|---|
| Source | Type III SS | df | Mean Squares | F-Ratio | p-Value |
| DELAY | 2.687 | 2 | 1.344 | 35.691 | 0.000 |
| WINDOW_TYPE | 0.729 | 1 | 0.729 | 19.371 | 0.000 |
| DELAY*WINDOW_TYPE | 0.295 | 2 | 0.148 | 3.918 | 0.025 |
| Error | 2.259 | 60 | 0.038 | | |

**Table 7.9** ANOVA analysis for the before and after stop heading error

From the interaction of the two trends, we see that as delay increases, the benefit from stopping increases as well. We believe this is because a stop is basically a mechanism of regaining control, and thus the After Window heading error (which represents return to control) does not rise as fast as the Before Window heading error for increasing Feedback Delay.

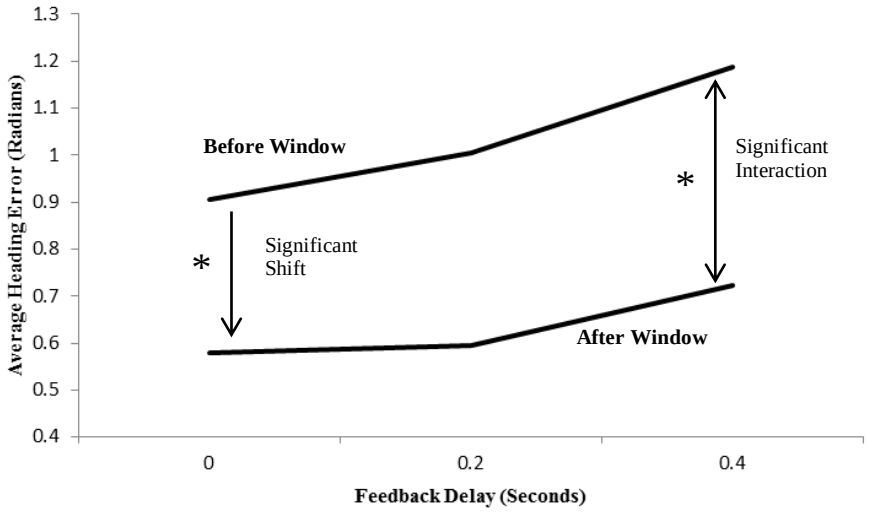


**Figure 7.14** The Before and After Window heading errors are plotted with the ANOVA results. The '*' denotes significance.

The forgoing analysis leads us to propose that humans are choosing to stop to regain control. A stop aids in regaining vehicle control by purging past delayed commands from the command cue. Once all commands in the cue are zero the operator can be confident that the next command they issue will be executed relative to a vehicle position that they know (the one at rest).

This conclusion is consistent with the assumptions and observations made in [26] regarding how humans cope with feedback delay. The researchers in [26] suggest that there are only two basic strategies observed in human operators who are facing feedback delay. The operator can either come to complete rest regularly or simply offer commands at a very slow rate. All operators observed by [26] adopted one of these two coping mechanisms without being told to do so, most operators chose to stop and wait. In our work we also observed similar behavior.

## 7.5. Conclusion

In this Chapter we have shown that human performance is impacted in many ways by delay and fit statistically significant models to this interaction showing either linear or quadratic impact. We also show that humans cope with the increased delay by bringing the vehicle to rest more and more often as Feedback Delay increases. This inspired us to apply the same stop-to-regain-control strategy to the receding horizon controller. In the next chapter, we look at the impact of delay on the receding horizon controller and show how a strategy similar to the humans can be captured by adding a constraint to the receding horizon formulation. We will also explore the cost-benefit of such a strategy.

# Chapter 8

# Explicitly Considering the Time Delay in the Controller Formulation

Throughout the course of this study, we have considered delay as a tuning knob used to introduce regulated uncertainty into the system. From the experiments we saw that introducing feedback delay results in loss of the convergence guarantee for the receding horizon controller. In this chapter we examine the theoretical implications of delay on the receding horizon controller and explore two methods of mitigating the effect of delay.

In Section 8.1 an over bound for the error introduced on one execution horizon by delay is given as a function of the delay itself. In Section 8.2.1 we show that for the original receding horizon control formulation, the convergence guarantee is lost. In Section 8.2.2 we present an error bound as a function of time delay for a receding horizon control operating in a world without obstacles. In Section 8.2.3 we present results of explicitly adding delay to the receding horizon control formulation, but show that this is a non-robust method of dealing with delay. Finally, in Section 8.2.4 we present a human-inspired robust method of dealing with delay and describe the attendant performance impact. Simulations are provided showing the efficacy of the method. Section 8.3 offers concluding thoughts.

## 8.1 Over Bound of the Uncertainty Introduced by Delay

During the delay of $d$ seconds, leftover commands from the previous solution horizon are being executed by the vehicle. Figure 8.1 shows how this occurs. To upper bound the position error introduced by the unknown commands

we will consider a worst case scenario. We will compute the maximum translation error due to the unknown delayed velocity commands and maximum rotation error due to unknown rotation commands separately and then add them together to get an overall upper bound for the error introduced by the delay. For the purpose of our work, we define *p* as the difference *n* – *d*. This is shown in Figure 8.1.

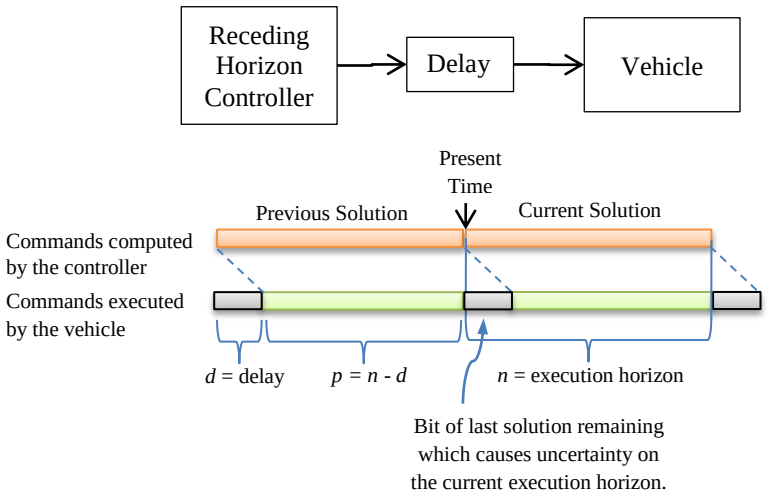


**Figure 8.1** This figure shows the impact of delay on commands executed by the vehicle.

Before computing the errors introduced by the unknown delayed commands, an important invariance property of the unicycle model needs to be mentioned. The vehicle model is first order thus purely kinematic. This means that if a command string, say

$$[u1, u2, u3],$$

will move the vehicle from point A to point B, then any command string with the same order of commands which includes zero commands will result in the same movement from A to B along the same path. For instance,

$$[u1, 0, u2, 0, u3] \text{ or } [0\ 0\ 0\ u1\ u2\ u3]$$

will both result in movement along the same path from A to B, see Figure 8.2. The difference among the paths created by the three sample command strings above will be noticed only in their velocity profiles. This invariance of the x-y path to inserted zero commands is exploited throughout the analysis that follows. In the real world, the assumption that a vehicle is purely kinematic will be reasonable if the vehicle has low mass or low speed or overall low momentum.

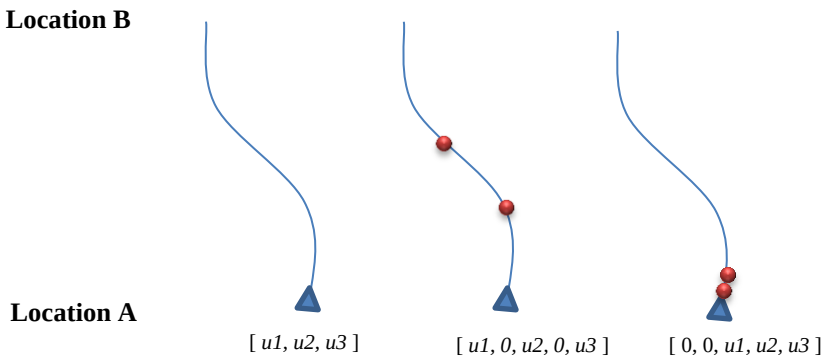


**Figure 8.2** Path from Location A to Location B. The path on the left is generated without any zero commands. The path in the middle and the path on the right are identical to the path on the left, except that they both have stops marked by red dots. This example shows the vehicle path invariance to zero commands.

To compute the error due to delayed velocity commands, assume the vehicle drives full speed straight ahead for the full length of the delay, $d$ seconds, see Figure 8.3. The maximum amount of translation error that could be introduced by the unknown delayed commands becomes the following:

$$e_{trans} = d\,\bar{v}\,,$$

where $\bar{v}$ is the maximum allowed forward speed command.

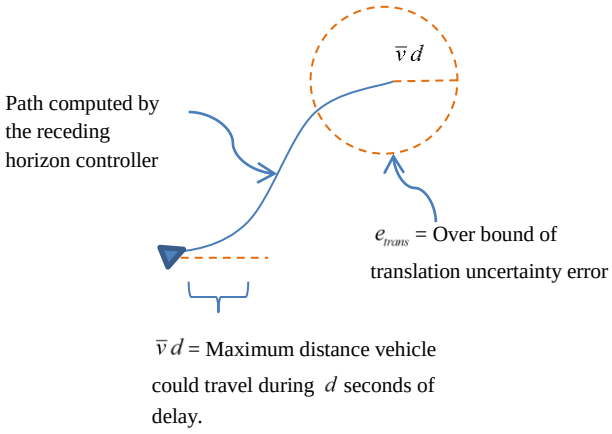


**Figure 8.3** Error that occurs due to delayed speed commands

To compute the error due to delayed heading commands**,** assume the vehicle spins in place for the entire time of the delay. The heading error would be as follows:

$$\text{Angular Heading Error} = d\,\bar{\omega}, \tag{1}$$

where $\bar{\omega}$ is the maximum allowed rotation rate. The ultimate translation error introduced by this unexpected change of heading which occurs before the execution of the computed trajectory will be over bounded by the arc swept by the maximum length of the computed trajectory twisted by the heading error:

$$\text{Error Due to Heading Uncertainty} = \text{Angular Heading Error} \cdot (\bar{v} \cdot \Delta t \cdot n) \tag{2}$$

We denote this error due to heading uncertainty $e_\theta$, see Figure 8.4.

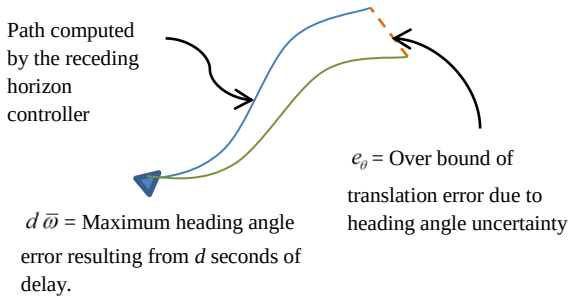


**Figure 8.4** Error due to delayed rotation commands.

The overall uncertainty error between the *location the receding horizon controller expects the vehicle to occupy after the execution of p steps on the next horizon* and the *actual location the vehicle will end up after executing the unknown delayed commands and first p computed commands for the present execution horizon* is what we call the delay uncertainty. The delay uncertainty can be upper bounded by adding together (1) and (2) from above:

$$\text{Delay Uncertainty Error: } e(d) = d\,\bar{v} + d\,\bar{\omega}\,\bar{v}\,\Delta t\,n\,. \tag{3}$$

See Figure 8.5.

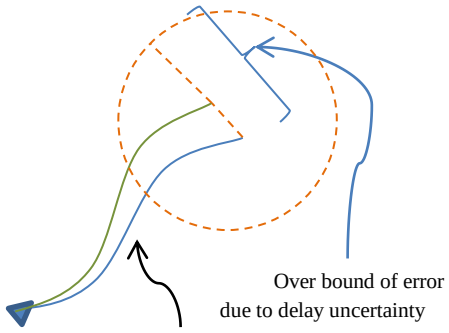


**Figure 8.5** Total maximum error due to delayed commands.

## 8.2 Four ways of looking at the effects of delay

In this section we offer four perspectives on the impact that feedback delay has on the performance of the receding horizon controller. First, in Subsection 8.2.1, we assess the impact of delay on the original receding horizon controller formulation. Then in Subsection 8.2.2, we offer an error over bound as a function of feedback delay for the modified case of no obstacles. Subsection 8.2.3 discusses the tradeoffs of dealing with delay in the vehicle model formulation, and in Subsection 8.2.4, we present a modification to the original receding horizon controller formulation that recovers the guaranteed goal convergence found in Chapter 3.

### 8.2.1 Effect of Delay on the Receding Horizon Controller with No Modification to the Formulation

The boundedness and convergence results we reported in Chapter 3 are based on the assumption of zero delay. For non-zero delay, an error between the vehicles actual location and the pre-computed location may occur. An upper bound for this error is given by equation (3). If no modification is made to the receding horizon control formulation we lose the guarantee that a path pre-computed to be collision free actually will be. This is because our formulation assumes vehicles may pass arbitrarily close to obstacles. With delay position uncertainty affecting the paths, passing arbitrarily close to an obstacle can now result in collision. Thus feasibility of the pre-computed path is no longer guaranteed. With the loss of feasibility, we lose convergence as well.

In Chapter 3 we saw in the experimental data for the receding horizon controller, at zero delay, 100% of the paths reach the goal, but for even a low delay of 0.2 seconds some paths no longer reached the goal. This empirically agrees with the theoretical conclusion that guaranteed convergence is lost with the introduction of delay.

### 8.2.2 Delay Uncertainty Bounds for the Case without Obstacles

For short delay we can still show convergence to a set of states close to the goal if we do not have obstacles and with slight modification to the receding horizon controller's interpretation of the contractive constraint. The modification requires the contractive constraint to be satisfied on a shorter horizon than the execution horizon. We now require the constraint to be met on the shorter horizon $p$, (recall, $p=n-d$), which means that during the next execution horizon, the commands over which the contraction has been computed are guaranteed to be executed. This is important, because due to the delay, some of the computed commands for the next horizon will not be executed before re-computation occurs. This modification foreshadows a much stronger result presented in Section 8.2.4.

The new contractive constraint becomes:

$$\max_{i\in\{1,\ldots,p\}}\{V(x^{pos}_{k+i\,|\,k})\} \le c \max_{j\in\{1,\ldots,n\}}\{V(x^{pos}_{k-n+j})\}$$

The difference between this and the original contractive constraint from Chapter 3 is in the range over which the left maximum is computed. It runs from $i=1:p$ instead of $i=1:n$ as previous. This constraint is a contraction of the predicted future distance between the vehicle and the goal. Of course, because of the delay error, the future path will not actually be the one predicted. The basic idea will be to ensure that the predicted contraction will be more than the maximum uncertainty error: even for the worst case delay error, some contraction will still occur. Note that because we are considering a case with no obstacles, $V(x^{pos})$ is simply the straight line distance to the goal.

To show contraction of $V(x^{pos})$ we simplify notation by introducing the terms:

$V^{\max}_{prev}$ = Maximum vehicle distance from the goal on the previous execution horizon $n$.

$V^{\max}_{pred}$ = Maximum vehicle distance to the goal, found by forward propagating the new solution $p$ steps forward from the present vehicle state, no delay considered.

$V^{\max}_{actual}$ = Greatest actual distance between the vehicle and the goal on the next execution horizon.

We have from the construction of $e(d)$ and the contractive constraint that

$$V^{\max}_{actual} < V^{\max}_{pred} + e(d),$$

$$V^{\max}_{pred} < cV^{\max}_{prev}.$$

We will impose a new condition,

$$e(d) < (1-c)V_{prev}^{\max}, \quad (4)$$

which means that the uncertainty due to delay must be less than the decrement. Now combining above we can show the following:

$$V_{actual}^{\max} < V_{pred}^{\max} + (1-c)V_{prev}^{\max} = V_{pred}^{\max} + V_{prev}^{\max} - cV_{prev}^{\max}$$

$$V_{pred}^{\max} + V_{prev}^{\max} - cV_{prev}^{\max} < cV_{prev}^{\max} + V_{prev}^{\max} - cV_{prev}^{\max} = V_{prev}^{\max}$$

Thus,

$$V_{actual}^{\max} < V_{prev}^{\max}, \quad (5)$$

giving contraction of the overall distance to the goal. See Figure 8.6. Equation (5) can be used to repeat all the feasibility and convergence arguments from Chapter 3, giving us both feasibility and convergence for this delayed modified controller, but there are limitations. Condition (4) means that contraction can only occur while the following is true:

$$V_{prev}^{\max} > \frac{e(d)}{1-c}.$$

After the error $V_{prev}^{\max}$ drops below the right side term, contraction is no longer guaranteed. Thus the vehicle goal error is guaranteed to contract only until this limit is reached. This gives bounded error and contract at least to the set $x \in D \ \forall x$ such that $V(x^{pos}) \leq \frac{e(d)}{1-c}$.

Practically, $e(d)$ grows very quickly as a function of $d$ and thus the region around the goal to which we can guarantee convergence may be quite large, which is not desirable, even for relatively small $d$. Also troubling is the recollection that there is an upper bound on $V(x^{pos})$ (from Chapter 3). This means that if $\frac{e(d)}{1-c}$ is larger than $\frac{1}{c}\Delta t\,\bar{v}$ (from Assumption A3), there will be no guarantee a feasible solution exists. Thus this method of dealing with delay is somewhat impractical. Because of this impracticality and its inability to handle obstacles we turn to more robust methods in the following subsections.

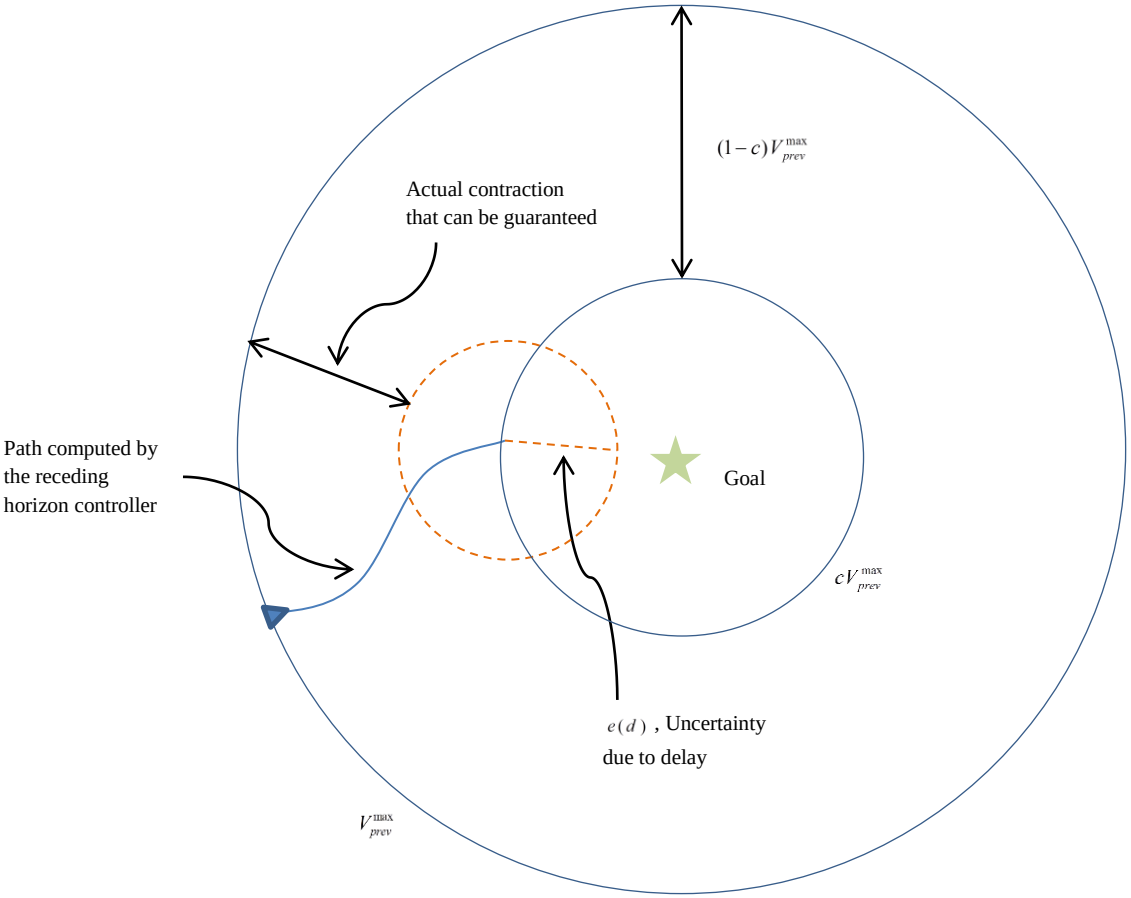


**Figure 8.6** This figure shows amount of contraction that can be guaranteed.

### 8.2.3 Explicitly Considering the Delay as a Part of the Vehicle Model

Another approach to handling delay is to explicitly include the delay in the vehicle model we give to the receding horizon controller. This is perfectly acceptable as a receding horizon controller can make use of any discrete causal vehicle model. See Figure 8.7. This approach would return to us all the guarantees of feasibility and convergence in the presence of concave obstacles that we previously enjoyed.

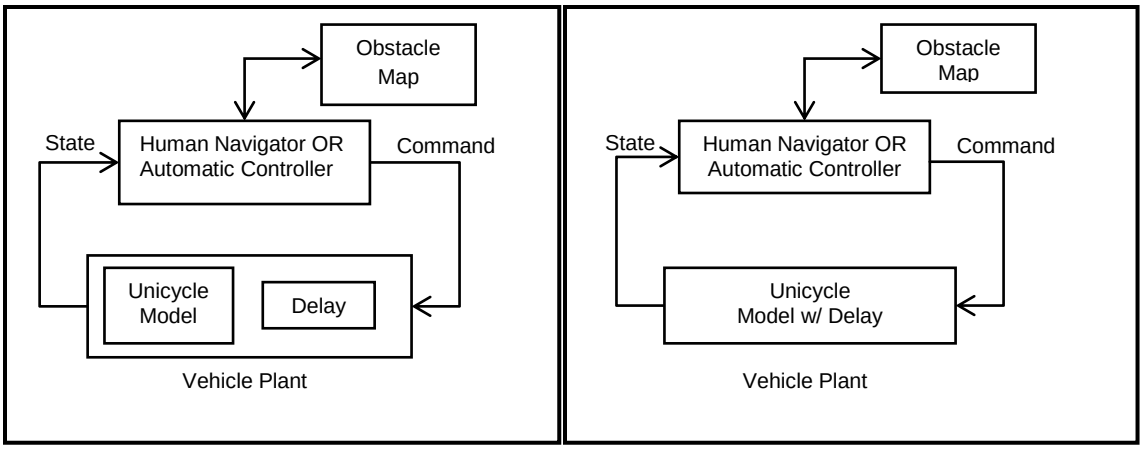


**Figure 8.7** In the original receding horizon controller formulation (on left), the delay was not part of the Unicycle Model and was thus not 'captured' by the receding horizon controller. If the delay is fixed and known exactly, it can be easily incorporated into the vehicle model, in which case it is now 'known' to the receding horizon controller and its effect is completely eliminated (on right). This is not robust because if the delay is not exactly what we expect, the system immediately reverts to something similar to the model on the left where there is a 'masked' unknown delay in addition to the Unicycle Model.

Unfortunately, incorporating a known value for the delay into the vehicle model does nothing to improve the robustness of the controller. If the delay in the real world differs from that assumed by the receding horizon controller's model, we revert immediately to the case presented in Section 8.2.1, where all guarantees are lost due to an unknown delay. This lack of robustness to variation in the real world delay leads us to consider another alternative for dealing with delay.

### 8.2.4 Robust Over-Bound for Delay

If an over bound for the delay is known then by a modification to the receding horizon controller formulation, all feasibility and convergence guarantees originally given can be recovered for *any* delay less than the over bound. The tradeoff is worse performance as the vehicle must make frequent stops.

Let the delay $d$, be over bounded by $q\Delta t$ where $q$ is an integer number of steps:

$$d < q\Delta t\,.$$

We will add one additional constrain to the receding horizon controller formulation:

$$u_{k+i\,|\,k} = 0 \;\forall\, k = n-q,\ldots,n\,. \tag{6}$$

We will also use the contractive constraint from Section 8.2.1,

$$\max_{i\in\{1,\ldots,p\}}\{V(x^{pos}_{\hat{k}+i\,|\,\hat{k}})\} \le c \max_{j\in\{1,\ldots,n\}}\{V(x^{pos}_{\hat{k}-n+j})\}$$

Other than these two modifications, the receding horizon controller will be identical to the one presented in Chapter 3.

The new constraint (6) causes a pause for $q$ steps at the end of each execution horizon. This pause ensures that any commands which are held in the delay cue and executed later will be zero, and any delayed commands executed on the present horizon will also be zero. The result is that while the vehicle may not move when expected, the resulting motion will be exactly the same as the receding horizon controller predicted so long as the delay is less than the bound. This works because the path produced by our vehicle model is invariant to zero magnitude commands. Figure 8.8 shows how the new constraint (6) works.

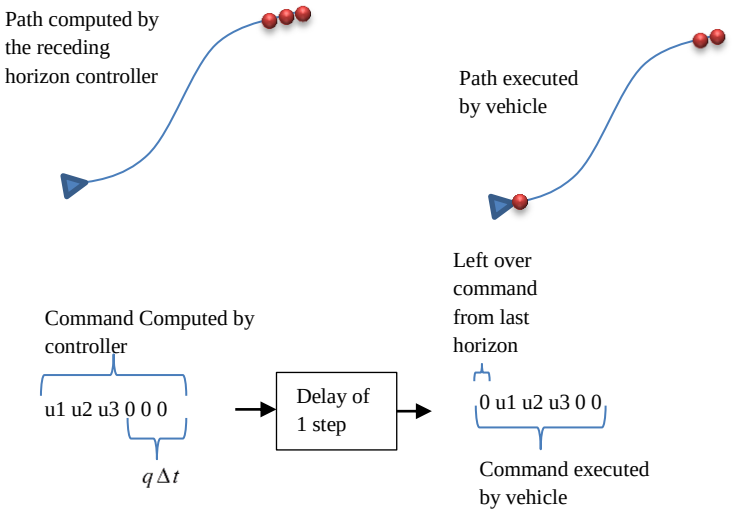


**Figure 8.8** Because all the delayed commands executed by the vehicle will now be zero, no unexpected movement happens. The delay has shifted the location of the stops (red dots) but has not changed the x-y path.

The delay means the vehicle is not executing its maneuver at the time we expected, but because the computed command is zero 'padded,' the result is that the vehicle does move from and to the points expected by the receding horizon controller. Thus any delay less than $q\Delta t$ will never result in unexpected movement. This means that all the conditions for collision-free error-contracting behavior from Chapter 3 still hold.

We show by simulation example how the new constraint works. Using the original formulation without delay compensation we show that for increasing delay the path becomes progressively more erratic, as displayed in Figure 8.9. The paths generated with the new constraint (6) included in the receding horizon control formulation are shown

in Figure 8.10. Notice in Figure 8.10 that for 0.4 seconds the path is identical to the path for 0.0 seconds delay. This is because both of these delay values are below the threshold, $q\Delta t = 0.5$ seconds, selected for this simulator.

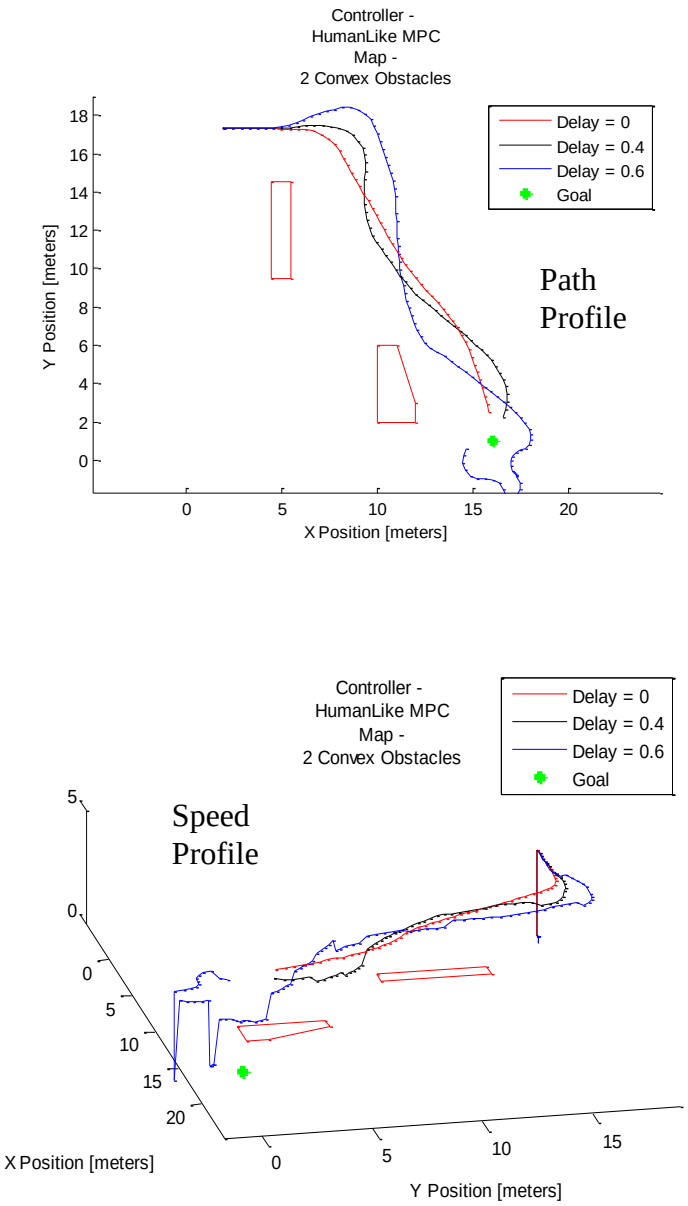


**Figure 8.9** Without delay compensation the path becomes increasingly erratic as delay increases.

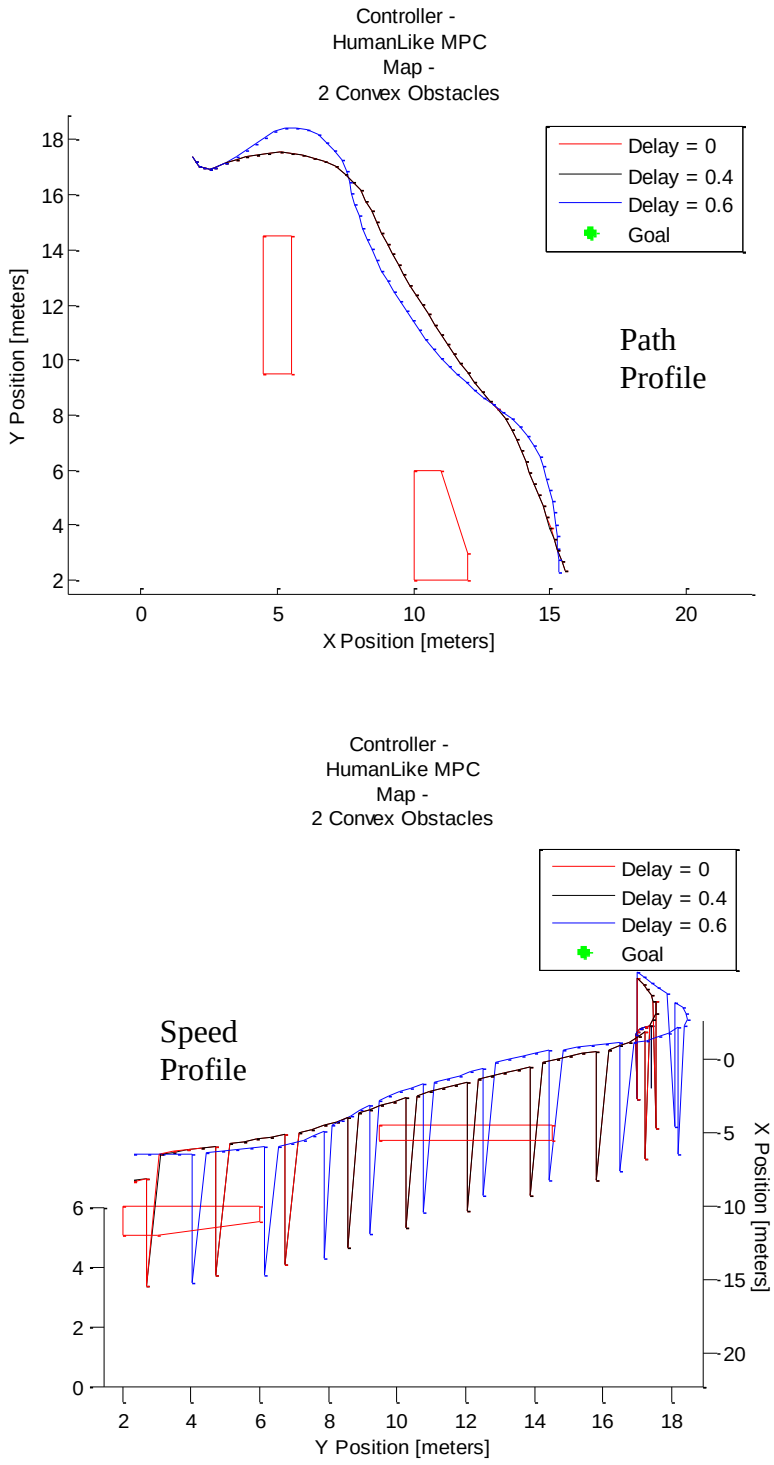


**Figure 8.10** Delay compensation constraint is active. $q$ = 0.5 seconds. The 0.4 second delay path is exactly the same as the 0 second delay path. The 0.6 second delay path shows slight perturbation but it is significantly less perturbed than the 0.6 second delay path from Figure 8.9. Notice that frequent stops are the performance impact of this delay compensation method.

## 8.3 Conclusion

The choice of constraint (6) was inspired by the human strategy of stopping to regain control as described in Chapter 7. The constraint leads to frequent stops that purge error from the vehicle control loop, which represents a "miniature" version of the human strategy which called for stops when the heading error was large. In this inspired strategy the controller stops at regular intervals before it loses control. Thus the strategy captured by constraint (6) is not identical to human behavior but similar in that stops are made to maintain control in the face of feedback delay. We show by argument and by simulation that the x-y path of the vehicle is unaffected by feedback delays below the threshold value of $q\Delta t$.

# Chapter 9

# Conclusions and Future Work

The work in this dissertation looks at the remote navigation problem from the human and automatic controller perspectives. Below, in Section 9.1, we discuss ways in which this work has met its stated goals. In Section 9.2, we discuss future directions in more detail.

## 9.1 Fulfillment of Stated Goals

In the introduction we laid out two broad goals for our work. The first was to learn from the study of humans how to improve fully autonomous remote navigation. The second was to glean insight that will allow better controllers to be designed for the situation where there is a human in the remote navigation control loop. We revisit these goals now to consider what contributions our work has made in these areas.

### 9.1.1 Insights from human remote navigation that can be applied to fully autonomous navigation

In this category our work makes four comments.

1. Time/Distance optimizing paths are not the most robust.

   The original receding horizon control created paths that ran aggressively close to the obstacles. As long as there was no uncertainty, this behavior was fine and produced good completion time and success rate results. When uncertainty in the form of unmolded feedback delay was introduced, however, performance

dropped significantly. The lesson here for application to autonomous navigators is that broader context needs to be considered before making a simple choice to optimize path length or completion time. A simple path length optimizing approach may work fine in simulation, but our study showed that it was brittle and extremely sensitive to perturbation that is found in real applications.

2. Robustness for a receding horizon controller can be improved by making changes only to the objective function.

   In our study, the only difference between the original and human-like receding horizon controller was found in the objective function. We showed that statistically significant improvements in robustness to delay uncertainty could be achieved simply by making contextually smart additions to the objective function. While every application and its context will differ, the three terms we developed — obstacle avoidance, speed limit and stop-to-turn — can be a starting point for other researchers.

3. Following a human strategy for dealing with delay, full robustness can be recovered for the receding horizon controller navigating a kinematic vehicle.

   The human operators were observed to make more and more frequent stops as feedback delay increased. By comparing the before and after stop heading error, it appeared the human operators were using the stops to help maintain or regain control, especially for cases with high feedback delay. This observation led us to develop a new constraint for the receding horizon controller which imitated the human's strategy. We showed through analysis and simulation that this new constraint resulted in the complete recovery of the controller's path performance for *any* delay less than a threshold (which is chosen by the designer). The drawback of this approach is that the receding horizon controller, like the humans, makes frequent stops. These stops result in a choppy speed profile.

4. A method for training a receding horizon controller to perform the navigation task in a human-like way, was developed.

   The methodology we employ, the specific terms we designed for addition to the objective function, and the path comparison metric are all developments unique to this work. It should be noted that while they are unique, they are also inspired by much similar work, noted in the citations given throughout the text. The method we develop (for training a receding horizon controller from human path data to perform the navigation task) stands complete, produces statistically significant learning (as measured by improvement from the baseline and greater similarity of paths to humans), and captures human-like behavior. It serves as a starting point for future researchers or practitioners.

### 9.1.2 Insights that will help researchers design smarter controllers for situations when humans are in the navigation control loop

We again mention four areas of contribution: two of them are not finished and represent future research directions. These will be dealt with more fully in the next section.

1. We have measured the impact of time delay on 5 metrics of human performance and characterized the impact as linear or superlinear.

   The human operator data was analyzed for the perspective of five independent performance metrics to assess the impact of feedback delay. The metrics were chosen to capture various elements of the remote navigation task that might be of interest to a researcher developing a human in-the-loop remote navigation platform. By characterizing the impact of increasing feedback delay on each metric as either linear or superliner, we provide insight that can inform engineering decisions based on the context of the task to be accomplished.

2. Humans are robust.

   Humans are robust and they are better at dealing with delay than the original receding horizon controller that we introduced. Because of their robust ability to adapt, humans will continue to be considered for inclusion in remote navigation control applications.

3. Maps verses automation.

   See future work, Section 9.2.

4. Experimentally establishing the delay level at which humans switch their compensatory strategy.

   See future work, Section 9.2.

## 9.2 Future Work

In this section we discuss two ideas for future research. The Maze Study has been partially carried out although final data processing is yet to be completed. The Thresholding Study is an idea for experimentally establishing specific levels of feedback delay for which humans change their compensation strategy.

### 9.2.1 Maze Study

One objective of this study is to help quantify the impact of map data and navigation automation on a human operator's performance of a remote search and spatial learning task. The maze study involved human subjects and real robotic hardware. A maze was constructed through which wirelessly controlled robots were navigated by human operators. The robot relayed a video feed to the operators. The human's task was to find and identify two types of targets located throughout the maze. Upon seeing a target, the human depressed a button to signal that they had seen a target come into view. At the end of the trial, the operators were asked to place marks on a map indicating the location of the targets. The study followed a factorial design: *map given to humans* (Yes, No), *level of automation* (driver, passive viewer), *and target type* (color, text, distractor). Performance was measured by three metrics: *button press accuracy* (discrete), *response time* (continuous), and *memory accuracy* (discrete).

This work is related to how humans update their spatial understandings of environments, an area that my co-advisor Frances Wang has been publishing in for some time [65, 66]. This study was jointly done with Whitney Street, a psychology graduate student at the University of Illinois, and a manuscript is being prepared for release. Detailed analysis of the data and conclusions will appear in this manuscript. Here we simply note that the preliminary data analysis suggests an interaction between the level of map data presented, level of driver involvement, and performance of the task.

### 9.2.2 Human Strategy Threshold for Feedback Delay

In this follow-on study, we would like to better understand how and why humans tradeoff between the strategies of stop-and-wait and go-slow. To better understand this, we could simply run additional experiments using the setup we already have for collecting human navigation data. We'd select to run these new experiments at several new values of delay, above and below the values for which we have currently collected data. We would need to develop quantitative measures by which to categorize a particular human path as having been executed by either the stop-and-wait or go-slow strategy.

## 9.3 Conclusion

In this work a provably convergent receding horizon controller formulation that deals with obstacles is presented. Human navigation data was collected and compared to data from the receding horizon controller. Key differences were noted and a human-like receding horizon controller was trained. We show through experiments and analysis that the human-like receding horizon controller indeed produces paths that are human-like. Moreover, the success rates of the human-like controller surpassed not only the baseline receding horizon controller but also the human operators, even under untrained delay conditions.

Future work will focus on continuing to better understand integration into remote navigation control loops. Using the simulator and analysis tools developed in this paper, we wish to further investigate and quantify how human

strategy and performance change as a function of feedback delay. An investigation that looks into remote navigator map use has already begun. Experimental data has been collected ad post-processing is in progress by collaborators from the psychology department. Another investigation which we see as a natural extension would be to study the interaction between the two identified human methods of coping with delay (stop-and-wait verses go-slow).

# Appendix A Explanation of Simple Linear Regression and the Statistical Significance of the Regression Terms

This study explores 5 measures of human performance (dependent variable) and how they are affected by feedback delay (the independent variable). In Section 7.3 we offered detailed explanation of the 5 metrics, how the data was collected and the implications of the analysis results. In Chapter 7 the analysis is done using SYSTAT, here, in Appendix A, we will describe similar analysis techniques step-by-step. The techniques are tests of statistical significance coupled with linear modeling of the interaction between the dependent and independent variables.

A model can always be fit to a data set with some error. Simply noting that the error is "small" is little justification for the model. To justify fitting any model to data we must show statistically significant connection between changes in the dependent variable and the independent variable. Once this is statistically established, we can begin looking for a model that describes the data well.

The model fitting technique we will use is linear regression. Regression refers to the mathematical technique of comparing dependent variable change with the independent variable, while linear means that the model we fit will be linear in its parameters (though the model need not be linear in the independent variable). Thus, linear regression can be used to fit a one-parameter model (a basic mean), a two-parameter model (linear), or a three parameter model (quadratic), etc. The nature of linear regression means that models with more parameters will always have "error" that is less than or equal to the error of a model with fewer parameters. In this work, model order and number of parameters are related as follows: model order = number of parameter – 1.

Higher order models will always have lower or equal error to lower order models, but what order makes statistically significant sense? To answer this question we use an analysis of variance to compare linear models that was proposed in [18].

## A.1 Establishing Movement in the Data

The first step in the analysis is to show that the dependent variable is experiencing statistically significant change with respect to the independent variable. Because the independent variable is discrete we can establish this by running a one-way ANOVA on Feedback Time Delay. At its most basic level, an ANOVA is a comparison of variance. It compares the variance within groups to the variance between groups. For a discrete independent variable, the ANOVA answers the question of how likely it is that the sets of dependent data came from the same

population. In hypothesis structure the question becomes can we reject the Null Hypothesis (NH) in favor of the Alternative Hypothesis (AH). The hypotheses in this case would be formulated as follows:

> NH: The independent variable has had no effect. All the data was drawn from a population with the same mean.
> AH: The independent variable affected the outcome. The data was drawn from populations of varying means.

To make this determination the F-statistic is computed according to standard ANOVA methods [17]. The F-statistic is a ratio of variability:

$$F = \frac{\text{between group variance}}{\text{within group variance}}$$

This statistic comes from a distribution known as the Fisher distribution, and we can determine the likelihood that the NH produced the given data by looking at the CDF of the Fisher distribution. The area to the right of the value of F returned by the ANOVA is the probability of the NH producing more between group variance than we have seen. So this probability is the significance of the test and it is the probability of rejecting the NH incorrectly. We set a significance level for our experiments of 0.05, meaning that if the significance of the test is less than the significance level (0.05), we reject the NH.

Once the ANOVA confirms there is a significant probability that the independent variable is affecting the dependent variable, we can look for a model to capture that interaction.

## A.2 Mean: The One Parameter Model

The general form of regression we use is linear regression based on minimizing the square error between the model and the data. The data will be viewed as a set of paired values: $\{y_i; x_i\}$ where $i$ goes from one up to the number of data points we have. The model we are using is expressed as follows:

$$y = X\beta + \varepsilon \tag{1}$$

The variables take the form,

$$X = \begin{bmatrix} (x_i)^0 & (x_i)^1 & \cdots & (x_i)^p \\ \vdots & \vdots & & \vdots \\ (x_N)^0 & (x_N)^1 & \cdots & (x_N)^p \end{bmatrix} \qquad y = \begin{bmatrix} y_1 \\ \vdots \\ y_N \end{bmatrix}$$

$$\beta = \begin{bmatrix} \beta_0 & \beta_1 & \cdots & \beta_p \end{bmatrix} \qquad \varepsilon = \begin{bmatrix} \varepsilon_i \\ \vdots \\ \varepsilon_N \end{bmatrix}$$

where $p$ is the order of the model. For each data point the individual error between the model and the value is given by $\varepsilon_i$. This is the distance between the model and the data as shown in Figure A.1.

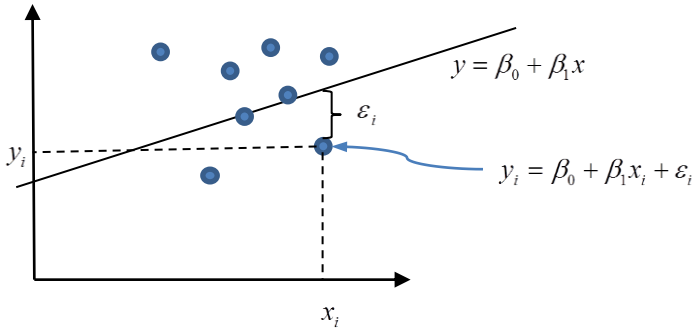


**Figure A.1** The error term is illustrated as the vertical distance between the data point and the model.

The regression takes place when values for beta are found that minimize the error. We choose to minimize the sum of the squared error, leading to a least-squares regression fit. This error is given as follows:

$$RSS = \sum_i (\varepsilon_i)^2 = \varepsilon^T \varepsilon$$

The formula for the $\beta$ minimizing RSS for a given data set $\{y_i; x_i\}$ *for* $i = 1{:}\,N$ is given by the following:

$$\beta = (X^T X)^{-1} X^T y\,.$$

This value is found by setting the derivative of the square error (as a function of $\beta$) equal to zero and solving for $\beta$. Even for fitting higher order models, like quadratic, we can still use the simple linear regression because the regression is still linear in the regression variable $\beta$.

For a single parameter model the equation for one data pair becomes as follows:

$$y_i = (x_i)^0 \beta_0 + \varepsilon_i = \beta_0 + \varepsilon_i .$$

The vectorized version follows the form of equation (1) and the variables are as follows:

$$X = \begin{bmatrix} (x_i)^0 & (x_i)^1 & \cdots & (x_i)^p \\ \vdots & \vdots & & \vdots \\ (x_N)^0 & (x_N)^1 & \cdots & (x_N)^p \end{bmatrix} = \begin{bmatrix} 1 \\ 1 \\ 1 \end{bmatrix}$$

$$\beta = [\beta_0]$$

Where $\beta_0$ will become the simple average of the data, see Figure A.2.

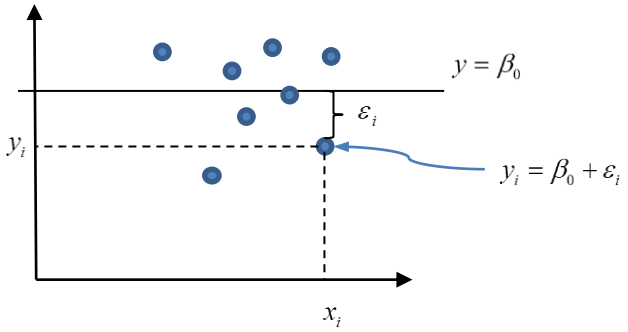


**Figure A.2** The single term model is a simple average. The residuals or error between each data point and the model prediction are captured by $\varepsilon_i$.

The purpose of this single parameter model is to give a point of comparison for us to use when justifying the two-parameter linear model discussed in the next section. In the event that variance analysis rejects the single-parameter model in favor of a higher order model no additional consideration is needed. If the variance analysis fails to reject the single-parameter model, additional questions about the data must be considered. In our study the single-parameter model was rejected in favor of a higher order model for all 5 metrics.

## A.3 Linear Model: The Two-Parameter Fit

Adding a parameter takes the model from a simple description of the data as a mean to describing the data as a line with a slope. The model becomes as follows:

$$y_i = (x_i)^0 \beta_0 + (x_i)^1 \beta_1 + \varepsilon_i$$

which is pictured in Figure A.1. For the vectorized version,

$$X = \begin{bmatrix} (x_i)^0 & (x_i)^1 & \cdots & (x_i)^p \\ \vdots & \vdots & & \vdots \\ (x_N)^0 & (x_N)^1 & \cdots & (x_N)^p \end{bmatrix} = \begin{bmatrix} 1 & x_i \\ 1 & \vdots \\ 1 & x_N \end{bmatrix} \text{ and,}$$

$$\beta = \begin{bmatrix} \beta_0 & \beta_1 \end{bmatrix}.$$

The linear model will have a smaller RSS than the mean model, but to determine the significance of this reduction, variance analysis must be carried out.

To compare the two models we first state the comparison in hypothesis form:

NH: $y_i = (x_i)^0 \beta_0 + \varepsilon_i$

AH: $y_i = (x_i)^0 \beta_0 + (x_i)^1 \beta_1 + \varepsilon_i$

The following analysis was adapted from [Book2]. Significance will again be read from a Fisher distribution, which is a function of the numerator and denominator degrees of freedom in the computation of the F value given by

$$F = \frac{(RSS_{NH} - RSS_{AH}) / (df_{NH} - df_{AH})}{RSS_{AH} / df_{AH}}$$

where the degrees of freedom for the Null Hypothesis, $df_{NH}$, is simply the number of parameters used in the regression, so for this case 1. The degrees of freedom for the Alternative Hypothesis are also computed as one less than the number of parameters, or for this case 2.

The Fisher distribution to which the F-value computed will be compared to is as follows:

$$F(df_{NH} - df_{AH}\ ,\ df_{AH}).$$

If the probability of the computed value of F falling at or above this level for the given Fisher distribution is less than the significance level, then we reject the NH.

## A.4 Quadratic Model: The Three-Parameter Fit

When the model has three parameters, a quadratic relationship between the independent variable and the dependent variable can be captured. For three parameters the model equation becomes as follows:

$$y = \beta_0 + x\beta_1 + x^2\beta_2$$

We again use linear regression to find the values of the parameters which will minimize the square of the error between the model and each data point. This error appears as $\varepsilon_i$ in the following equation:

$$y_i = (x_i)^0\beta_0 + (x_i)^1\beta_1 + (x_i)^2\beta_2 + \varepsilon_i$$

Where the stacked versions of $X$ and $\beta$ becomes as follows:

$$X = \begin{bmatrix} 1 & x_i & x_i^2 \\ 1 & \vdots & \vdots \\ 1 & x_i & x_N^2 \end{bmatrix}$$

$$\beta = \begin{bmatrix} \beta_0 & \beta_1 & \beta_2 \end{bmatrix}.$$

After regression, the quadratic model will then be tested against the linear model to determine if the additional term is statistically significant using the procedure explained in Section A.2.3.

Because the independent variable in all this analysis is Feedback Delay, and because the Feedback Delay takes only three values in these experiments all the dependent variable data is ‘stacked’ over just three independent values. These values are 0, 0.2 and 0.4 seconds of feedback delay. Figure A.3 illustrates this.

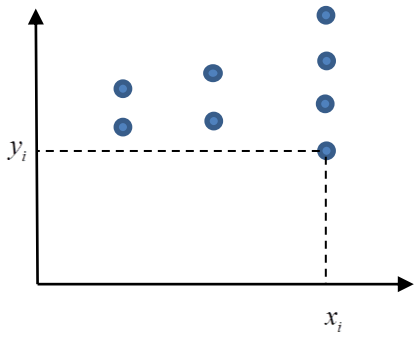


**Figure A.3** Because the independent variable of Feedback Time Delay takes only three values the data is stacked above these values

The fact that there are only 3 values for Feedback Delay and the data in all five cases is monotone means that it does not make sense to fit a model to the data of order beyond quadratic. Mathematically this is because three parameters are sufficient to capture any monotone trend in the three independent variable data. Practically this is the case because a quadratic curve can pass through the mean of each data set, meaning that no better fit is possible, see Figure A.4.

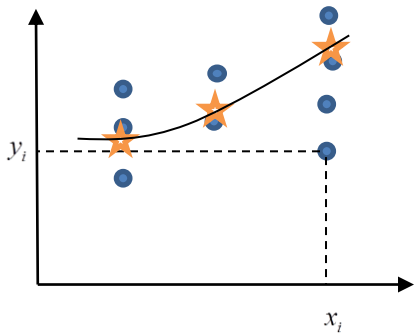


**Figure A.4** Because the independent variable of Feedback Delay takes only three values and the data is monotone a quadratic curve is capable of passing through all three means. In this cartoon the yellow stars represent the mean value of the metric for each Feedback Delay.

Once a model has passed through the means of all the data sets it is impossible for another model to have lower error, thus no higher order model will ever be statically significant compared to the quadratic. Thus we do not attempt to fit any models to the data that are of order higher than quadratic.

# Appendix B Experimental Data from the Study of Feedback Delay Impact on the Human Operator

This Table contains all the raw data used for analysis in Chapter 7. It is given only to provide context for readers.

| | A | B | C | D | E | F | G | H | I | J | K | L | M |
|---|---|---|---|---|---|---|---|---|---|---|---|---|---|
| Notes: | Each line of data represents two human path attempts. Total Successful indicates how many of these attempts were successful. | | | | | | If this column is "0" dependant data will be listed as Not A Number, "NaN" | This is the completion time for successful paths averaged | The median is from zero delay human data, even when compariing to a path with delay. | A stop is only recorded if there is are at least 10 steps follow the resumption of forward movment. | This is measured by computing the heading error at each point on the path and averaging. | This is error based on a window of 10 steps before the stop. For delay cases the window is shifted back by the delay amount. | This error is based on a window of 10 step (.5 sec) following the resumption of forward movment. |
| | Subject | Map | Delay | IC | num obst | concave | Total Successful summed across both paths | Avg Cmpltn Time **(Seconds)** | Average error relative to nearest median human path **(Unitless)** | Number of Stops summed across both paths | Average heading error for two paths, calculated for every point **(Radians)** | Average before stop heading error **(Radians)** | Average after stop heading error **(Radians)** |
| | 4 | 1 | 1 | 1 | 1 | 0 | 2 | 6.23 | 585 | 0 | 0.70 | 0.00 | 0.00 |
| | 4 | 1 | 1 | 2 | 1 | 0 | 2 | 5.65 | 641 | 0 | 0.56 | 0.00 | 0.00 |
| | 4 | 1 | 1 | 3 | 1 | 0 | 1 | 5.65 | 422 | 0 | 0.66 | 0.00 | 0.00 |
| | 4 | 1 | 1 | 4 | 1 | 0 | 2 | 4.75 | 449 | 0 | 0.42 | 0.00 | 0.00 |
| | 4 | 1 | 2 | 1 | 1 | 0 | 2 | 7.03 | 397 | 0 | 0.65 | 0.00 | 0.00 |
| | 4 | 1 | 2 | 2 | 1 | 0 | 2 | 7.15 | 736 | 0 | 0.87 | 0.00 | 0.00 |
| | 4 | 1 | 2 | 3 | 1 | 0 | 2 | 9.63 | 667 | 0 | 0.87 | 0.00 | 0.00 |
| | 4 | 1 | 2 | 4 | 1 | 0 | 2 | 6.18 | 499 | 0 | 0.72 | 0.00 | 0.00 |
| | 4 | 1 | 3 | 1 | 1 | 0 | 2 | 10.55 | 782 | 1 | 0.79 | 0.54 | 0.03 |
| | 4 | 1 | 3 | 2 | 1 | 0 | 2 | 15.65 | 1242 | 6 | 0.95 | 0.57 | 0.38 |
| | 4 | 1 | 3 | 3 | 1 | 0 | 2 | 9.43 | 785 | 0 | 0.87 | 0.00 | 0.00 |
| | 4 | 1 | 3 | 4 | 1 | 0 | 2 | 14.90 | 1038 | 6 | 0.83 | 1.38 | 0.38 |
| | 4 | 2 | 1 | 1 | 2 | 0 | 2 | 10.10 | 1131 | 1 | 1.04 | 1.26 | 0.61 |
| | 4 | 2 | 1 | 2 | 2 | 0 | 2 | 7.58 | 531 | 0 | 0.87 | 0.00 | 0.00 |
| | 4 | 2 | 1 | 3 | 2 | 0 | 2 | 5.53 | 278 | 0 | 0.46 | 0.00 | 0.00 |
| | 4 | 2 | 1 | 4 | 2 | 0 | 2 | 6.15 | 474 | 0 | 0.62 | 0.00 | 0.00 |
| | 4 | 2 | 2 | 1 | 2 | 0 | 2 | 12.95 | 669 | 3 | 0.94 | 0.38 | 0.40 |
| | 4 | 2 | 2 | 2 | 2 | 0 | 1 | 6.90 | 967 | 0 | 0.65 | 0.00 | 0.00 |
| | 4 | 2 | 2 | 3 | 2 | 0 | 2 | 8.40 | 497 | 0 | 0.83 | 0.00 | 0.00 |
| | 4 | 2 | 2 | 4 | 2 | 0 | 2 | 8.75 | 880 | 1 | 0.92 | 1.11 | 0.25 |
| | 4 | 2 | 3 | 1 | 2 | 0 | 2 | 15.53 | 1008 | 3 | 1.01 | 0.82 | 0.16 |
| | 4 | 2 | 3 | 2 | 2 | 0 | 2 | 19.50 | 723 | 8 | 0.88 | 0.67 | 0.40 |
| | 4 | 2 | 3 | 3 | 2 | 0 | 2 | 25.40 | 1100 | 9 | 1.06 | 1.51 | 0.82 |
| | 4 | 2 | 3 | 4 | 2 | 0 | 2 | 20.08 | 1233 | 6 | 1.05 | 1.75 | 0.81 |
| | 4 | 3 | 1 | 1 | 1 | 1 | 1 | 8.50 | 457 | 0 | 0.92 | 0.00 | 0.00 |
| | 4 | 3 | 1 | 2 | 1 | 1 | 2 | 5.50 | 107 | 0 | 0.54 | 0.00 | 0.00 |
| | 4 | 3 | 1 | 3 | 1 | 1 | 1 | 5.95 | 326 | 0 | 0.69 | 0.00 | 0.00 |
| | 4 | 3 | 1 | 4 | 1 | 1 | 2 | 5.18 | 439 | 0 | 0.49 | 0.00 | 0.00 |
| | 4 | 3 | 2 | 1 | 1 | 1 | 2 | 11.80 | 1014 | 1 | 1.07 | 0.63 | 0.77 |
| | 4 | 3 | 2 | 2 | 1 | 1 | 2 | 9.98 | 420 | 1 | 0.70 | 0.26 | 0.38 |
| | 4 | 3 | 2 | 3 | 1 | 1 | 2 | 7.00 | 256 | 0 | 0.70 | 0.00 | 0.00 |
| | 4 | 3 | 2 | 4 | 1 | 1 | 2 | 5.73 | 575 | 0 | 0.56 | 0.00 | 0.00 |
| | 4 | 3 | 3 | 1 | 1 | 1 | 1 | 26.30 | 1568 | 4 | 1.27 | 1.80 | 0.43 |
| | 4 | 3 | 3 | 2 | 1 | 1 | 1 | 13.50 | 1598 | 1 | 1.02 | 1.36 | 0.34 |
| | 4 | 3 | 3 | 3 | 1 | 1 | 2 | 11.60 | 951 | 1 | 0.79 | 0.50 | 0.18 |
| | 4 | 3 | 3 | 4 | 1 | 1 | 2 | 24.70 | 1696 | 10 | 0.99 | 1.88 | 0.74 |
| | 4 | 4 | 1 | 1 | 2 | 1 | 2 | 9.38 | 605 | 2 | 0.94 | 0.92 | 0.43 |
| | 4 | 4 | 1 | 2 | 2 | 1 | 2 | 5.30 | 227 | 0 | 0.54 | 0.00 | 0.00 |
| | 4 | 4 | 1 | 3 | 2 | 1 | 2 | 14.78 | 684 | 6 | 0.93 | 0.63 | 0.48 |
| | 4 | 4 | 1 | 4 | 2 | 1 | 2 | 7.80 | 568 | 0 | 0.84 | 0.00 | 0.00 |
| | 4 | 4 | 2 | 1 | 2 | 1 | 2 | 13.00 | 934 | 2 | 1.02 | 1.55 | 1.75 |
| | 4 | 4 | 2 | 2 | 2 | 1 | 2 | 8.80 | 443 | 1 | 0.85 | 0.36 | 0.31 |
| | 4 | 4 | 2 | 3 | 2 | 1 | 2 | 8.83 | 586 | 1 | 0.72 | 0.36 | 0.66 |
| | 4 | 4 | 2 | 4 | 2 | 1 | 2 | 13.50 | 1008 | 1 | 1.04 | 1.14 | 0.19 |
| | 4 | 4 | 3 | 1 | 2 | 1 | 2 | 31.60 | 979 | 11 | 1.07 | 0.91 | 0.57 |
| | 4 | 4 | 3 | 2 | 2 | 1 | 2 | 16.88 | 602 | 3 | 0.70 | 0.66 | 0.20 |
| | 4 | 4 | 3 | 3 | 2 | 1 | 2 | 13.05 | 782 | 5 | 0.81 | 0.93 | 0.41 |
| | 4 | 4 | 3 | 4 | 2 | 1 | 2 | 23.68 | 1090 | 12 | 1.06 | 1.59 | 0.77 |
| | 5 | 1 | 1 | 1 | 1 | 0 | 2 | 7.85 | 417 | 0 | 0.50 | 0.00 | 0.00 |
| | 5 | 1 | 1 | 2 | 1 | 0 | 2 | 7.70 | 711 | 0 | 0.68 | 0.00 | 0.00 |
| | 5 | 1 | 1 | 3 | 1 | 0 | 2 | 6.00 | 214 | 1 | 0.41 | 0.11 | 0.17 |
| | 5 | 1 | 1 | 4 | 1 | 0 | 2 | 8.68 | 704 | 6 | 0.69 | 0.66 | 0.36 |
| | 5 | 1 | 2 | 1 | 1 | 0 | 2 | 8.68 | 678 | 0 | 0.91 | 0.00 | 0.00 |
| | 5 | 1 | 2 | 2 | 1 | 0 | 2 | 8.05 | 629 | 1 | 0.80 | 0.73 | 0.46 |
| | 5 | 1 | 2 | 3 | 1 | 0 | 2 | 9.55 | 493 | 3 | 0.71 | 0.94 | 0.74 |
| | 5 | 1 | 2 | 4 | 1 | 0 | 2 | 5.45 | 275 | 0 | 0.50 | 0.00 | 0.00 |
| | 5 | 1 | 3 | 1 | 1 | 0 | 2 | 25.33 | 954 | 6 | 1.10 | 1.35 | 0.77 |
| | 5 | 1 | 3 | 2 | 1 | 0 | 2 | 14.40 | 766 | 4 | 0.87 | 1.15 | 0.61 |
| | 5 | 1 | 3 | 3 | 1 | 0 | 2 | 28.63 | 927 | 11 | 1.05 | 1.54 | 0.64 |
| | 5 | 1 | 3 | 4 | 1 | 0 | 1 | 13.20 | 595 | 2 | 0.83 | 1.38 | 0.68 |
| | 5 | 2 | 1 | 1 | 2 | 0 | 2 | 8.43 | 245 | 0 | 0.74 | 0.00 | 0.00 |
| | 5 | 2 | 1 | 2 | 2 | 0 | 2 | 7.00 | 329 | 1 | 0.53 | 0.17 | 0.02 |
| | 5 | 2 | 1 | 3 | 2 | 0 | 2 | 11.00 | 501 | 5 | 0.68 | 0.45 | 0.17 |
| | 5 | 2 | 1 | 4 | 2 | 0 | 2 | 7.18 | 161 | 0 | 0.57 | 0.00 | 0.00 |
| | 5 | 2 | 2 | 1 | 2 | 0 | 2 | 11.45 | 1217 | 4 | 0.86 | 1.23 | 0.43 |
| | 5 | 2 | 2 | 2 | 2 | 0 | 2 | 9.33 | 439 | 1 | 0.73 | 0.28 | 0.47 |
| | 5 | 2 | 2 | 3 | 2 | 0 | 2 | 14.53 | 1104 | 6 | 0.95 | 0.73 | 0.54 |
| | 5 | 2 | 2 | 4 | 2 | 0 | 2 | 9.25 | 764 | 0 | 0.91 | 0.00 | 0.00 |
| | 5 | 2 | 3 | 1 | 2 | 0 | 2 | 13.80 | 726 | 5 | 0.92 | 1.22 | 0.37 |
| | 5 | 2 | 3 | 2 | 2 | 0 | 2 | 12.03 | 638 | 4 | 0.67 | 1.28 | 0.29 |
| | 5 | 2 | 3 | 3 | 2 | 0 | 1 | 10.60 | 510 | 0 | 0.78 | 0.00 | 0.00 |
| | 5 | 2 | 3 | 4 | 2 | 0 | 2 | 10.65 | 645 | 2 | 0.74 | 1.84 | 0.21 |
| | 5 | 3 | 1 | 1 | 1 | 1 | 2 | 7.08 | 310 | 0 | 0.65 | 0.00 | 0.00 |
| | 5 | 3 | 1 | 2 | 1 | 1 | 2 | 7.08 | 147 | 0 | 0.65 | 0.00 | 0.00 |
| | 5 | 3 | 1 | 3 | 1 | 1 | 2 | 13.18 | 711 | 9 | 0.68 | 0.96 | 0.37 |
| | 5 | 3 | 1 | 4 | 1 | 1 | 2 | 5.85 | 379 | 0 | 0.36 | 0.00 | 0.00 |
| | 5 | 3 | 2 | 1 | 1 | 1 | 2 | 9.48 | 472 | 4 | 0.59 | 0.89 | 0.20 |
| | 5 | 3 | 2 | 2 | 1 | 1 | 2 | 9.40 | 795 | 0 | 1.08 | 0.00 | 0.00 |
| | 5 | 3 | 2 | 3 | 1 | 1 | 2 | 8.55 | 435 | 1 | 0.60 | 0.24 | 0.12 |
| | 5 | 3 | 2 | 4 | 1 | 1 | 2 | 7.95 | 502 | 3 | 0.46 | 0.27 | 0.33 |
| | 5 | 3 | 3 | 1 | 1 | 1 | 2 | 11.70 | 466 | 3 | 0.67 | 1.10 | 0.38 |
| | 5 | 3 | 3 | 2 | 1 | 1 | 2 | 14.40 | 906 | 12 | 0.68 | 0.98 | 0.37 |
| | 5 | 3 | 3 | 3 | 1 | 1 | 2 | 17.63 | 876 | 6 | 0.85 | 0.97 | 0.53 |
| | 5 | 3 | 3 | 4 | 1 | 1 | 2 | 9.33 | 659 | 3 | 0.59 | 0.70 | 0.19 |
| | 5 | 4 | 1 | 1 | 2 | 1 | 2 | 7.90 | 210 | 0 | 0.89 | 0.00 | 0.00 |
| | 5 | 4 | 1 | 2 | 2 | 1 | 2 | 8.28 | 341 | 3 | 0.64 | 0.50 | 0.31 |
| | 5 | 4 | 1 | 3 | 2 | 1 | 2 | 8.13 | 532 | 1 | 0.77 | 0.53 | 0.47 |
| | 5 | 4 | 1 | 4 | 2 | 1 | 2 | 6.35 | 457 | 0 | 0.63 | 0.00 | 0.00 |
| | 5 | 4 | 2 | 1 | 2 | 1 | 2 | 11.50 | 551 | 4 | 0.97 | 1.69 | 0.93 |
| | 5 | 4 | 2 | 2 | 2 | 1 | 1 | 10.00 | 473 | 2 | 0.82 | 1.21 | 0.17 |
| | 5 | 4 | 2 | 3 | 2 | 1 | 2 | 7.98 | 438 | 2 | 0.70 | 0.21 | 0.07 |
| | 5 | 4 | 2 | 4 | 2 | 1 | 2 | 13.83 | 1078 | 3 | 1.06 | 1.22 | 0.48 |
| | 5 | 4 | 3 | 1 | 2 | 1 | 2 | 17.78 | 725 | 13 | 0.98 | 1.36 | 0.71 |
| | 5 | 4 | 3 | 2 | 2 | 1 | 1 | 16.15 | 731 | 8 | 0.86 | 1.44 | 0.89 |
| | 5 | 4 | 3 | 3 | 2 | 1 | 1 | 12.20 | 633 | 2 | 0.74 | 0.59 | 0.29 |

Continued:

| | | | | | | | | | | | | |
|---|---|---|---|---|---|---|---|---|---|---|---|---|
| 5 | 4 | 3 | 4 | 2 | 1 | 1 | 10.40 | 559 | 1 | 0.79 | 0.97 | 0.14 |
| 6 | 1 | 1 | 1 | 1 | 0 | 2 | 5.10 | 175 | 0 | 0.46 | 0.00 | 0.00 |
| 6 | 1 | 1 | 2 | 1 | 0 | 2 | 5.55 | 382 | 0 | 0.50 | 0.00 | 0.00 |
| 6 | 1 | 1 | 3 | 1 | 0 | 2 | 6.08 | 155 | 0 | 0.56 | 0.00 | 0.00 |
| 6 | 1 | 1 | 4 | 1 | 0 | 2 | 4.73 | 201 | 0 | 0.30 | 0.00 | 0.00 |
| 6 | 1 | 2 | 1 | 1 | 0 | 2 | 5.48 | 392 | 0 | 0.57 | 0.00 | 0.00 |
| 6 | 1 | 2 | 2 | 1 | 0 | 2 | 7.15 | 533 | 0 | 0.86 | 0.00 | 0.00 |
| 6 | 1 | 2 | 3 | 1 | 0 | 2 | 7.50 | 560 | 0 | 0.81 | 0.00 | 0.00 |
| 6 | 1 | 2 | 4 | 1 | 0 | 2 | 8.20 | 623 | 0 | 0.92 | 0.00 | 0.00 |
| 6 | 1 | 3 | 1 | 1 | 0 | 2 | 16.93 | 1108 | 8 | 0.84 | 1.23 | 0.37 |
| 6 | 1 | 3 | 2 | 1 | 0 | 2 | 12.73 | 817 | 4 | 0.78 | 1.37 | 0.39 |
| 6 | 1 | 3 | 3 | 1 | 0 | 2 | 18.18 | 740 | 10 | 1.01 | 0.83 | 1.28 |
| 6 | 1 | 3 | 4 | 1 | 0 | 2 | 13.88 | 1135 | 5 | 0.79 | 1.36 | 0.24 |
| 6 | 2 | 1 | 1 | 2 | 0 | 2 | 5.88 | 490 | 0 | 0.63 | 0.00 | 0.00 |
| 6 | 2 | 1 | 2 | 2 | 0 | 2 | 7.33 | 235 | 1 | 0.60 | 0.61 | 0.57 |
| 6 | 2 | 1 | 3 | 2 | 0 | 2 | 6.60 | 233 | 0 | 0.52 | 0.00 | 0.00 |
| 6 | 2 | 1 | 4 | 2 | 0 | 2 | 5.78 | 407 | 0 | 0.58 | 0.00 | 0.00 |
| 6 | 2 | 2 | 1 | 2 | 0 | 2 | 9.30 | 508 | 2 | 0.84 | 0.83 | 0.16 |
| 6 | 2 | 2 | 2 | 2 | 0 | 2 | 6.03 | 224 | 0 | 0.48 | 0.00 | 0.00 |
| 6 | 2 | 2 | 3 | 2 | 0 | 2 | 6.60 | 228 | 0 | 0.55 | 0.00 | 0.00 |
| 6 | 2 | 2 | 4 | 2 | 0 | 2 | 8.08 | 825 | 0 | 0.82 | 0.00 | 0.00 |
| 6 | 2 | 3 | 1 | 2 | 0 | 2 | 16.10 | 840 | 5 | 0.90 | 0.50 | 0.39 |
| 6 | 2 | 3 | 2 | 2 | 0 | 2 | 16.60 | 731 | 10 | 0.81 | 1.78 | 0.48 |
| 6 | 2 | 3 | 3 | 2 | 0 | 2 | 30.10 | 819 | 10 | 0.93 | 1.06 | 0.60 |
| 6 | 2 | 3 | 4 | 2 | 0 | 2 | 9.83 | 771 | 3 | 0.71 | 1.09 | 0.85 |
| 6 | 3 | 1 | 1 | 1 | 1 | 2 | 6.48 | 130 | 0 | 0.54 | 0.00 | 0.00 |
| 6 | 3 | 1 | 2 | 1 | 1 | 2 | 5.93 | 384 | 0 | 0.63 | 0.00 | 0.00 |
| 6 | 3 | 1 | 3 | 1 | 1 | 2 | 6.88 | 328 | 0 | 0.73 | 0.00 | 0.00 |
| 6 | 3 | 1 | 4 | 1 | 1 | 2 | 4.60 | 278 | 0 | 0.46 | 0.00 | 0.00 |
| 6 | 3 | 2 | 1 | 1 | 1 | 2 | 11.28 | 576 | 4 | 0.70 | 1.58 | 0.70 |
| 6 | 3 | 2 | 2 | 1 | 1 | 2 | 8.38 | 424 | 0 | 0.69 | 0.00 | 0.00 |
| 6 | 3 | 2 | 3 | 1 | 1 | 2 | 7.35 | 377 | 0 | 0.67 | 0.00 | 0.00 |
| 6 | 3 | 2 | 4 | 1 | 1 | 2 | 5.53 | 393 | 0 | 0.69 | 0.00 | 0.00 |
| 6 | 3 | 3 | 1 | 1 | 1 | 2 | 12.13 | 574 | 2 | 0.75 | 1.18 | 0.62 |
| 6 | 3 | 3 | 2 | 1 | 1 | 2 | 16.33 | 583 | 6 | 0.93 | 1.14 | 0.82 |
| 6 | 3 | 3 | 3 | 1 | 1 | 2 | 13.75 | 663 | 5 | 0.86 | 1.55 | 0.60 |
| 6 | 3 | 3 | 4 | 1 | 1 | 2 | 7.05 | 565 | 0 | 0.58 | 0.00 | 0.00 |
| 6 | 4 | 1 | 1 | 2 | 1 | 1 | 5.80 | 565 | 0 | 0.53 | 0.00 | 0.00 |
| 6 | 4 | 1 | 2 | 2 | 1 | 2 | 6.20 | 122 | 0 | 0.58 | 0.00 | 0.00 |
| 6 | 4 | 1 | 3 | 2 | 1 | 2 | 9.08 | 210 | 0 | 0.84 | 0.00 | 0.00 |
| 6 | 4 | 1 | 4 | 2 | 1 | 2 | 6.03 | 409 | 0 | 0.84 | 0.00 | 0.00 |
| 6 | 4 | 2 | 1 | 2 | 1 | 2 | 14.73 | 976 | 3 | 0.98 | 0.73 | 0.85 |
| 6 | 4 | 2 | 2 | 2 | 1 | 2 | 9.00 | 328 | 2 | 0.70 | 0.63 | 0.30 |
| 6 | 4 | 2 | 3 | 2 | 1 | 2 | 8.18 | 463 | 2 | 0.64 | 0.49 | 0.18 |
| 6 | 4 | 2 | 4 | 2 | 1 | 2 | 9.73 | 891 | 2 | 0.80 | 0.34 | 0.18 |
| 6 | 4 | 3 | 1 | 2 | 1 | 2 | 16.60 | 755 | 7 | 0.97 | 1.70 | 0.67 |
| 6 | 4 | 3 | 2 | 2 | 1 | 2 | 14.25 | 1076 | 4 | 0.68 | 1.08 | 0.36 |
| 6 | 4 | 3 | 3 | 2 | 1 | 2 | 11.73 | 696 | 2 | 0.79 | 1.05 | 0.20 |
| 6 | 4 | 3 | 4 | 2 | 1 | 2 | 16.90 | 874 | 7 | 0.90 | 1.31 | 0.84 |
| 8 | 1 | 1 | 1 | 1 | 0 | 2 | 7.13 | 313 | 0 | 0.34 | 0.00 | 0.00 |
| 8 | 1 | 1 | 2 | 1 | 0 | 2 | 5.50 | 447 | 0 | 0.40 | 0.00 | 0.00 |
| 8 | 1 | 1 | 3 | 1 | 0 | 2 | 6.48 | 412 | 0 | 0.46 | 0.00 | 0.00 |
| 8 | 1 | 1 | 4 | 1 | 0 | 2 | 5.15 | 260 | 0 | 0.30 | 0.00 | 0.00 |
| 8 | 1 | 2 | 1 | 1 | 0 | 2 | 7.65 | 517 | 0 | 0.76 | 0.00 | 0.00 |
| 8 | 1 | 2 | 2 | 1 | 0 | 2 | 5.83 | 455 | 0 | 0.42 | 0.00 | 0.00 |
| 8 | 1 | 2 | 3 | 1 | 0 | 2 | 7.28 | 381 | 1 | 0.44 | 0.66 | 0.35 |
| 8 | 1 | 2 | 4 | 1 | 0 | 2 | 5.48 | 307 | 0 | 0.26 | 0.00 | 0.00 |
| 8 | 1 | 3 | 1 | 1 | 0 | 2 | 21.15 | 931 | 7 | 0.88 | 0.86 | 0.61 |
| 8 | 1 | 3 | 2 | 1 | 0 | 2 | 9.73 | 1188 | 0 | 0.93 | 0.00 | 0.00 |
| 8 | 1 | 3 | 3 | 1 | 0 | 2 | 11.80 | 555 | 1 | 0.57 | 0.54 | 0.04 |
| 8 | 1 | 3 | 4 | 1 | 0 | 2 | 20.78 | 1549 | 11 | 0.94 | 0.86 | 0.79 |
| 8 | 2 | 1 | 1 | 2 | 0 | 2 | 7.73 | 207 | 0 | 0.50 | 0.00 | 0.00 |
| 8 | 2 | 1 | 2 | 2 | 0 | 2 | 6.65 | 353 | 0 | 0.44 | 0.00 | 0.00 |
| 8 | 2 | 1 | 3 | 2 | 0 | 2 | 8.35 | 710 | 1 | 0.57 | 0.33 | 1.00 |
| 8 | 2 | 1 | 4 | 2 | 0 | 2 | 7.95 | 824 | 0 | 0.86 | 0.00 | 0.00 |
| 8 | 2 | 2 | 1 | 2 | 0 | 2 | 8.53 | 216 | 0 | 0.54 | 0.00 | 0.00 |
| 8 | 2 | 2 | 2 | 2 | 0 | 2 | 6.98 | 377 | 0 | 0.41 | 0.00 | 0.00 |
| 8 | 2 | 2 | 3 | 2 | 0 | 2 | 6.30 | 472 | 0 | 0.57 | 0.00 | 0.00 |
| 8 | 2 | 2 | 4 | 2 | 0 | 2 | 7.40 | 447 | 0 | 0.78 | 0.00 | 0.00 |
| 8 | 2 | 3 | 1 | 2 | 0 | 1 | 11.00 | 288 | 0 | 0.57 | 0.00 | 0.00 |
| 8 | 2 | 3 | 2 | 2 | 0 | 2 | 8.65 | 609 | 1 | 0.46 | 0.29 | 0.16 |
| 8 | 2 | 3 | 3 | 2 | 0 | 1 | 8.95 | 542 | 1 | 0.56 | 0.61 | 0.23 |
| 8 | 2 | 3 | 4 | 2 | 0 | 2 | 9.40 | 607 | 1 | 0.87 | 1.23 | 1.34 |
| 8 | 3 | 1 | 1 | 1 | 1 | 2 | 6.08 | 153 | 0 | 0.44 | 0.00 | 0.00 |
| 8 | 3 | 1 | 2 | 1 | 1 | 2 | 5.95 | 270 | 0 | 0.43 | 0.00 | 0.00 |
| 8 | 3 | 1 | 3 | 1 | 1 | 2 | 8.53 | 321 | 1 | 0.87 | 1.26 | 1.09 |
| 8 | 3 | 1 | 4 | 1 | 1 | 2 | 6.58 | 402 | 0 | 0.33 | 0.00 | 0.00 |
| 8 | 3 | 2 | 1 | 1 | 1 | 2 | 7.85 | 302 | 1 | 0.54 | 0.13 | 0.51 |
| 8 | 3 | 2 | 2 | 1 | 1 | 2 | 16.48 | 811 | 2 | 1.01 | 0.44 | 0.44 |
| 8 | 3 | 2 | 3 | 1 | 1 | 2 | 6.78 | 276 | 0 | 0.56 | 0.00 | 0.00 |
| 8 | 3 | 2 | 4 | 1 | 1 | 2 | 5.13 | 208 | 0 | 0.44 | 0.00 | 0.00 |
| 8 | 3 | 3 | 1 | 1 | 1 | 2 | 9.15 | 445 | 1 | 0.62 | 0.82 | 0.02 |
| 8 | 3 | 3 | 2 | 1 | 1 | 1 | 13.95 | 676 | 2 | 0.92 | 1.40 | 1.12 |
| 8 | 3 | 3 | 3 | 1 | 1 | 2 | 9.73 | 542 | 1 | 0.89 | 0.99 | 1.46 |
| 8 | 3 | 3 | 4 | 1 | 1 | 1 | 8.65 | 637 | 1 | 0.78 | 1.29 | 0.17 |
| 8 | 4 | 1 | 1 | 2 | 1 | 2 | 6.35 | 438 | 0 | 0.72 | 0.00 | 0.00 |
| 8 | 4 | 1 | 2 | 2 | 1 | 2 | 7.25 | 364 | 0 | 0.50 | 0.00 | 0.00 |
| 8 | 4 | 1 | 3 | 2 | 1 | 2 | 10.00 | 980 | 2 | 0.85 | 0.94 | 1.04 |
| 8 | 4 | 1 | 4 | 2 | 1 | 2 | 5.93 | 506 | 0 | 0.61 | 0.00 | 0.00 |
| 8 | 4 | 2 | 1 | 2 | 1 | 2 | 6.30 | 468 | 0 | 0.40 | 0.00 | 0.00 |
| 8 | 4 | 2 | 2 | 2 | 1 | 2 | 6.80 | 426 | 0 | 0.71 | 0.00 | 0.00 |
| 8 | 4 | 2 | 3 | 2 | 1 | 2 | 6.35 | 324 | 0 | 0.58 | 0.00 | 0.00 |
| 8 | 4 | 2 | 4 | 2 | 1 | 2 | 6.33 | 504 | 0 | 0.77 | 0.00 | 0.00 |
| 8 | 4 | 3 | 1 | 2 | 1 | 2 | 17.70 | 835 | 2 | 0.97 | 0.89 | 0.76 |
| 8 | 4 | 3 | 2 | 2 | 1 | 2 | 14.08 | 1000 | 4 | 0.90 | 0.80 | 0.41 |
| 8 | 4 | 3 | 3 | 2 | 1 | 2 | 10.30 | 626 | 0 | 0.88 | 0.00 | 0.00 |
| 8 | 4 | 3 | 4 | 2 | 1 | 2 | 18.93 | 856 | 2 | 1.12 | 0.98 | 0.49 |
| 9 | 1 | 1 | 1 | 1 | 0 | 2 | 8.18 | 391 | 2 | 0.54 | 0.79 | 0.39 |
| 9 | 1 | 1 | 2 | 1 | 0 | 2 | 6.88 | 129 | 0 | 0.44 | 0.00 | 0.00 |
| 9 | 1 | 1 | 3 | 1 | 0 | 2 | 9.68 | 485 | 2 | 0.69 | 0.38 | 0.12 |
| 9 | 1 | 1 | 4 | 1 | 0 | 2 | 8.98 | 404 | 1 | 0.39 | 0.56 | 0.13 |
| 9 | 1 | 2 | 1 | 1 | 0 | 2 | 9.73 | 637 | 3 | 0.63 | 0.31 | 0.13 |
| 9 | 1 | 2 | 2 | 1 | 0 | 2 | 10.50 | 496 | 1 | 0.65 | 0.12 | 0.25 |
| 9 | 1 | 2 | 3 | 1 | 0 | 2 | 11.18 | 600 | 5 | 0.57 | 0.97 | 0.27 |
| 9 | 1 | 2 | 4 | 1 | 0 | 2 | 8.05 | 437 | 1 | 0.49 | 0.37 | 0.13 |
| 9 | 1 | 3 | 1 | 1 | 0 | 1 | 10.60 | 689 | 2 | 0.47 | 0.76 | 0.50 |
| 9 | 1 | 3 | 2 | 1 | 0 | 1 | 17.50 | 521 | 3 | 0.68 | 0.66 | 0.31 |
| 9 | 1 | 3 | 3 | 1 | 0 | 2 | 28.58 | 778 | 22 | 0.89 | 1.00 | 0.85 |
| 9 | 1 | 3 | 4 | 1 | 0 | 2 | 10.25 | 723 | 5 | 0.62 | 0.78 | 0.50 |
| 9 | 2 | 1 | 1 | 2 | 0 | 2 | 9.63 | 601 | 4 | 0.71 | 0.65 | 0.45 |
| 9 | 2 | 1 | 2 | 2 | 0 | 2 | 9.45 | 458 | 3 | 0.63 | 0.53 | 0.24 |
| 9 | 2 | 1 | 3 | 2 | 0 | 2 | 12.63 | 687 | 3 | 0.78 | 0.39 | 0.37 |
| 9 | 2 | 1 | 4 | 2 | 0 | 2 | 7.20 | 304 | 0 | 0.58 | 0.00 | 0.00 |
| 9 | 2 | 2 | 1 | 2 | 0 | 2 | 15.10 | 980 | 7 | 0.93 | 1.37 | 0.74 |
| 9 | 2 | 2 | 2 | 2 | 0 | 2 | 16.60 | 956 | 6 | 1.03 | 1.33 | 0.57 |
| 9 | 2 | 2 | 3 | 2 | 0 | 2 | 15.98 | 646 | 4 | 0.63 | 1.18 | 0.31 |
| 9 | 2 | 2 | 4 | 2 | 0 | 2 | 9.20 | 494 | 3 | 0.64 | 0.63 | 0.44 |
| 9 | 2 | 3 | 1 | 2 | 0 | 2 | 20.78 | 841 | 12 | 0.84 | 1.23 | 0.63 |
| 9 | 2 | 3 | 2 | 2 | 0 | 2 | 19.18 | 982 | 8 | 0.99 | 1.44 | 1.01 |
| 9 | 2 | 3 | 3 | 2 | 0 | 1 | 15.55 | 580 | 3 | 0.82 | 1.10 | 0.50 |
| 9 | 2 | 3 | 4 | 2 | 0 | 2 | 15.45 | 1090 | 5 | 0.99 | 1.16 | 0.27 |
| 9 | 3 | 1 | 1 | 1 | 1 | 2 | 9.53 | 379 | 3 | 0.58 | 0.50 | 0.10 |
| 9 | 3 | 1 | 2 | 1 | 1 | 2 | 11.68 | 652 | 0 | 0.71 | 0.00 | 0.00 |
| 9 | 3 | 1 | 3 | 1 | 1 | 2 | 13.13 | 694 | 6 | 0.76 | 1.11 | 0.81 |
| 9 | 3 | 1 | 4 | 1 | 1 | 2 | 8.25 | 432 | 1 | 0.65 | 0.63 | 0.11 |
| 9 | 3 | 2 | 1 | 1 | 1 | 2 | 13.20 | 942 | 5 | 0.82 | 1.68 | 0.84 |
| 9 | 3 | 2 | 2 | 1 | 1 | 2 | 14.20 | 805 | 5 | 0.93 | 0.98 | 0.28 |
| 9 | 3 | 2 | 3 | 1 | 1 | 2 | 11.95 | 489 | 3 | 0.60 | 1.04 | 0.46 |
| 9 | 3 | 2 | 4 | 1 | 1 | 2 | 10.18 | 624 | 3 | 0.54 | 0.98 | 0.16 |
| 9 | 3 | 3 | 1 | 1 | 1 | 2 | 17.48 | 705 | 5 | 0.68 | 0.97 | 0.62 |
| 9 | 3 | 3 | 2 | 1 | 1 | 2 | 15.98 | 551 | 5 | 0.76 | 0.81 | 0.37 |
| 9 | 3 | 3 | 3 | 1 | 1 | 2 | 16.38 | 980 | 8 | 0.66 | 0.96 | 0.40 |
| 9 | 3 | 3 | 4 | 1 | 1 | 2 | 9.88 | 483 | 5 | 0.63 | 1.01 | 0.34 |
| 9 | 4 | 1 | 1 | 2 | 1 | 2 | 11.60 | 521 | 5 | 0.72 | 0.49 | 0.38 |
| 9 | 4 | 1 | 2 | 2 | 1 | 2 | 10.98 | 434 | 3 | 0.56 | 0.90 | 0.43 |
| 9 | 4 | 1 | 3 | 2 | 1 | 2 | 12.48 | 432 | 4 | 0.67 | 1.10 | 0.39 |
| 9 | 4 | 1 | 4 | 2 | 1 | 2 | 12.68 | 294 | 6 | 0.71 | 0.69 | 0.44 |
| 9 | 4 | 2 | 1 | 2 | 1 | 2 | 11.05 | 380 | 1 | 0.43 | 0.57 | 0.40 |
| 9 | 4 | 2 | 2 | 2 | 1 | 2 | 15.13 | 758 | 4 | 0.77 | 1.22 | 0.26 |
| 9 | 4 | 2 | 3 | 2 | 1 | 2 | 13.85 | 781 | 2 | 0.92 | 0.17 | 0.07 |
| 9 | 4 | 2 | 4 | 2 | 1 | 2 | 12.40 | 806 | 4 | 0.85 | 1.52 | 0.40 |
| 9 | 4 | 3 | 1 | 2 | 1 | 2 | 19.45 | 582 | 7 | 0.82 | 1.24 | 0.75 |
| 9 | 4 | 3 | 2 | 2 | 1 | 2 | 22.70 | 1312 | 10 | 0.96 | 1.27 | 0.83 |
| 9 | 4 | 3 | 3 | 2 | 1 | 2 | 18.85 | 897 | 4 | 0.67 | 1.10 | 0.16 |
| 9 | 4 | 3 | 4 | 2 | 1 | 2 | 15.48 | 873 | 5 | 0.87 | 1.15 | 0.82 |
| 10 | 1 | 1 | 1 | 1 | 0 | 2 | 5.50 | 327 | 0 | 0.64 | 0.00 | 0.00 |
| 10 | 1 | 1 | 2 | 1 | 0 | 2 | 7.93 | 1104 | 0 | 0.91 | 0.00 | 0.00 |
| 10 | 1 | 1 | 3 | 1 | 0 | 2 | 5.55 | 356 | 0 | 0.60 | 0.00 | 0.00 |
| 10 | 1 | 1 | 4 | 1 | 0 | 2 | 5.05 | 359 | 0 | 0.41 | 0.00 | 0.00 |
| 10 | 1 | 2 | 1 | 1 | 0 | 2 | 6.58 | 464 | 0 | 0.66 | 0.00 | 0.00 |
| 10 | 1 | 2 | 2 | 1 | 0 | 2 | 8.35 | 949 | 0 | 0.81 | 0.00 | 0.00 |

Continued:

| | | | | | | | | | | | | | |
|---|---|---|---|---|---|---|---|---|---|---|---|---|---|
| | 10 | 1 | 2 | 3 | 1 | 0 | 2 | 7.08 | 424 | 3 | 0.55 | 0.21 | 0.17 |
| | 10 | 1 | 2 | 4 | 1 | 0 | 2 | 5.38 | 291 | 0 | 0.43 | 0.00 | 0.00 |
| | 10 | 1 | 3 | 1 | 1 | 0 | 2 | 12.33 | 716 | 5 | 0.91 | 0.83 | 0.32 |
| | 10 | 1 | 3 | 2 | 1 | 0 | 2 | 13.23 | 771 | 6 | 0.94 | 0.78 | 0.78 |
| | 10 | 1 | 3 | 3 | 1 | 0 | 2 | 8.68 | 535 | 1 | 0.78 | 0.58 | 0.44 |
| | 10 | 1 | 3 | 4 | 1 | 0 | 0 | NaN | NaN | 0 | NaN | NaN | NaN |
| | 10 | 2 | 1 | 1 | 2 | 0 | 2 | 6.10 | 423 | 0 | 0.44 | 0.00 | 0.00 |
| | 10 | 2 | 1 | 2 | 2 | 0 | 2 | 6.13 | 248 | 0 | 0.55 | 0.00 | 0.00 |
| | 10 | 2 | 1 | 3 | 2 | 0 | 2 | 7.00 | 539 | 0 | 0.67 | 0.00 | 0.00 |
| | 10 | 2 | 1 | 4 | 2 | 0 | 2 | 7.30 | 337 | 0 | 0.62 | 0.00 | 0.00 |
| | 10 | 2 | 2 | 1 | 2 | 0 | 2 | 8.38 | 386 | 0 | 0.54 | 0.00 | 0.00 |
| | 10 | 2 | 2 | 2 | 2 | 0 | 2 | 8.43 | 426 | 0 | 0.64 | 0.00 | 0.00 |
| | 10 | 2 | 2 | 3 | 2 | 0 | 2 | 6.65 | 377 | 0 | 0.60 | 0.00 | 0.00 |
| | 10 | 2 | 2 | 4 | 2 | 0 | 2 | 7.03 | 547 | 1 | 0.66 | 0.59 | 0.19 |
| | 10 | 2 | 3 | 1 | 2 | 0 | 2 | 11.48 | 632 | 5 | 0.79 | 0.73 | 0.39 |
| | 10 | 2 | 3 | 2 | 2 | 0 | 1 | 9.20 | 648 | 0 | 0.76 | 0.00 | 0.00 |
| | 10 | 2 | 3 | 3 | 2 | 0 | 1 | 12.80 | 569 | 4 | 0.79 | 0.41 | 0.58 |
| | 10 | 2 | 3 | 4 | 2 | 0 | 2 | 16.28 | 651 | 3 | 0.61 | 0.30 | 0.28 |
| | 10 | 3 | 1 | 1 | 1 | 1 | 2 | 5.98 | 270 | 0 | 0.67 | 0.00 | 0.00 |
| | 10 | 3 | 1 | 2 | 1 | 1 | 2 | 6.93 | 567 | 0 | 0.79 | 0.00 | 0.00 |
| | 10 | 3 | 1 | 3 | 1 | 1 | 2 | 5.85 | 403 | 0 | 0.56 | 0.00 | 0.00 |
| | 10 | 3 | 1 | 4 | 1 | 1 | 2 | 5.00 | 472 | 0 | 0.52 | 0.00 | 0.00 |
| | 10 | 3 | 2 | 1 | 1 | 1 | 2 | 8.08 | 338 | 1 | 0.60 | 0.07 | 0.29 |
| | 10 | 3 | 2 | 2 | 1 | 1 | 2 | 11.73 | 1132 | 6 | 0.92 | 0.82 | 0.47 |
| | 10 | 3 | 2 | 3 | 1 | 1 | 2 | 6.53 | 368 | 0 | 0.64 | 0.00 | 0.00 |
| | 10 | 3 | 2 | 4 | 1 | 1 | 2 | 8.83 | 1054 | 4 | 0.69 | 0.66 | 0.25 |
| | 10 | 3 | 3 | 1 | 1 | 1 | 2 | 10.58 | 416 | 3 | 0.73 | 0.74 | 0.42 |
| | 10 | 3 | 3 | 2 | 1 | 1 | 2 | 13.30 | 1625 | 5 | 0.83 | 1.59 | 0.38 |
| | 10 | 3 | 3 | 3 | 1 | 1 | 2 | 11.85 | 1156 | 5 | 0.89 | 0.81 | 0.33 |
| | 10 | 3 | 3 | 4 | 1 | 1 | 2 | 6.00 | 272 | 0 | 0.51 | 0.00 | 0.00 |
| | 10 | 4 | 1 | 1 | 2 | 1 | 2 | 8.08 | 357 | 0 | 0.67 | 0.00 | 0.00 |
| | 10 | 4 | 1 | 2 | 2 | 1 | 2 | 6.30 | 352 | 0 | 0.70 | 0.00 | 0.00 |
| | 10 | 4 | 1 | 3 | 2 | 1 | 2 | 11.65 | 640 | 0 | 0.80 | 0.00 | 0.00 |
| | 10 | 4 | 1 | 4 | 2 | 1 | 2 | 8.45 | 398 | 3 | 0.72 | 0.32 | 0.29 |
| | 10 | 4 | 2 | 1 | 2 | 1 | 2 | 8.85 | 427 | 5 | 0.55 | 0.41 | 0.54 |
| | 10 | 4 | 2 | 2 | 2 | 1 | 2 | 15.03 | 1115 | 3 | 0.92 | 0.40 | 0.33 |
| | 10 | 4 | 2 | 3 | 2 | 1 | 2 | 6.35 | 397 | 0 | 0.60 | 0.00 | 0.00 |
| | 10 | 4 | 2 | 4 | 2 | 1 | 2 | 11.25 | 567 | 7 | 0.62 | 0.82 | 0.20 |
| | 10 | 4 | 3 | 1 | 2 | 1 | 2 | 15.38 | 690 | 6 | 0.82 | 1.16 | 0.66 |
| | 10 | 4 | 3 | 2 | 2 | 1 | 2 | 12.70 | 539 | 13 | 0.60 | 0.45 | 0.19 |
| | 10 | 4 | 3 | 3 | 2 | 1 | 2 | 14.08 | 671 | 21 | 0.52 | 0.89 | 0.44 |
| | 10 | 4 | 3 | 4 | 2 | 1 | 2 | 12.13 | 634 | 5 | 0.82 | 1.19 | 0.51 |
| | 11 | 1 | 1 | 1 | 1 | 0 | 2 | 9.90 | 362 | 0 | 0.57 | 0.00 | 0.00 |
| | 11 | 1 | 1 | 2 | 1 | 0 | 2 | 9.00 | 599 | 0 | 0.54 | 0.00 | 0.00 |
| | 11 | 1 | 1 | 3 | 1 | 0 | 2 | 8.40 | 318 | 0 | 0.50 | 0.00 | 0.00 |
| | 11 | 1 | 1 | 4 | 1 | 0 | 2 | 10.80 | 533 | 1 | 0.48 | 0.56 | 0.12 |
| | 11 | 1 | 2 | 1 | 1 | 0 | 2 | 9.93 | 402 | 0 | 0.67 | 0.00 | 0.00 |
| | 11 | 1 | 2 | 2 | 1 | 0 | 2 | 10.53 | 683 | 1 | 0.70 | 0.76 | 0.09 |
| | 11 | 1 | 2 | 3 | 1 | 0 | 2 | 10.78 | 346 | 1 | 0.61 | 0.09 | 0.07 |
| | 11 | 1 | 2 | 4 | 1 | 0 | 2 | 8.48 | 759 | 1 | 0.51 | 0.53 | 0.55 |
| | 11 | 1 | 3 | 1 | 1 | 0 | 1 | 12.70 | 526 | 2 | 0.71 | 0.57 | 0.46 |
| | 11 | 1 | 3 | 2 | 1 | 0 | 2 | 12.85 | 755 | 4 | 0.74 | 0.52 | 0.57 |
| | 11 | 1 | 3 | 3 | 1 | 0 | 2 | 26.63 | 1296 | 10 | 1.06 | 1.36 | 1.09 |
| | 11 | 1 | 3 | 4 | 1 | 0 | 2 | 10.98 | 533 | 0 | 0.55 | 0.00 | 0.00 |
| | 11 | 2 | 1 | 1 | 2 | 0 | 2 | 10.40 | 179 | 1 | 0.67 | 0.29 | 0.42 |
| | 11 | 2 | 1 | 2 | 2 | 0 | 2 | 11.38 | 604 | 1 | 0.73 | 0.36 | 0.68 |
| | 11 | 2 | 1 | 3 | 2 | 0 | 2 | 12.85 | 533 | 0 | 0.68 | 0.00 | 0.00 |
| | 11 | 2 | 1 | 4 | 2 | 0 | 2 | 8.28 | 395 | 0 | 0.57 | 0.00 | 0.00 |
| | 11 | 2 | 2 | 1 | 2 | 0 | 2 | 13.45 | 441 | 2 | 0.69 | 0.41 | 0.51 |
| | 11 | 2 | 2 | 2 | 2 | 0 | 2 | 10.28 | 618 | 2 | 0.68 | 0.34 | 0.51 |
| | 11 | 2 | 2 | 3 | 2 | 0 | 2 | 8.93 | 343 | 0 | 0.51 | 0.00 | 0.00 |
| | 11 | 2 | 2 | 4 | 2 | 0 | 2 | 9.95 | 849 | 3 | 0.78 | 0.69 | 1.07 |
| | 11 | 2 | 3 | 1 | 2 | 0 | 2 | 24.98 | 702 | 11 | 0.82 | 0.76 | 0.69 |
| | 11 | 2 | 3 | 2 | 2 | 0 | 2 | 16.95 | 844 | 6 | 0.63 | 0.65 | 0.47 |
| | 11 | 2 | 3 | 3 | 2 | 0 | 2 | 34.38 | 1398 | 18 | 1.06 | 0.95 | 1.02 |
| | 11 | 2 | 3 | 4 | 2 | 0 | 2 | 14.78 | 593 | 2 | 0.69 | 0.41 | 0.29 |
| | 11 | 3 | 1 | 1 | 1 | 1 | 2 | 13.85 | 293 | 1 | 0.77 | 0.64 | 0.61 |
| | 11 | 3 | 1 | 2 | 1 | 1 | 2 | 11.65 | 377 | 0 | 0.69 | 0.00 | 0.00 |
| | 11 | 3 | 1 | 3 | 1 | 1 | 2 | 8.80 | 508 | 1 | 0.56 | 0.27 | 0.21 |
| | 11 | 3 | 1 | 4 | 1 | 1 | 2 | 7.05 | 326 | 0 | 0.45 | 0.00 | 0.00 |
| | 11 | 3 | 2 | 1 | 1 | 1 | 2 | 17.13 | 545 | 5 | 0.75 | 0.74 | 0.56 |
| | 11 | 3 | 2 | 2 | 1 | 1 | 2 | 12.75 | 668 | 0 | 0.83 | 0.00 | 0.00 |
| | 11 | 3 | 2 | 3 | 1 | 1 | 2 | 10.70 | 522 | 0 | 0.60 | 0.00 | 0.00 |
| | 11 | 3 | 2 | 4 | 1 | 1 | 2 | 8.05 | 383 | 0 | 0.53 | 0.00 | 0.00 |
| | 11 | 3 | 3 | 1 | 1 | 1 | 2 | 21.80 | 1111 | 10 | 0.99 | 1.34 | 0.92 |
| | 11 | 3 | 3 | 2 | 1 | 1 | 2 | 15.18 | 703 | 2 | 0.76 | 0.61 | 0.44 |
| | 11 | 3 | 3 | 3 | 1 | 1 | 2 | 18.08 | 1089 | 7 | 0.87 | 0.36 | 0.37 |
| | 11 | 3 | 3 | 4 | 1 | 1 | 2 | 12.93 | 698 | 2 | 0.58 | 0.21 | 0.13 |
| | 11 | 4 | 1 | 1 | 2 | 1 | 2 | 11.33 | 413 | 0 | 0.78 | 0.00 | 0.00 |
| | 11 | 4 | 1 | 2 | 2 | 1 | 2 | 10.50 | 322 | 0 | 0.65 | 0.00 | 0.00 |
| | 11 | 4 | 1 | 3 | 2 | 1 | 2 | 14.68 | 580 | 3 | 0.68 | 0.69 | 0.64 |
| | 11 | 4 | 1 | 4 | 2 | 1 | 2 | 9.45 | 531 | 0 | 0.78 | 0.00 | 0.00 |
| | 11 | 4 | 2 | 1 | 2 | 1 | 2 | 13.73 | 615 | 1 | 0.80 | 0.46 | 0.41 |
| | 11 | 4 | 2 | 2 | 2 | 1 | 2 | 10.95 | 334 | 0 | 0.71 | 0.00 | 0.00 |
| | 11 | 4 | 2 | 3 | 2 | 1 | 2 | 9.93 | 282 | 0 | 0.71 | 0.00 | 0.00 |
| | 11 | 4 | 2 | 4 | 2 | 1 | 2 | 8.93 | 589 | 1 | 0.70 | 0.15 | 0.30 |
| | 11 | 4 | 3 | 1 | 2 | 1 | 2 | 23.85 | 628 | 11 | 0.92 | 0.97 | 0.64 |
| | 11 | 4 | 3 | 2 | 2 | 1 | 2 | 20.80 | 689 | 9 | 0.62 | 0.31 | 0.30 |
| | 11 | 4 | 3 | 3 | 2 | 1 | 2 | 17.98 | 734 | 7 | 0.72 | 0.61 | 0.31 |
| | 11 | 4 | 3 | 4 | 2 | 1 | 2 | 13.40 | 510 | 4 | 0.66 | 0.55 | 0.53 |
| | 12 | 1 | 1 | 1 | 1 | 0 | 2 | 7.60 | 715 | 6 | 0.63 | 1.20 | 0.41 |
| | 12 | 1 | 1 | 2 | 1 | 0 | 2 | 4.88 | 293 | 0 | 0.44 | 0.00 | 0.00 |
| | 12 | 1 | 1 | 3 | 1 | 0 | 2 | 5.25 | 371 | 0 | 0.34 | 0.00 | 0.00 |
| | 12 | 1 | 1 | 4 | 1 | 0 | 2 | 4.43 | 253 | 0 | 0.33 | 0.00 | 0.00 |
| | 12 | 1 | 2 | 1 | 1 | 0 | 2 | 8.73 | 593 | 4 | 0.78 | 1.87 | 0.64 |
| | 12 | 1 | 2 | 2 | 1 | 0 | 2 | 7.65 | 708 | 1 | 0.91 | 0.98 | 1.11 |
| | 12 | 1 | 2 | 3 | 1 | 0 | 2 | 9.25 | 674 | 7 | 0.64 | 1.13 | 0.23 |
| | 12 | 1 | 2 | 4 | 1 | 0 | 1 | 5.05 | 481 | 0 | 0.61 | 0.00 | 0.00 |
| | 12 | 1 | 3 | 1 | 1 | 0 | 2 | 7.50 | 436 | 2 | 0.51 | 0.99 | 0.20 |
| | 12 | 1 | 3 | 2 | 1 | 0 | 2 | 8.63 | 744 | 0 | 0.95 | 0.00 | 0.00 |
| | 12 | 1 | 3 | 3 | 1 | 0 | 1 | 13.75 | 764 | 6 | 0.86 | 1.46 | 0.69 |
| | 12 | 1 | 3 | 4 | 1 | 0 | 1 | 11.35 | 731 | 4 | 0.87 | 1.56 | 0.54 |
| | 12 | 2 | 1 | 1 | 2 | 0 | 2 | 9.33 | 248 | 5 | 0.48 | 0.53 | 0.39 |
| | 12 | 2 | 1 | 2 | 2 | 0 | 2 | 6.35 | 286 | 4 | 0.47 | 0.38 | 0.16 |
| | 12 | 2 | 1 | 3 | 2 | 0 | 2 | 9.08 | 222 | 5 | 0.58 | 0.85 | 0.30 |
| | 12 | 2 | 1 | 4 | 2 | 0 | 2 | 7.83 | 239 | 3 | 0.63 | 0.19 | 0.13 |
| | 12 | 2 | 2 | 1 | 2 | 0 | 2 | 11.48 | 558 | 10 | 0.61 | 0.57 | 0.46 |
| | 12 | 2 | 2 | 2 | 2 | 0 | 2 | 8.13 | 630 | 4 | 0.66 | 0.35 | 0.44 |
| | 12 | 2 | 2 | 3 | 2 | 0 | 2 | 12.73 | 828 | 14 | 0.68 | 0.84 | 0.40 |
| | 12 | 2 | 2 | 4 | 2 | 0 | 2 | 6.43 | 676 | 2 | 0.60 | 0.34 | 0.40 |
| | 12 | 2 | 3 | 1 | 2 | 0 | 2 | 16.45 | 1237 | 5 | 1.11 | 2.31 | 0.88 |
| | 12 | 2 | 3 | 2 | 2 | 0 | 2 | 6.70 | 638 | 2 | 0.57 | 0.40 | 0.14 |
| | 12 | 2 | 3 | 3 | 2 | 0 | 1 | 19.40 | 725 | 2 | 0.91 | 2.05 | 0.84 |
| | 12 | 2 | 3 | 4 | 2 | 0 | 2 | 14.68 | 974 | 11 | 0.85 | 1.13 | 0.78 |
| | 12 | 3 | 1 | 1 | 1 | 1 | 2 | 5.93 | 456 | 4 | 0.32 | 0.47 | 0.31 |
| | 12 | 3 | 1 | 2 | 1 | 1 | 2 | 5.93 | 424 | 2 | 0.40 | 0.46 | 0.15 |
| | 12 | 3 | 1 | 3 | 1 | 1 | 2 | 5.73 | 508 | 1 | 0.55 | 0.20 | 0.32 |
| | 12 | 3 | 1 | 4 | 1 | 1 | 2 | 6.38 | 851 | 2 | 0.52 | 0.19 | 0.03 |
| | 12 | 3 | 2 | 1 | 1 | 1 | 2 | 10.38 | 565 | 6 | 0.74 | 0.99 | 0.69 |
| | 12 | 3 | 2 | 2 | 1 | 1 | 2 | 11.55 | 602 | 8 | 0.56 | 0.77 | 0.37 |
| | 12 | 3 | 2 | 3 | 1 | 1 | 2 | 10.28 | 1096 | 7 | 0.72 | 1.29 | 0.60 |
| | 12 | 3 | 2 | 4 | 1 | 1 | 2 | 7.55 | 602 | 8 | 0.42 | 0.71 | 0.34 |
| | 12 | 3 | 3 | 1 | 1 | 1 | 2 | 11.48 | 637 | 12 | 0.63 | 0.84 | 0.54 |
| | 12 | 3 | 3 | 2 | 1 | 1 | 2 | 24.58 | 1330 | 17 | 0.91 | 1.26 | 0.79 |
| | 12 | 3 | 3 | 3 | 1 | 1 | 1 | 16.35 | 1247 | 7 | 0.74 | 1.25 | 0.38 |
| | 12 | 3 | 3 | 4 | 1 | 1 | 2 | 9.78 | 882 | 7 | 0.70 | 0.85 | 0.40 |
| | 12 | 4 | 1 | 1 | 2 | 1 | 2 | 5.45 | 361 | 0 | 0.53 | 0.00 | 0.00 |
| | 12 | 4 | 1 | 2 | 2 | 1 | 2 | 5.73 | 465 | 0 | 0.52 | 0.00 | 0.00 |
| | 12 | 4 | 1 | 3 | 2 | 1 | 2 | 7.25 | 443 | 3 | 0.61 | 0.48 | 0.17 |
| | 12 | 4 | 1 | 4 | 2 | 1 | 2 | 5.83 | 493 | 4 | 0.52 | 0.46 | 0.23 |
| | 12 | 4 | 2 | 1 | 2 | 1 | 2 | 14.25 | 973 | 11 | 0.85 | 1.05 | 0.65 |
| | 12 | 4 | 2 | 2 | 2 | 1 | 2 | 11.88 | 926 | 10 | 0.72 | 0.41 | 0.32 |
| | 12 | 4 | 2 | 3 | 2 | 1 | 1 | 7.60 | 934 | 1 | 0.72 | 0.58 | 0.13 |
| | 12 | 4 | 2 | 4 | 2 | 1 | 2 | 7.03 | 766 | 6 | 0.65 | 0.86 | 0.57 |
| | 12 | 4 | 3 | 1 | 2 | 1 | 2 | 14.38 | 703 | 9 | 0.96 | 1.44 | 0.86 |
| | 12 | 4 | 3 | 2 | 2 | 1 | 2 | 14.15 | 1091 | 6 | 0.92 | 1.41 | 1.06 |
| | 12 | 4 | 3 | 3 | 2 | 1 | 2 | 16.68 | 1110 | 13 | 0.92 | 1.15 | 0.80 |
| | 12 | 4 | 3 | 4 | 2 | 1 | 0 | NaN | NaN | 0 | NaN | NaN | NaN |
| | 13 | 1 | 1 | 1 | 1 | 0 | 2 | 8.40 | 146 | 3 | 0.24 | 0.17 | 0.04 |
| | 13 | 1 | 1 | 2 | 1 | 0 | 2 | 7.78 | 507 | 2 | 0.53 | 0.26 | 0.07 |
| | 13 | 1 | 1 | 3 | 1 | 0 | 2 | 15.35 | 678 | 12 | 0.47 | 0.57 | 0.40 |
| | 13 | 1 | 1 | 4 | 1 | 0 | 2 | 7.18 | 471 | 2 | 0.34 | 0.49 | 0.15 |
| | 13 | 1 | 2 | 1 | 1 | 0 | 2 | 8.10 | 423 | 2 | 0.34 | 0.21 | 0.07 |
| | 13 | 1 | 2 | 2 | 1 | 0 | 2 | 8.65 | 854 | 3 | 0.60 | 0.32 | 0.21 |
| | 13 | 1 | 2 | 3 | 1 | 0 | 1 | 8.95 | 485 | 1 | 0.37 | 0.75 | 0.26 |
| | 13 | 1 | 2 | 4 | 1 | 0 | 2 | 8.63 | 381 | 2 | 0.32 | 0.29 | 0.04 |
| | 13 | 1 | 3 | 1 | 1 | 0 | 2 | 12.83 | 983 | 5 | 0.65 | 0.88 | 0.52 |
| | 13 | 1 | 3 | 2 | 1 | 0 | 2 | 19.70 | 1009 | 6 | 0.68 | 0.42 | 0.17 |
| | 13 | 1 | 3 | 3 | 1 | 0 | 2 | 18.93 | 587 | 7 | 0.63 | 0.58 | 0.21 |

Continued:

| | | | | | | | | | | | | | | |
|---|---|---|---|---|---|---|---|---|---|---|---|---|---|---|
| | 13 | 1 | 3 | 4 | 1 | 0 | 2 | 18.90 | 476 | 5 | 0.47 | 0.63 | 0.28 |
| | 13 | 2 | 1 | 1 | 2 | 0 | 2 | 19.15 | 787 | 8 | 0.57 | 0.97 | 0.54 |
| | 13 | 2 | 1 | 2 | 2 | 0 | 2 | 11.05 | 537 | 4 | 0.48 | 0.12 | 0.11 |
| | 13 | 2 | 1 | 3 | 2 | 0 | 2 | 11.45 | 582 | 5 | 0.56 | 0.32 | 0.19 |
| | 13 | 2 | 1 | 4 | 2 | 0 | 2 | 10.65 | 569 | 0 | 0.56 | 0.00 | 0.00 |
| | 13 | 2 | 2 | 1 | 2 | 0 | 2 | 13.13 | 491 | 2 | 0.61 | 0.50 | 0.41 |
| | 13 | 2 | 2 | 2 | 2 | 0 | 2 | 14.43 | 974 | 8 | 0.58 | 0.56 | 0.38 |
| | 13 | 2 | 2 | 3 | 2 | 0 | 2 | 10.70 | 654 | 4 | 0.49 | 0.46 | 0.28 |
| | 13 | 2 | 2 | 4 | 2 | 0 | 1 | 12.90 | 1240 | 1 | 0.72 | 1.47 | 0.65 |
| | 13 | 2 | 3 | 1 | 2 | 0 | 2 | 15.98 | 872 | 6 | 0.62 | 0.81 | 0.45 |
| | 13 | 2 | 3 | 2 | 2 | 0 | 2 | 12.83 | 777 | 4 | 0.67 | 0.85 | 0.29 |
| | 13 | 2 | 3 | 3 | 2 | 0 | 2 | 31.08 | 738 | 18 | 0.98 | 1.13 | 0.53 |
| | 13 | 2 | 3 | 4 | 2 | 0 | 2 | 14.83 | 769 | 5 | 0.69 | 0.45 | 0.39 |
| | 13 | 3 | 1 | 1 | 1 | 1 | 2 | 10.95 | 774 | 3 | 0.42 | 0.60 | 0.52 |
| | 13 | 3 | 1 | 2 | 1 | 1 | 2 | 11.73 | 590 | 3 | 0.65 | 0.41 | 0.25 |
| | 13 | 3 | 1 | 3 | 1 | 1 | 2 | 9.53 | 702 | 1 | 0.54 | 0.39 | 0.21 |
| | 13 | 3 | 1 | 4 | 1 | 1 | 2 | 8.18 | 329 | 1 | 0.38 | 0.23 | 0.04 |
| | 13 | 3 | 2 | 1 | 1 | 1 | 2 | 11.18 | 612 | 3 | 0.49 | 0.75 | 0.13 |
| | 13 | 3 | 2 | 2 | 1 | 1 | 2 | 14.05 | 800 | 3 | 0.74 | 0.79 | 0.38 |
| | 13 | 3 | 2 | 3 | 1 | 1 | 2 | 12.03 | 871 | 1 | 0.74 | 0.63 | 0.01 |
| | 13 | 3 | 2 | 4 | 1 | 1 | 2 | 8.25 | 702 | 2 | 0.41 | 0.87 | 0.12 |
| | 13 | 3 | 3 | 1 | 1 | 1 | 2 | 14.75 | 660 | 3 | 0.52 | 0.97 | 0.25 |
| | 13 | 3 | 3 | 2 | 1 | 1 | 2 | 13.83 | 756 | 8 | 0.81 | 1.10 | 0.77 |
| | 13 | 3 | 3 | 3 | 1 | 1 | 2 | 21.35 | 1228 | 5 | 1.01 | 1.71 | 1.06 |
| | 13 | 3 | 3 | 4 | 1 | 1 | 1 | 9.00 | 394 | 1 | 0.44 | 1.00 | 0.30 |
| | 13 | 4 | 1 | 1 | 2 | 1 | 2 | 13.13 | 543 | 2 | 0.44 | 0.49 | 0.26 |
| | 13 | 4 | 1 | 2 | 2 | 1 | 2 | 12.08 | 759 | 3 | 0.69 | 1.13 | 0.88 |
| | 13 | 4 | 1 | 3 | 2 | 1 | 2 | 11.85 | 641 | 4 | 0.64 | 0.31 | 0.23 |
| | 13 | 4 | 1 | 4 | 2 | 1 | 2 | 14.35 | 560 | 7 | 0.77 | 0.78 | 0.53 |
| | 13 | 4 | 2 | 1 | 2 | 1 | 2 | 9.58 | 336 | 1 | 0.44 | 0.44 | 0.10 |
| | 13 | 4 | 2 | 2 | 2 | 1 | 2 | 15.20 | 773 | 9 | 0.46 | 0.51 | 0.24 |
| | 13 | 4 | 2 | 3 | 2 | 1 | 2 | 12.83 | 751 | 3 | 0.72 | 0.42 | 0.23 |
| | 13 | 4 | 2 | 4 | 2 | 1 | 2 | 10.23 | 474 | 4 | 0.67 | 0.70 | 0.41 |
| | 13 | 4 | 3 | 1 | 2 | 1 | 2 | 19.20 | 591 | 5 | 0.69 | 0.81 | 0.77 |
| | 13 | 4 | 3 | 2 | 2 | 1 | 2 | 14.73 | 700 | 5 | 0.69 | 1.27 | 0.34 |
| | 13 | 4 | 3 | 3 | 2 | 1 | 2 | 27.25 | 888 | 5 | 0.98 | 1.20 | 0.44 |
| | 13 | 4 | 3 | 4 | 2 | 1 | 1 | 12.00 | 547 | 3 | 0.87 | 1.07 | 0.33 |
| | 14 | 1 | 1 | 1 | 1 | 0 | 2 | 8.83 | 554 | 0 | 0.66 | 0.00 | 0.00 |
| | 14 | 1 | 1 | 2 | 1 | 0 | 2 | 7.35 | 398 | 0 | 0.62 | 0.00 | 0.00 |
| | 14 | 1 | 1 | 3 | 1 | 0 | 2 | 7.00 | 483 | 0 | 0.68 | 0.00 | 0.00 |
| | 14 | 1 | 1 | 4 | 1 | 0 | 2 | 5.23 | 116 | 0 | 0.28 | 0.00 | 0.00 |
| | 14 | 1 | 2 | 1 | 1 | 0 | 2 | 8.25 | 735 | 0 | 0.80 | 0.00 | 0.00 |
| | 14 | 1 | 2 | 2 | 1 | 0 | 2 | 7.23 | 305 | 0 | 0.75 | 0.00 | 0.00 |
| | 14 | 1 | 2 | 3 | 1 | 0 | 2 | 8.85 | 785 | 1 | 0.76 | 0.76 | 0.58 |
| | 14 | 1 | 2 | 4 | 1 | 0 | 2 | 5.63 | 365 | 0 | 0.45 | 0.00 | 0.00 |
| | 14 | 1 | 3 | 1 | 1 | 0 | 2 | 11.40 | 688 | 0 | 0.95 | 0.00 | 0.00 |
| | 14 | 1 | 3 | 2 | 1 | 0 | 2 | 12.43 | 779 | 0 | 0.79 | 0.00 | 0.00 |
| | 14 | 1 | 3 | 3 | 1 | 0 | 2 | 11.70 | 1234 | 0 | 1.04 | 0.00 | 0.00 |
| | 14 | 1 | 3 | 4 | 1 | 0 | 1 | 6.95 | 257 | 0 | 0.53 | 0.00 | 0.00 |
| | 14 | 2 | 1 | 1 | 2 | 0 | 2 | 8.13 | 340 | 0 | 0.76 | 0.00 | 0.00 |
| | 14 | 2 | 1 | 2 | 2 | 0 | 2 | 7.63 | 185 | 0 | 0.70 | 0.00 | 0.00 |
| | 14 | 2 | 1 | 3 | 2 | 0 | 2 | 9.88 | 125 | 1 | 0.65 | 0.15 | 0.12 |
| | 14 | 2 | 1 | 4 | 2 | 0 | 2 | 7.83 | 337 | 0 | 0.51 | 0.00 | 0.00 |
| | 14 | 2 | 2 | 1 | 2 | 0 | 2 | 10.58 | 426 | 0 | 0.78 | 0.00 | 0.00 |
| | 14 | 2 | 2 | 2 | 2 | 0 | 2 | 12.08 | 903 | 2 | 1.02 | 1.46 | 2.24 |
| | 14 | 2 | 2 | 3 | 2 | 0 | 2 | 12.18 | 804 | 2 | 0.90 | 1.13 | 1.53 |
| | 14 | 2 | 2 | 4 | 2 | 0 | 2 | 7.58 | 398 | 0 | 0.71 | 0.00 | 0.00 |
| | 14 | 2 | 3 | 1 | 2 | 0 | 2 | 10.60 | 434 | 1 | 0.77 | 1.18 | 0.28 |
| | 14 | 2 | 3 | 2 | 2 | 0 | 2 | 18.25 | 977 | 1 | 1.16 | 0.85 | 0.89 |
| | 14 | 2 | 3 | 3 | 2 | 0 | 2 | 26.48 | 1024 | 7 | 1.07 | 1.20 | 1.10 |
| | 14 | 2 | 3 | 4 | 2 | 0 | 2 | 10.68 | 619 | 1 | 0.77 | 0.56 | 0.09 |
| | 14 | 3 | 1 | 1 | 1 | 1 | 2 | 7.83 | 288 | 0 | 0.72 | 0.00 | 0.00 |
| | 14 | 3 | 1 | 2 | 1 | 1 | 2 | 6.55 | 426 | 0 | 0.73 | 0.00 | 0.00 |
| | 14 | 3 | 1 | 3 | 1 | 1 | 2 | 7.88 | 399 | 2 | 0.78 | 0.91 | 0.64 |
| | 14 | 3 | 1 | 4 | 1 | 1 | 2 | 5.53 | 110 | 0 | 0.43 | 0.00 | 0.00 |
| | 14 | 3 | 2 | 1 | 1 | 1 | 2 | 10.38 | 729 | 0 | 0.84 | 0.00 | 0.00 |
| | 14 | 3 | 2 | 2 | 1 | 1 | 2 | 11.78 | 374 | 2 | 0.69 | 0.84 | 0.60 |
| | 14 | 3 | 2 | 3 | 1 | 1 | 2 | 10.38 | 557 | 1 | 0.60 | 0.32 | 0.61 |
| | 14 | 3 | 2 | 4 | 1 | 1 | 2 | 7.60 | 711 | 1 | 0.61 | 0.65 | 0.44 |
| | 14 | 3 | 3 | 1 | 1 | 1 | 2 | 9.60 | 313 | 0 | 0.73 | 0.00 | 0.00 |
| | 14 | 3 | 3 | 2 | 1 | 1 | 2 | 12.25 | 791 | 2 | 1.02 | 0.98 | 0.67 |
| | 14 | 3 | 3 | 3 | 1 | 1 | 2 | 14.15 | 746 | 5 | 0.98 | 1.08 | 1.23 |
| | 14 | 3 | 3 | 4 | 1 | 1 | 2 | 9.45 | 730 | 2 | 0.80 | 0.60 | 0.79 |
| | 14 | 4 | 1 | 1 | 2 | 1 | 2 | 9.75 | 317 | 0 | 0.89 | 0.00 | 0.00 |
| | 14 | 4 | 1 | 2 | 2 | 1 | 2 | 11.28 | 0 | 0 | 0.88 | 0.00 | 0.00 |
| | 14 | 4 | 1 | 3 | 2 | 1 | 2 | 13.43 | 209 | 2 | 0.77 | 0.27 | 1.00 |
| | 14 | 4 | 1 | 4 | 2 | 1 | 2 | 7.50 | 148 | 0 | 0.72 | 0.00 | 0.00 |
| | 14 | 4 | 2 | 1 | 2 | 1 | 2 | 14.73 | 748 | 2 | 0.94 | 1.05 | 0.53 |
| | 14 | 4 | 2 | 2 | 2 | 1 | 2 | 14.28 | 554 | 1 | 0.96 | 0.36 | 0.88 |
| | 14 | 4 | 2 | 3 | 2 | 1 | 2 | 12.63 | 501 | 1 | 0.86 | 0.35 | 0.34 |
| | 14 | 4 | 2 | 4 | 2 | 1 | 2 | 8.08 | 453 | 0 | 0.74 | 0.00 | 0.00 |
| | 14 | 4 | 3 | 1 | 2 | 1 | 2 | 25.68 | 1246 | 7 | 1.17 | 0.97 | 1.01 |
| | 14 | 4 | 3 | 2 | 2 | 1 | 2 | 24.43 | 1240 | 4 | 1.17 | 1.29 | 1.23 |
| | 14 | 4 | 3 | 3 | 2 | 1 | 2 | 18.65 | 876 | 6 | 1.08 | 1.40 | 0.72 |
| | 14 | 4 | 3 | 4 | 2 | 1 | 1 | 12.00 | 570 | 2 | 0.82 | 0.97 | 0.63 |
| | 15 | 1 | 1 | 1 | 1 | 0 | 2 | 4.80 | 442 | 0 | 0.43 | 0.00 | 0.00 |
| | 15 | 1 | 1 | 2 | 1 | 0 | 2 | 5.65 | 603 | 1 | 0.51 | 0.06 | 0.09 |
| | 15 | 1 | 1 | 3 | 1 | 0 | 2 | 7.93 | 843 | 0 | 0.85 | 0.00 | 0.00 |
| | 15 | 1 | 1 | 4 | 1 | 0 | 2 | 4.23 | 235 | 0 | 0.21 | 0.00 | 0.00 |
| | 15 | 1 | 2 | 1 | 1 | 0 | 1 | 5.95 | 392 | 0 | 0.82 | 0.00 | 0.00 |
| | 15 | 1 | 2 | 2 | 1 | 0 | 2 | 7.48 | 761 | 0 | 0.80 | 0.00 | 0.00 |
| | 15 | 1 | 2 | 3 | 1 | 0 | 2 | 7.23 | 599 | 0 | 0.79 | 0.00 | 0.00 |
| | 15 | 1 | 2 | 4 | 1 | 0 | 2 | 6.43 | 736 | 0 | 0.71 | 0.00 | 0.00 |
| | 15 | 1 | 3 | 1 | 1 | 0 | 2 | 13.20 | 1274 | 6 | 0.97 | 0.41 | 0.50 |
| | 15 | 1 | 3 | 2 | 1 | 0 | 2 | 9.73 | 855 | 0 | 0.80 | 0.00 | 0.00 |
| | 15 | 1 | 3 | 3 | 1 | 0 | 1 | 7.85 | 296 | 0 | 0.82 | 0.00 | 0.00 |
| | 15 | 1 | 3 | 4 | 1 | 0 | 2 | 6.18 | 424 | 0 | 0.74 | 0.00 | 0.00 |
| | 15 | 2 | 1 | 1 | 2 | 0 | 2 | 7.60 | 823 | 0 | 0.87 | 0.00 | 0.00 |
| | 15 | 2 | 1 | 2 | 2 | 0 | 2 | 6.18 | 299 | 0 | 0.68 | 0.00 | 0.00 |
| | 15 | 2 | 1 | 3 | 2 | 0 | 2 | 8.78 | 604 | 1 | 0.88 | 1.14 | 0.49 |
| | 15 | 2 | 1 | 4 | 2 | 0 | 2 | 5.33 | 489 | 0 | 0.54 | 0.00 | 0.00 |
| | 15 | 2 | 2 | 1 | 2 | 0 | 1 | 6.60 | 231 | 0 | 0.64 | 0.00 | 0.00 |
| | 15 | 2 | 2 | 2 | 2 | 0 | 2 | 10.25 | 1026 | 0 | 1.03 | 0.00 | 0.00 |
| | 15 | 2 | 2 | 3 | 2 | 0 | 2 | 9.58 | 861 | 0 | 1.01 | 0.00 | 0.00 |
| | 15 | 2 | 2 | 4 | 2 | 0 | 2 | 5.18 | 416 | 0 | 0.63 | 0.00 | 0.00 |
| | 15 | 2 | 3 | 1 | 2 | 0 | 2 | 12.78 | 1011 | 6 | 0.94 | 0.69 | 0.64 |
| | 15 | 2 | 3 | 2 | 2 | 0 | 0 | NaN | NaN | 0 | NaN | NaN | NaN |
| | 15 | 2 | 3 | 3 | 2 | 0 | 1 | 6.70 | 268 | 0 | 0.55 | 0.00 | 0.00 |
| | 15 | 2 | 3 | 4 | 2 | 0 | 2 | 7.18 | 750 | 0 | 0.88 | 0.00 | 0.00 |
| | 15 | 3 | 1 | 1 | 1 | 1 | 1 | 5.60 | 381 | 0 | 0.59 | 0.00 | 0.00 |
| | 15 | 3 | 1 | 2 | 1 | 1 | 2 | 4.98 | 323 | 0 | 0.45 | 0.00 | 0.00 |
| | 15 | 3 | 1 | 3 | 1 | 1 | 2 | 6.10 | 468 | 0 | 0.60 | 0.00 | 0.00 |
| | 15 | 3 | 1 | 4 | 1 | 1 | 2 | 4.98 | 489 | 0 | 0.52 | 0.00 | 0.00 |
| | 15 | 3 | 2 | 1 | 1 | 1 | 1 | 7.15 | 340 | 0 | 0.62 | 0.00 | 0.00 |
| | 15 | 3 | 2 | 2 | 1 | 1 | 2 | 7.98 | 639 | 2 | 0.83 | 0.27 | 0.37 |
| | 15 | 3 | 2 | 3 | 1 | 1 | 2 | 9.35 | 856 | 1 | 0.97 | 1.55 | 0.41 |
| | 15 | 3 | 2 | 4 | 1 | 1 | 2 | 4.78 | 351 | 0 | 0.47 | 0.00 | 0.00 |
| | 15 | 3 | 3 | 1 | 1 | 1 | 1 | 7.85 | 677 | 0 | 0.97 | 0.00 | 0.00 |
| | 15 | 3 | 3 | 2 | 1 | 1 | 2 | 7.35 | 456 | 1 | 0.74 | 0.25 | 0.53 |
| | 15 | 3 | 3 | 3 | 1 | 1 | 2 | 7.55 | 561 | 0 | 0.83 | 0.00 | 0.00 |
| | 15 | 3 | 3 | 4 | 1 | 1 | 2 | 16.40 | 1219 | 1 | 1.05 | 1.37 | 1.12 |
| | 15 | 4 | 1 | 1 | 2 | 1 | 2 | 8.23 | 232 | 0 | 0.80 | 0.00 | 0.00 |
| | 15 | 4 | 1 | 2 | 2 | 1 | 2 | 5.38 | 253 | 0 | 0.55 | 0.00 | 0.00 |
| | 15 | 4 | 1 | 3 | 2 | 1 | 2 | 9.63 | 204 | 2 | 0.72 | 0.79 | 1.04 |
| | 15 | 4 | 1 | 4 | 2 | 1 | 2 | 5.93 | 531 | 0 | 0.67 | 0.00 | 0.00 |
| | 15 | 4 | 2 | 1 | 2 | 1 | 2 | 10.00 | 880 | 0 | 0.86 | 0.00 | 0.00 |
| | 15 | 4 | 2 | 2 | 2 | 1 | 1 | 6.65 | 512 | 0 | 0.73 | 0.00 | 0.00 |
| | 15 | 4 | 2 | 3 | 2 | 1 | 1 | 6.50 | 547 | 0 | 0.75 | 0.00 | 0.00 |
| | 15 | 4 | 2 | 4 | 2 | 1 | 2 | 9.85 | 1131 | 1 | 0.97 | 0.47 | 0.26 |
| | 15 | 4 | 3 | 1 | 2 | 1 | 2 | 15.50 | 893 | 3 | 1.12 | 0.29 | 0.77 |
| | 15 | 4 | 3 | 2 | 2 | 1 | 1 | 7.55 | 683 | 0 | 0.69 | 0.00 | 0.00 |
| | 15 | 4 | 3 | 3 | 2 | 1 | 1 | 11.25 | 662 | 0 | 0.79 | 0.00 | 0.00 |
| | 15 | 4 | 3 | 4 | 2 | 1 | 2 | 8.48 | 514 | 0 | 0.88 | 0.00 | 0.00 |

# Appendix C Delay Impact Averaged by Subject

This Table is a pivot table of data from Appendix B. Here all the data is averaged across maps and ICs to give one data point for each Subject for each Delay. This averaged data was used in the SYSTAT analysis performed in Chapter 7.

| Row Labels | Average of Total Successful summed across both paths | Average of Avg Cmpltn Time (Seconds) | Average of Average error relative to nearest median human path (Unitless) | Average of Number of Stops summed across both paths | Average of Average heading error for two paths, calculated for every point (Radians) | Average of Average before stop heading error (Radians) | Average of Average after stop heading error (Radians) |
|---|---|---|---|---|---|---|---|
| **1** | **1.971590909** | **8.009943182** | **424.656641** | **1.147727273** | **0.604910094** | **0.211205271** | **0.140730033** |
| 4 | 1.8125 | 7.125 | 495.3073674 | 0.5625 | 0.702343766 | 0.175795528 | 0.094884083 |
| 5 | 2 | 7.978125 | 398.0710443 | 1.625 | 0.629201185 | 0.211935825 | 0.116496025 |
| 6 | 1.9375 | 6.125 | 294.0266698 | 0.0625 | 0.580441409 | 0.038418924 | 0.035326405 |
| 8 | 2 | 6.9734375 | 434.9425143 | 0.25 | 0.537909229 | 0.158410042 | 0.195980405 |
| 9 | 2 | 10.18125 | 456.1167561 | 2.6875 | 0.631703419 | 0.543860168 | 0.272444298 |
| 10 | 2 | 6.7984375 | 446.9127845 | 0.1875 | 0.641555629 | 0.020235794 | 0.017909277 |
| 11 | 2 | 10.51875 | 429.6503999 | 0.5 | 0.632057328 | 0.175544831 | 0.16693698 |
| 12 | 2 | 6.4328125 | 414.3409736 | 2.4375 | 0.491459649 | 0.338651853 | 0.161425226 |
| 13 | 2 | 11.4234375 | 573.3848985 | 3.75 | 0.517874933 | 0.453039436 | 0.275163307 |
| 14 | 2 | 8.2234375 | 277.123819 | 0.3125 | 0.672639002 | 0.08324438 | 0.110145395 |
| 15 | 1.9375 | 6.3296875 | 451.3458238 | 0.25 | 0.616825489 | 0.124121202 | 0.101318966 |
| **2** | **1.9375** | **9.485653409** | **603.6090641** | **1.892045455** | **0.704045096** | **0.428847652** | **0.259045297** |
| 4 | 1.9375 | 9.1 | 659.3052918 | 0.6875 | 0.819570667 | 0.362412589 | 0.29436724 |
| 5 | 1.9375 | 9.684375 | 646.4681459 | 2.125 | 0.791496906 | 0.603050285 | 0.309206056 |
| 6 | 2 | 8.2796875 | 520.0504674 | 0.9375 | 0.731304688 | 0.287840571 | 0.148984008 |
| 8 | 2 | 7.3390625 | 405.7579602 | 0.25 | 0.575262151 | 0.07660144 | 0.081474414 |
| 9 | 2 | 12.3921875 | 676.8865046 | 3.5625 | 0.712977513 | 0.901698469 | 0.356903591 |
| 10 | 2 | 8.4046875 | 578.8123707 | 1.875 | 0.650706737 | 0.247513563 | 0.152753416 |
| 11 | 2 | 10.903125 | 523.7187495 | 1.0625 | 0.674314996 | 0.25981859 | 0.2538654 |
| 12 | 1.875 | 9.3703125 | 725.6274611 | 6.1875 | 0.679100912 | 0.797205812 | 0.459093928 |
| 13 | 1.875 | 11.175 | 676.4667024 | 3.0625 | 0.54331508 | 0.604956585 | 0.244043896 |
| 14 | 2 | 10.1359375 | 584.2778251 | 0.8125 | 0.777105874 | 0.43295064 | 0.483903941 |
| 15 | 1.6875 | 7.5578125 | 642.328226 | 0.25 | 0.789340529 | 0.143275629 | 0.064902379 |
| **3** | **1.795454545** | **14.98800578** | **793.8583961** | **4.75** | **0.819823045** | **0.86046843** | **0.468429093** |
| 4 | 1.875 | 18.2703125 | 1073.521997 | 5.375 | 0.947302263 | 1.053359563 | 0.413873923 |
| 5 | 1.6875 | 14.8875 | 707.2795678 | 5.125 | 0.821476023 | 1.116586233 | 0.441030932 |
| 6 | 2 | 15.190625 | 796.7240956 | 5.5 | 0.828373958 | 1.139038274 | 0.543609122 |
| 8 | 1.75 | 12.7453125 | 742.8753127 | 2.1875 | 0.803689685 | 0.722744348 | 0.476297348 |
| 9 | 1.8125 | 17.128125 | 786.6483062 | 6.8125 | 0.770832038 | 1.040746415 | 0.554159681 |
| 10 | 1.75 | 11.99833333 | 701.6035929 | 5.125 | 0.75272674 | 0.69771429 | 0.381568117 |
| 11 | 1.9375 | 18.6390625 | 800.5946195 | 6.5625 | 0.774036569 | 0.635586763 | 0.515080946 |
| 12 | 1.625 | 13.72166667 | 883.3665322 | 6.4375 | 0.827855938 | 1.206824253 | 0.591821614 |
| 13 | 1.875 | 17.321875 | 748.466604 | 5.6875 | 0.710939299 | 0.929534012 | 0.444784276 |
| 14 | 1.875 | 14.6671875 | 782.6450621 | 2.375 | 0.927616898 | 0.692720613 | 0.541005831 |
| 15 | 1.5625 | 9.701666667 | 702.8574406 | 1.0625 | 0.851491929 | 0.200526714 | 0.237327616 |
| **Grand Total** | **1.901515152** | **10.80409524** | **606.3090793** | **2.596590909** | **0.708962858** | **0.498114958** | **0.28837846** |

# References


[1] Held, R., & Durlach, N. (1991). Telepresence, time delay and adoption. In S. Ellis, M. K. Kaiser, & A. C. Grunwdd (Ed.), Pictorial communication in virtual and real environments (pp. 232-245). London: Taylor & Francis.

[2] Aerospace America. Volume 49, No. 3. Edited by Elaine J. Camhi, et. al. Reston, Va., March 2011

[3] Lewis, M.; Huadong Wang; Velagapudi, P.; Scerri, P.; Sycara, K.; , "Using humans as sensors in robotic search," Information Fusion, 2009. FUSION '09. 12th International Conference on , vol., no., pp.1249-1256, 6-9 July 2009

[4] Chardard, Y.; Copros, T.; , "Swimmer: final sea demonstration of this innovative hybrid AUV/ROV system," Underwater Technology, 2002. Proceedings of the 2002 International Symposium on , vol., no., pp. 17- 23, 2002

[5] Lam, T.M.; Mulder, M.; van Paassen, M.M.; , "Collision avoidance in UAV tele-operation with time delay," Systems, Man and Cybernetics, 2007. ISIC. IEEE International Conference on , vol., no., pp.997-1002, 7-10 Oct. 2007

[6] Beltran-Gonzalez, C.; Gasteratos, A.; Amanatiadis, A.; Chrysostomou, D.; Guzman, R.; Toth, A.; Szollosi, L.; Juhasz, A.; Galambos, P.; , "Methods and techniques for intelligent navigation and manipulation for bomb disposal and rescue operations," Safety, Security and Rescue Robotics, 2007. SSRR 2007. IEEE International Workshop on , vol., no., pp.1-6, 27-29 Sept. 2007

[7] Pradel, G.; Comfaits, O.; , "A framework for a Web-based supervisory control of mobile robots ," Robot and Human Interactive Communication, 2001. Proceedings. 10th IEEE International Workshop on , vol., no., pp.249-255, 2001

[8] Murphy, R.R.; Steimle, E.; Hall, M.; Lindemuth, M.; Trejo, D.; Hurlebaus, S.; Medina-Cetina, Z.; Slocum, D.; , "Robot-assisted bridge inspection after Hurricane Ike," Safety, Security & Rescue Robotics (SSRR), 2009 IEEE International Workshop on , vol., no., pp.1-5, 3-6 Nov. 2009

[9] Suzuki, S.; Tomomatsu, N.; Harashima, F.; Furuta, K.; , "Skill evaluation based on state-transition model for human adaptive mechatronics (HAM)," Industrial Electronics Society, 2004. IECON 2004. 30th Annual Conference of IEEE , vol.1, no., pp. 641- 646 Vol. 1, 2-6 Nov. 2004

[10] Meng Wang; Liu, J.N.K.; , "A novel teleoperation paradigm for human-robot interaction," Robotics, Automation and Mechatronics, 2004 IEEE Conference on , vol.1, no., pp. 13- 18 vol.1, 1-3 Dec. 2004

[11] Burns, V. J.; , "Aircraft Navigation: Design Theory for A Self-Organizing, High Accuracy Navigation System," Aerospace and Navigational Electronics, IEEE Transactions on , vol.Technical_Paper, no.0, pp.3.4.5-1-3.4.5-6, Oct. 1963

[12] Chaojian Shi; Jingyuan Li; Jing Peng; , "A new approach for ARPA display and collision danger assessment," Radar Symposium, 2008 International , vol., no., pp.1-4, 21-23 May 2008

[13] Kutila, M.; Jokela, M.; Markkula, G.; Rue, M.R.; , "Driver Distraction Detection with a Camera Vision System," Image Processing, 2007. ICIP 2007. IEEE International Conference on , vol.6, no., pp.VI-201-VI-204, Sept. 16 2007-Oct. 19 2007

[14] Goralski, R.; Gold, C.; Dakowicz, M.; , "Application of the Kinetic Voronoi Diagram to the Real-Time Navigation of Marine Vessels," Computer Information Systems and Industrial Management Applications, 2007. CISIM '07. 6th International Conference on , vol., no., pp.129-134, 28-30 June 2007

[15] Obata, T.; Daimon, T.; Kawashima, H.; , "A cognitive study of in-vehicle navigation systems: Applying verbal protocol analysis to usability evaluation," Vehicle Navigation and Information Systems Conference, 1993., Proceedings of the IEEE-IEE , vol., no., pp.232-237, 12-15 Oct 1993

[16] Hai Chen; Xin-min Wang; Yan Li; , "A Survey of Autonomous Control for UAV," Artificial Intelligence and Computational Intelligence, 2009. AICI '09. International Conference on , vol.2, no., pp.267-271, 7-8 Nov. 2009

[17] Weiss, David J. Analysis of variance and functional measurement: a practical guide, Oxford; New York: Oxford University Press, 2006

[18] Weisberg, Sanford, Applied Linear Regression, Wiley series in probability and statistics, 3rd ed., Hoboken, N.H., 2005.

[19] Lam, T.M.; Mulder, M.; van Paassen, M.M.; , "Collision avoidance in UAV tele-operation with time delay," Systems, Man and Cybernetics, 2007. ISIC. IEEE International Conference on , vol., no., pp.997-1002, 7-10 Oct. 2007

[20] Hassan-Zadeh, I.; Janabi-Sharifi, F.; Yang, A.X.; , "Internet-based teleoperation of a mobile robot using shared impedance control scheme: a pilot study," Control Applications, 2005. CCA 2005. Proceedings of 2005 IEEE Conference on , vol., no., pp.346-351, 28-31 Aug. 2005

[21] Davis, J.; Smyth, C.; McDowell, K.; , "The Effects of Time Lag on Driving Performance and a Possible Mitigation," Robotics, IEEE Transactions on , vol.26, no.3, pp.590-593, June 2010.

[22] James F. Parker, Jr., Raymond E. Reilb, Richard F, Dillon, Thornas G. Andrews, and Edwin A, Fleishman. Development of Tests for Measurement of Primary Perceptual-Motor Performance. NASA Technical Report, National Aeronautics and Space Administration, Washington, D.C., December 1965.

[23] G. Lee Bourassa, Robert M. Guion. A factorial study of dexterity tests. Journal of Applied Psychology, Vol. 43, No. 3, 1959.

[24] J. Tang, A. Singh, N. Goehausen, and P. Abbeel, “Parameterized maneuver learning for autonomous helicopter flight,” in Proc. of the IEEE Int. Conf. on Robotics and Automation, Anchorage, AK, May 2010, pp. 1142–1148.

[25] Abbeel, P., Dolgov, D., Ng, A.Y., Thrun, S.: Apprenticeship learning for motion planning with application to parking lot navigation. In: Conference on Intelligent Robots and Systems (2008)

[26] Ferrell, W. R. Remote Manipulation with Transmission Delay, NASA Technical Note, National Aeronautics and Space Administration, Washington, D.C., February, 1965

[27] Ferrell, W. R. (1965). Remote manipulation with transmission delay. IEEE Transactions on Human Factors in Electronics, 6, 24–32.

[28] Sheridan, T. B. (1993). Space teleoperation through time delay: Review and prognosis. IEEE Transactions on Robotics and Automation, 9(5), 592–606.

[29] Burridge, R.R.; Hambuchen, K.A.; , "Using prediction to enhance remote robot supervision across time delay," Intelligent Robots and Systems, 2009. IROS 2009. IEEE/RSJ International Conference on , vol., no., pp.5628-5634, 10-15 Oct. 2009

[30] Janabi-Sharifi, F.; Hassanzadeh, I.; , "Experimental Analysis of Mobile-Robot Teleoperation via Shared Impedance Control," Systems, Man, and Cybernetics, Part B: Cybernetics, IEEE Transactions on , vol.41, no.2, pp.591-606, April 2011

[31] C. Burns, R. F. Wang, D. Stipanović, "A Study of Human and Receding Horizon Controller Performance of a Remote Navigation Task with Obstacles and Feedback Delays." Paladyn. Journal of Behavioral Robotics. Accepted May 12th, 2011.

[32] Fajen, B. R.; Warren, W. H. 2003. Behavioral Dynamics of Steering, Obstacle Avoidance,and Route Selection. Journal of Experimental Psychology: Human Perception and Performance, Vol. 29, No. 2, 343–362

[33] Huang, W. H.; Fajen, B. R.; Fink, R. J.; Warren, W. H. 2006. Visual navigation and obstacle avoidance using a steering potential function. Robotics and Autonomous Systems, 54 (2006) 288–299.

[34] Arechavaleta, G.; Laumond, J.-P.; Hicheur, H.; Berthoz, A.; , "An Optimality Principle Governing Human Walking," Robotics, IEEE Transactions on , vol.24, no.1, pp.5-14, Feb. 2008

[35] Fajen, B. R., Warren, W. H., Temizer, S., & Kaelbling, L. P. (2003). A dynamical model of visually-guided steering, obstacle avoidance, and route selection. International Journal of Computer Vision, 54(1/2/3): 13-34.

[36] Mejia, J.S.; Stipanović, D.M., "A modified contractive model predictive control approach," Decision and Control, 2009 held jointly with the 2009 28th Chinese Control Conference. CDC/CCC 2009. Proceedings of the 48th IEEE Conference on , vol., no., pp.1968-1973, 15-18 Dec. 2009

[37] S. de Oliveira and M. Morari, "Contractive model predictive control for constrained nonlinear systems," IEEE Transactions on Automatic Control, vol. 45, no. 6, pp. 1053–1071, 2000.

[38] Mejia, J.S.; Stipanović, D.M.; , "Safe coordination control policy for multiple input constrained nonholonomic vehicles," Decision and Control, 2009 held jointly with the 2009 28th Chinese Control Conference. CDC/CCC 2009. Proceedings of the 48th IEEE Conference on , vol., no., pp.5679-5684, 15-18 Dec. 2009

[39] Kuwata, Y.; How, J.P.; , "Stable trajectory design for highly constrained environments using receding horizon control," American Control Conference, 2004. Proceedings of the 2004 , vol.1, no., pp. 902- 907 vol.1, 30 June-2 July 2004

[40] Ogren, P.; Leonard, N.E.; , "A convergent dynamic window approach to obstacle avoidance," Robotics, IEEE Transactions on , vol.21, no.2, pp. 188- 195, April 2005

[41] B3 – Abbeel, Pieter and Ng, Andrew Y. "Apprenticeship Learning via Inverse Reinforcement Learning." Proceedings of the 21st International Conference on Machine Learning. Banff, Canada, 2004.

[42] C. Burns, J. Zearing, R. F. Wang, D. Stipanović, "Autonomous and Semiautonomous Control Simulator", 2010 AAAI Spring Symposium, Technical Report SS-10-04. Published by The AAAI Press, Menlo Park, California.

[43] S. Lavalle. Planning Algorithms. Cambridge University Press, 2006.

[44] Inalhan, G.; Stipanović, D.; and Tomlin, C. 2002. Decentralized optimization, with application to multiple aircraft coordination. In Proceedings of the IEEE 41st Conference on Decision and Control, Las Vegas, Nevada.

[45] D. J. Weiss, Analysis of Variance and Functional Measurement, Oxford University Press, Oxford NY, 2006.

[46] D. Q. Mayne, J. B. Rawlings, C. V. Rao, P. O. M. Scokaert. Constrained model predictive control: Stability and optimality. Automatica vol. 36 no. 6: 789-814, 2000.

[47] Fujita, Y.; Nakamura, Y.; Shiller, Z.; , "Dual Dijkstra Search for paths with different topologies," Robotics and Automation, 2003. Proceedings. ICRA '03. IEEE International Conference on , vol.3, no., pp. 3359- 3364 vol.3, 14-19 Sept. 2003

[48] Gao Yang; , "An improved shortest route algorithm in Vehicle Navigation System," Advanced Computer Theory and Engineering (ICACTE), 2010 3rd International Conference on , vol.2, no., pp.V2-363-V2-366, 20-22 Aug. 2010

[49] Kambayashi, Y.; Yamachi, H.; Tsujimura, Y.; Yamamoto, H.; , "Dijkstra beats genetic algorithm: Integrating uncomfortable intersection-turns to subjectively optimal route selection," Computational Cybernetics, 2009. ICCC 2009. IEEE International Conference on , vol., no., pp.45-50, 26-29 Jan. 2009

[50] Ying-Fung Wu; Widmayer, P.; Schlag, M.D.F.; Wong, C.K.; , "Rectilinear Shortest Paths and Minimum Spanning Trees in the Presence of Rectilinear Obstacles," Computers, IEEE Transactions on , vol.C-36, no.3, pp.321-331, March 1987

[51] G. M. Phillips, "Algorithms for piecewise straight line approximations,", Comput. J., vol. II, pp. 211-212, 1968.

[52] Pavlidis, T.; Horowitz, S.L.; , "Segmentation of Plane Curves," Computers, IEEE Transactions on , vol.C-23, no.8, pp. 860- 870, Aug. 1974

[53] Dunham, James George; , "Optimum Uniform Piecewise Linear Approximation of Planar Curves," Pattern Analysis and Machine Intelligence, IEEE Transactions on , vol.PAMI-8, no.1, pp.67-75, Jan. 1986

[54] E.W. Dijkstra, "A note on two problems in connexion with graphs," NumerischeMathematik, vol. 1, pp. 269-271, 1959.

[55] R. G. Cleggs, "Bellman-Ford and Dijkstra's Algorithm," tech. rep., University of York.

[56] Curve Matching, Time Warping, and Light Fields: New Algorithms for Computing Similarity between Curves, ALON EFRAT AND QUANFU FAN, Department of Computer Science, University of Arizona SURESH VENKATASUBRAMANIAN, AT&T Labs – Research, Published online: 30 November 2006

[57] Helmut Alt and Michael Godau. 1992. Measuring the resemblance of polygonal curves. In Proceedings of the eighth annual symposium on Computational geometry (SCG '92). ACM, New York, NY, USA, 102-109.

[58] T. Eiter and H. Mannila, Computing discrete Fréchet distance, Technical Report CD-TR 94/64, Christian Doppler Laboratory for Expert Systems, TU Vienna, Austria, 1994.

[59] Sriraghavendra, R.; Karthik, K.; Bhattacharyya, C.; , "Fréchet Distance Based Approach for Searching Online Handwritten Documents," Document Analysis and Recognition, 2007. ICDAR 2007. Ninth International Conference on , vol.1, no., pp.461-465, 23-26 Sept. 2007

[60] A. Mosig and M. Clausen. Approximately matching polygonal curves with respect to the Frechet distance. Comput. Geom, 30(2):113–127, 2005.

[61] Fei Shao; Songmei Cai; Junzhong Gu; , "A modified Hausdorff distance based algorithm for 2-dimensional spatial trajectory matching," Computer Science and Education (ICCSE), 2010 5th International Conference on , vol., no., pp.166-172, 24-27 Aug. 2010

[62] Alt, Helmut, Behrends, Bernd, and Blömer, J. 1995. "Approximate matching of polygonal shapes." Ann. Math. Artif. Intell. 13, 251–266.

[63] Sakoe, H. & Chiba, S. (1978) Dynamic programming algorithm optimization for spoken word recognition. IEEE Trans. Acoustics, Speech, and Signal Proc., Vol. ASSP-26, 43-49.

[64] Audet, Charles and J. E. Dennis Jr., "Analysis of Generalized Pattern Searches", SIAM Journal on Optimization, Volume 13, Number 3, pages 889–903, 2003

[65] Wan, X. I.; Wang, R. F.; Crowell, J. A., Spatial updating in superimposed real and virtual environments. Attention Perception & Psychophysics 2009, 71, (1), 42-51.

[66] Wang, R.F. and Simons, D.J. (1999) Active and passive scene recognition across views. Cognition 70, 191–210